Analysis and Design of Blast-Resistant Structures

Yang Guichang

SCHOOL OF CIVIL & ENVIRONMENTAL ENGINEERING

A thesis submitted to the Nanyang Technological University
in fulfillment of the requirement for the degree of
doctor of philosophy

2006

ACKNOWLEDGMENT

The author is greatly indebted to various individuals for their encouragement and assistance in the course of this research. In particular, he wishes to thank his supervisor Prof. Lok Tat Seng, for his generous support and understanding.

TABLE OF CONTENTS

ABSTRACT

The response of reinforced concrete beams and plates with an attached external layer of FRP platekheet on the tension face and subjected to air-blast loading are investigated using a simplified analytical model. The model comprises a number of distinct elastic phases, of which each phase terminates due to failure at a cross-section, and finally the plastic phase, when the reinforced concrete structure becomes a free movable mechanism. Campbell's dynamic yield criterion is employed to take account of the strain rate effect of steel reinforcement. Closed-form formulae are derived to calculate the time when a cross-section yields using approximate numerical technique. With these formulae the time when a dynamic response phase terminates can be determined. Based on the simplified analytical model, the dynamic response of a reinforced concrete beam or plate is traced in accordance with a proposed algorithm. Full disclosure of the theoretical development is provided. A number of numerical examples are given to illustrate how the formulae and the algorithm can be used to analyze structures subjected to air-blast loading.

LIST OF TABLES

LIST OF FIGURES

LIST OF SYMBOLS

η	=	amplification factor to take account of static axial force effect
ω	=	frequency parameter of the equivalent SDOF system
Ω	=	domain of the plate in *xy*-plane
τ	=	yielding delay time of steel reinforcement
$\partial\Omega$	=	boundary of domain Ω
ε'_s	=	tension strain of steel reinforcement
$\sigma(t)$	=	dynamic stress of steel reinforcement
$\Omega(x,y)$	=	static deformation of plate in plastic phase
θ_A	=	rotational displacement of beam's left end
φ_a	=	rotation angle of left beam segment
θ_B	=	rotational displacement of beam's right end
ε_c	=	compressive strain of concrete
φ_c	=	rotation angle of right beam segment
σ_{dy}	=	dynamic yield stress of the steel reinforcement
α_s	=	ratio of E_s to E_c
α_f	=	ratio of E_f to E_c
α_{fs}	=	ratio of E_f to E_s
ε_{ft}	=	tension strain of FRP reinforcement
ψ_i	=	open angle of i^{th} plastic hinge
ψ_{id}	=	limit open angle of i^{th} plastic hinge
σ_{sy}	=	static yield stress of steel reinforcement

A_s'	=	area of steel reinforcement at top of beam's cross-section
A_f	=	effective area of FRP reinforcement at bottom of beam's cross-section
A_s	=	area of steel reinforcement at bottom of beam's cross-section
B	=	bending stiffness of beam
b	=	width of beam's cross-section
c	=	depth of compression zone of beam's cross-section
d	=	effective height of beam's cross-section
D	=	bending stiffness of plate
d_s	=	diameter of steel bar
E_c	=	Young's modulus of concrete
E_f	=	Young's modulus of FRP
E_s	=	Young's modulus of steel reinforcement
$f_l(x)$	=	load distribution function of the blast loading on beam
$f_l(x,y)$	=	distribution function of blast loading
f_c	=	compression strength of concrete
f_y	=	tension strength of steel reinforcement
H	=	height of beam's cross-section
I	=	second moment of area of beam's cross-section
K	=	stiffness of the rotational spring to join two beam segments
$K_{\theta A}$	=	rotational stiffness of elastic support at left end of beam
$K_{\theta B}$	=	rotational stiffness of elastic support at right end of beam
K_{yA}	=	vertical stiffness of elastic support at left end of beam
K_{yB}	=	vertical stiffness of elastic support at right end of beam
L	=	length of beam

L_A	=	length of left beam segment
L_B	=	length of right beam segment
L_y	=	length of yield beam segment
m	=	distributed mass of the beam or plate
$M(x,t)$	=	dynamic bending moment in beam
M_{AB}	=	joint moment on beam's left end
M_{BA}	=	joint moment on beam's right end
$M_x(x,y,t)$	=	dynamic x-bending moment of plate
$M_{xy}(x,y,t)$	=	dynamic torsional moment of plate
$M_y(x,y,t)$	=	dynamic y-bending moment of plate
p	=	amplitude of blast loading
$P(x,t)$	=	blast loading on beam
$P(x,y,t)$	=	distributed blast loading on plate
$Q(x,t)$	=	dynamic shear force in beam
q_A	=	value of load distribution function at left end of beam
q_B	=	value of load distribution function at right end of beam
$Q_x(x,y,t)$	=	dynamic x-shear force of plate
$Q_y(x,y,t)$	=	dynamic y-shear force of plate
R_{AY}	=	vertical joint force on beam's left end
R_{BY}	=	vertical joint force on beam's right end
T	=	dynamic function of equivalent SDOF system
t_d	=	duration of blast loading
t_f	=	time when fiber reinforced plastics rupture
v_A	=	vertical displacement of beam's left end

v_B	=	vertical displacement of beam's right end
$W(x)$	=	beam's static deflection.
$w(x,t)$	=	beam's dynamic deflection
$w(x,y,t)$	=	plate's dynamic deflection.

Chapter 1

INTRODUCTION

1.1 Background

The bombings at New York City's World Trade Center, Oklahoma City's Alfred P. Murrah Federal Office Building, Atlanta's Centennial Park, and more recently, the 11 September 2001 terrorist attack shocked the world. The design and construction of public buildings to provide life safety in the face of explosions is receiving renewed attention from structural engineers and planners. Much research and experiments have been done addressing the analysis, design and construction of military buildings and facilities. Increasingly, this technology is filtered down to address facilities in the civilian and commercial domain.

The design of civilian or commercial buildings to withstand the effects of air-blast is unlike the design of military installations. Military structures are typically associated with a specific requirement that must be maintained, and they must remain operational despite the attack. The form and function of a facility are governed by the mission that it is designed to perform. The blast-protection objective of any commercial or public building must be to prevent structural collapse, to save lives and to evacuate victims. Military structures occupy secure sites with substantial "keep-out" distances surrounding the assets; unfortunately, this is not possible for most civilian structures. Civilian real-estate owners typically want to attract the public to keep the property profitable and can rarely afford the real estate necessary to be a secured site. This "keep-out" distance is vital in the design of blast-resistant structures since it is the key parameter that determines, for a given charge weight, the blast overpressures that load the building and its structural elements. The degree of fenestration is another key parameter as it determines the pressure that enters the structure. The smaller the door and window openings the better protected the occupants are within the structure. Architectural and structural features play a significant role in determining how the building will respond to the blast loading. These features can include adjacent or underground parking, atriums, transfer girders, slab configurations, and structural-frame systems.

Designers of civilian structures are caught in a dilemma. Many of the features that make the structures desirable working space are the same features that make them more vulnerable to attack. Situated on urban sites, civilian structures are limited in their ability to restrict terrorist access to a prescribed keep-out distance. Windows and atriums enhance the working space by providing openness and natural light. Hence, the role of the blast engineer is further complicated by architectural criteria that directly contradict blast-mitigation objectives. Within these constraints the blast engineer is unable to make a building blast resistant. The objectives are therefore more modestly defined to permit significant localized damage while preventing catastrophic collapse. The casualties that will occur to occupants in the immediate vicinity of the explosion may be unavoidable, but by preventing progressive collapse, the remaining occupants may be spared injury or death. The means to achieve these objectives requires a thorough review of the design, to identify weaknesses that may put the occupants at risk. Attention must be given to the behavior of the structural elements to improve their redundancy, toughness, and ductility, and to provide adequate means to guarantee the keep-out distance available to the site. Therefore, the methods and techniques to design and construct military facilities should be developed further to make them suitable to the design and construction of civilian and commercial buildings.

Despite the need to construct new buildings to resist terrorism and occasional explosions, many existing civilian and commercial buildings should be strengthened to increase their blast resistance. Some techniques to strengthen concrete structures such as sprayed concrete, concrete jacketing, or externally bonded steel plates and composite materials like fiber reinforced plastics (FRP) may be used to increase the resistance of concrete structures, but the simple methods to analyze and design of the structures composed of externally strengthened structural components subjected to blast loads are still lacking. Research and experiments should be conducted to develop the effective strengthening techniques to increase the blast resistance of the building, and the step should be taken to develop a simple analysis and design method for strengthening structures.

The ability to design and construct blast resistant buildings depends on an understanding of how such buildings behave under the severe loads. Many analysis methods to predict how a structure will respond to explosion overpressures have been developed, and are still being developed further. There are basically three kinds of methods, which are widely used in the analysis and design of blast-resistant structures:

Pseudo-dynamic or pseudo-static methods. These are simplest to apply since they take the explosion overpressure as a blanket loading, and are usually combined with dynamic amplification factors. The methods can assess both elastic and inelastic response and can be applied to complex structures

Single-degree-of-freedom (SDOF) method. This is a dynamic analysis technique, which predicts the response of a structure by reducing the structure to a simplified spring/mass system. The method is effective for simple structures that behave in a manner analogous to a spring/mass system. The method can assess both linear and nonlinear response and, with care, can be applied to more complex structures.

Finite element analysis (FEA). FEA can be used effectively to solve explosion response problems, taking account of geometric and material non-linearity. The method has to be applied with care, since there is a fine line between a model which is detailed enough to predict the response, and coarse enough not to run for impracticable lengths of time and no good constitutive material model exists to describe brittle materials such as concrete. Many commercial FEA based software exist for the analysis of blast-resistant structures. These are EPSA-II (Atkash, *et. al.*, 1994), DYNA3D (Whirley and Engelmann, 1993), etc.

Among these methods, the SDOF approach is most widely used in design practice. This was developed for military applications many years ago, before availability and the common use of computers.

Explosion materials are designed to release large amounts of energy in a short time. The explosion arises through the reaction of solid or liquid chemicals or vapor to form more stable products, primarily gasses. A high explosive is one in which the speed of reaction (Typically 5,000 – 8,000 m/s) is faster than the speed of sound in the explosion. When an explosion occurs, a shock or pressure wave propagates outward from the source of explosion, encountering structures and components along its path. The shock wave or pressure wave includes a short duration of high-amplitude overpressure followed by a longer duration of negative pressure or suction. The overpressures can be range up to tens of megaPascals (MPa), and its duration ranges from a very few milliseconds to a hundred milliseconds. The suction phase is typically ignored in blast evaluation, except where it is necessary to evaluate the rebound effects from overpressure response.

Blast overpressure is typically a very high amplitude loading but of very short duration and generally over one cycle. The response of building to such loads is rooted in the dynamic response of their structural elements. Blast-resistant design therefore relies on significant levels of allowable inelastic behavior. As a result, blast-resistant structures must have the ductile detailing necessary to withstand inelastic deformations and still perform acceptably.

When a particular face of a building is struck with the blast shock wave traveling with a velocity greater than the speed of sound, it could move the exposed face of the building off its foundation and precipitate collapse or partial collapse. This depends on such features as the magnitude of the shock impulse of the blast wave, the natural period of the structure and elasticity of the structure.

The relatively low incident blast shock loads on roofs are generally acting downward and often sufficient in terrorist attack scenarios to either fail the roof slabs or panels or buckle the columns holding up the roof or both. Hardened roof design is then required as part of a blast-resistant design effort.

The exterior walls of building are subjected to higher reflected blast shock loads. When these walls fail, they often compromise the integrity of the structure and breach the building envelope allowing the blast wave to enter the building and do further internal damage.

Based on the understanding of the behavior of structures subjected to air blast load, the first step for the design of most buildings to resist blast loading is to break down the structure into a few simple structural components, which can be analyzed using simple dynamic analysis methods. This is where the SDOF method can be used. This SDOF method allows the designer to determine the maximum deformation of each main structural element or component of the building, and hence determine the degree of damage to the building ranging from insignificant or light damage to total destruction.

1.2 Research scope and objective

If the explosion originated at a sufficiently great scaled range (i.e., a small charge or a large distance from a structure), then the structure will be loaded in a manner that leads to global deformation, meaning that all the elements provide some degree of resistance to the loading. The definition of the expected loading, and the provision of resisting elements to accommodate the loading are the essence of dynamic design, analysis, and construction; these issues are addressed in design manuals such as TM 5-1300 (TM5-1300, 1987), DOE/TIC-11268 (DOE/TIC-11268, 1992), etc. and by computer programs such as DYNA3D (Whirley and Engelmann, 1993), BLASTX (Britt and Lumsden, 1994), etc. When the component of the structure is reinforced with combined steel bars and fiber mat or fiber reinforced plastic plates, the dynamic behavior of the structure will be essentially different from that of the structure reinforced with steel bars only. The dynamic analysis and design methods for such structures are still lacking. This thesis outlines and develops a simple analysis method for the design of concrete structures reinforced with combined steel bars and FRP plate/sheet subjected to air blast loading.

The typical dynamic response of reinforced concrete structures subjected to air blast load can be divided into elastic phase, elastic-plastic phases, and finally the plastic phase (i.e. the structure becomes a mechanism). Protective structures and some commercial and public buildings should have ample reserve of strength and stability to resist blast loading. In this respect, two design criteria are usually considered. The first is elastic criteria. It considers the possibility of the structure subjected to a series of blast loads. However, after each load there should be no residual strains in the structure. All the cracks that appear during the blast load phase should be closed. Thus, only elastic deformations are developed in the structure. To satisfy the elastic design criteria, elastic analysis is adequate. The second is plastic criteria. When the designed blast load acts on the structure, it should not collapse. However, some plastic deformation of the structure may be allowed but there should be stability to guarantee the safety of personnel and equipment inside the building. To satisfy the plastic design criteria, plastic analysis following a detailed analysis of the elastic phase is necessary.

The traditional approach to design reinforced concrete structural members subjected to air-blast loading is to transform the component into a Single-Degree-Of-Freedom (SDOF) system. Using simple dynamic analysis, the solution of this equivalent SDOF system may be derived. Currently, design manuals utilize this principle to outline procedures. To help engineers, a significant number of design charts have been produced. However, when such structural components are reinforced with an external layer of fiber reinforced polymer – perhaps to harden the existing structure or designing walls for a new facility – the engineer is unable to analyze the system because no such theory exists that would enable him to undertake a thorough dynamic analysis of the system. This vacuum has been recognized and is the subject of this research. To conduct this research, several progressive approaches have been identified. Therefore, the scope of this research includes:

(1) A review of analysis and design of blast-resistant structure and the Single-Degree-Of-Freedom (SDOF) method.

(2) The use of SDOF method to analyze concrete structures reinforced with both steel bars and external layer of fiber reinforced polymer (FRP).

(3) The use of rational functions to obtain approximate solution of nonlinear problems (or equations).

The ultimate aim of understanding a problem and conducting detailed analysis of systems is to improve existing design methodology and/or develop more accurate means of estimating the response of structures (from a complex loading system) so that greater economy can be achieved. This forms the basis of the objective in this research into the analysis and design of blast-resistant structures. Therefore, the objectives are:

Deriving (analytically) the mathematical model of a "general" beam reinforced with both steel bars and external layer of fiber reinforced polymer (FRP) – the system is subjected to air-blast loading.

Develop the mathematical model and to relate the model to real concrete structures.

Deriving the formulae to determine the yielding delay time of steel reinforcement of the concrete structure. This is an essential element of the research because the FRP system contributes significantly to the strength of the system. The difficulty lies in the formulation and solution of the problem.

(4) Deriving formulae for a plate reinforced with both steel bars and FRP plate/sheet and subjected to air-blast loading.

1.3 Organization of this thesis

This thesis consists of eight chapters describing the research conducted in the School of Civil & Environmental Engineering, Nanyang Technological

University.

Chapter 2 presents a review of existing knowledge on the analysis and design of blast-resistant structures. The review focuses on the analysis of blast-resistant structures which includes the SDOF method and finite element analysis (FEA) based methods, strain rate effect of reinforcing steel and structure strengthening with FRP plate/sheet.

Original and new formulae and derivations for analysis and design of concrete beams with arbitrary support conditions are developed in Chapter 3. The formulae for the analysis of a continuous beam loaded by static axial forces are also derived. These formulae can be used to analyze concrete buildings when a bomb explodes in an adjacent area.

In Chapter 4, formulae for analysis and design of plate structures reinforced with combined steel bars and FRP sheet are derived.

The formulae to determine the time when a dynamic deformation stage terminates are derived in Chapter 5.

The criteria which may be used for the design of blast-resistant structures are summarized in Chapter 6. The formulae can be found from the public literature. However it should be noted that these formulae are applicable for static problems. One should exercise due care when they are used for dynamic problems.

With these developed methods contained in the thesis, structural members reinforced with combined steel bars and FRP plate/sheet can be easily analyzed. A number of numerical examples are given in Chapter 7.

Finally, summary and recommendations for future study are presented in Chapter 8.

Chapter 2

LITERATURE REVIEW

2.1 Simplified analytical model

Explosive devices have been used for hundreds of years, yet the comprehensive treatment of blast-effects and their mitigation appeared only during and after World War II. World War II was the first international conflict that resulted in massive destruction of cities, mostly with high explosives, which also inflicted enormous casualties. In the later stages of the war, the use of two nuclear weapons demonstrated the destructive capacity of such weapons (Glasstone and Dolan, 1977). In addressing both the nuclear threat and the threat of conventional weapons, a lot of research coupled with test programs has been done to develop computational approaches for estimating the response and behavior of simple structures subjected to blast loading. In turn, based on experimental data, field-test observations and analytical procedures, a number of technical design manuals were developed, e.g. *Structures to Resist the Effects of Accidental Explosions* (TM 5-1300, 1987), *A Manual for the Prediction of Blast and Fragment Loadings on structures* (DOE/TIC-11268, 1992), *Protective Construction Design Manual* (ESL-TR-87-57, 1989). The analysis and design procedures in all of these design manuals are largely based on the synthesis of test data and simplified computational models. This simplified computational model is usually a mass-spring system with a single-degree-of-freedom (SDOF), which is simplified from the real structure to be analyzed. This approximate design method is usually called Biggs' Method (Biggs, 1964). This method can be briefly described as follows:

It is assumed that the structure - exposed to the dynamic pressure pulse - ultimately attains a deformed configuration comparable to the static deformation pattern. Using the static deformation pattern as the displacement shape function,

$$w(x,t) = W(x)T(t) \tag{2.1}$$

and the dynamic equations of equilibrium can be transformed (assuming an undamped single-degree-of- freedom system) to:

$$\bar{m}\ddot{T}(t) + \bar{k}T(t) = \bar{f}(t) \tag{2.2}$$

where

$W(x)$	=	displacement shape function
$T(t)$	=	dynamic function of the equivalent SDOF system
$\ddot{T}(t)$	=	second-order derivative of $T(t)$ with respect to time t
$\bar{m}$	=	generalized mass
$\bar{f}(t)$	=	generalized force
$\bar{k}$	=	generalized elastic bending stiffness

Alternatively the equilibrium equation can be expressed as:

$$k_{lm}M\ddot{T}(t) + KT(t) = F(t) \tag{2.3}$$

where

$k_{lm} = k_m / k_l$	=	load-mass transformation factor
$k_m = \bar{m}/M$	=	mass transformation factor
$k_l = \bar{f}(t)/F$	=	load transformation factor
$M = \int_\Omega m dx + \sum_i M_i$	=	total mass
$F = \int_\Omega p(x,t)dx + \sum_i F_i$	=	total load
$K = \bar{k}/k_m$	=	characteristic stiffness
M	=	distributed mass
M_i	=	concentrated mass at point x_i
$p(x,t)$	=	explosion pressure

F_i	=	concentrated load
x_i	=	position of concentrated mass/load
$W_i =$	=	value of shape function at x_i
Ω	=	domain of the structural components

The natural frequency of vibration for the equivalent system is given by

$$\omega = \sqrt{\frac{\bar{m}}{\bar{k}}} = \sqrt{\frac{K}{k_{lm} M}} \qquad (2.4)$$

The response, $T(t)$, is entirely governed by the total mass, load-mass factor, the characteristic stiffness and the load history.

For a linear system, the load factor and the characteristic stiffness are constant. The response is then alternatively governed by the eigenperiod and the characteristic stiffness.

For a nonlinear system, the load-mass factor and the characteristic stiffness depend on the response (deformation). Nonlinear systems may often be approximated by equivalent bi-linear or tri-linear systems. In such cases, the response can be expressed in terms of

K_1	=	characteristic stiffness in the initial, linear resistance domain
T_{el}	=	displacement at the end of the initial linear resistance domain
ω	=	circular frequency in the initial, linear resistance domain
K_3	=	normalized characteristic in the third linear resistance domain, if relevant

For a given explosion load history, the maximum displacement, T_{max}, is found by analytical or numerical integration of Eq. (2.3).

For standard load histories and standard resistance curves, maximum displacements are presented in design charts, which are given in design manuals mentioned earlier. For example, the normalized maximum displacement of a SDOF system with a bi-($K_3=0$) or trilinear ($K_3>0$) resistance function, exposed to a triangular pressure pulse with zero rise time is shown in Fig. 2.1. When ratio of the duration of the pressure pulse to the eigenperiod in the initial and linear resistance range is known, the maximum displacement can be determined directly from the diagram.

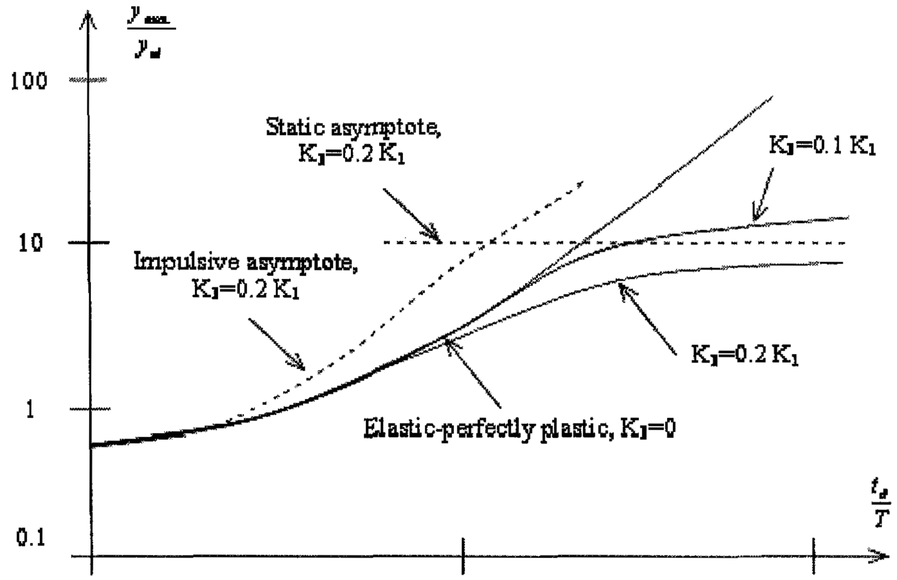

Fig. 2.1 Maximum response of SDOF system subjected to a triangle pressure pulse with zero rise time

Transformation factors for elastic-plastic deformation of beams and slabs with different boundary conditions can be found in design manuals. Diagrams showing the maximum displacements for a SDOF system exposed to different pressure histories can also be found in design manuals.

The characteristic response of the system is based upon the resistance in the linear range, $K=K_1$, where the equivalent stiffness is determined from the elastic solution to the actual system.

If the displacement shape function change as a nonlinear structure undergoes deformation, the transformation factors change. An average value of the combined load-mass transformation factor can be approximated as

$$k_{lm}^{average} = \frac{1}{\mu}\left[k_{lm}^{elastic} + (\mu - 1)\, k_{lm}^{plastic}\right] \tag{2.5}$$

where μ is the ductility ratio ($\mu = T_{\max}/T_{el}$).

With the formulae of the transformation factors and design charts, one can easily analyze and design a simple structure, such as beams, plates, etc., subjected to an idealized blast load.

2.2 Computational techniques

During the past 25 years, powerful computer programs have been developed for predicting blast loads and the resulting structural response (National Research Council, 1995). Computer programs for the prediction of blast effects can be subdivided in two groups: *first-principle* and *semi-empirical* programs, in which the mathematical equations describing the basic laws of physics governing a particular problem are solved. These principles are conservation of matter, momentum, and energy. In addition, mathematical relationships called constitutive equations, which describe the physical behavior of materials, are needed. If these equations are solved accurately with suitable mathematical modes, they should predict the blast loads and structural response. However, there are several barriers to accurate prediction of the effects of an explosion through the use of the first-principle programs. Among them are the following:

- In the calculation of blast due to explosions in air, the response of the air involves complicated phenomena, such as dust-air mixtures, boundary effects, and turbulence. Turbulent flow, for example, cannot be calculated without the addition of models governed by empirical parameters.

- Calculation of the pressures imparted by a detonating explosive on the structure involves multiscale phenomena that are very difficult to deal with; such phenomena also occur in the structure during failure.
- In the calculation of structural failure, the behavior of the materials is neither well understood nor readily characterized; in other words, accurate constitutive equations are not available for the materials, particularly in fracture or fragmentation.

While these deficiencies in first-principle codes are often compensated for by the use of engineering judgment, the main objective of *first-principle* technique is to provide predictions in new domains where experience that makes engineering judgment possible is not available.

Semi-empirical computational methods are based on simplified models of physical phenomena, which are developed through analysis of test results and application of engineering judgment. These methods rely on extensive data and case studies. They involve fewer equations and require far less computer time, which makes them more practical than first-principle codes for design purposes.

The computer programs applied in the evaluation of explosive effects cover two physical disciplines:

- Computational fluid dynamics (CFD), which is used for the prediction of the air blast caused by the explosion and pressures applied to surfaces exposed to the propagating air blast; and
- Computational solid mechanics (CSM), which deals with the prediction of the response of structures to loads.

The pressure and the response of the structure are inter-related, and in many cases "coupled" analysis of the fluid and structure are needed. Coupled CSM-CFD solutions entail the use of much larger computer programs and are more costly, but they can provide more accurate predictions. There are difficulties in understanding and mathematically modeling the structural behavior in transition regions of response from predominately flexural behavior into domains dominated by boundary or punching shear, and ultimately to material disintegration. Also, material constitutive relationships are less well understood in these transition regions. Nevertheless, computations can give valuable information about the magnitude and type of damage. The pressures resulting from complex, non-spherical explosive charges (e.g., car bombs) are not well understood and carefully controlled experiments are vital for a better understanding and validation of computer programs. Despite some success in re-creating the observed effects of actual bombings and cited examples where numerical codes were applied to specific design problems it is not clear that the routine application of these programs to civilian buildings will become widespread. However, where these programs could prove very valuable is in testing a wide range of building types and structural details over a broad range of hypothetical explosion events. The knowledge gained from such testing, verified by experimentation, could transfer directly to civilian practice through manuals and other design aids, and ultimately into building codes, in much the same way as the application of seismic design principles has become routine.

2.3 Strain rate effect

For the reinforcement of mild steel, the level of stress at which yield occurs can increase by up to 60% for very fast loading rates as shown schematically in Fig. 2.2 (Smith and Hetherington, 1994).

The laws of deformation of materials sensitive to the speed of deformation were dealt with in the literature (Goldsmith, 1965; Sdobirev, 1968; and Kotlyarevskii, 1961). Here, only the laws for mild steel are used for the design of reinforced concrete structures subjected to explosion loads. In the case of a single-axis state of stress, the dynamic yield point $\sigma(\tau)$ for an arbitrary regime of dynamic stress $\sigma(t)$ may be obtained from the expression for the universal criterion for dynamic creeping which determines the delay time τ on the basis of the theory of dislocations,

$$\int_0^{\tau}\left[\sigma(t)\right]^{\alpha} dt = t_0 f_y^{\alpha} \tag{2.6}$$

where

τ = yielding delay time (i.e. the time interval between the instant of loading and the commencement of yielding)

t_0 = a parameter depending on temperature, which is determined from test

α = non-dimension constant, which is determined from test

f_y = static yield strength of reinforcing steel

Within the interval $0<t<\tau$ or $0<\sigma<\sigma(\tau)$ mild steel behaves as a linearly elastic material. The dynamic modulus of elasticity E_d practically does not differ from the static modulus E. Experiments performed by Kotlyarevskii (1961) with mild steels have shown that at normal temperature (20^{O} C) t_0 = 0.895*s* and α=17. Campbell(1953) gives the values of α in range of 18.5 to 25.

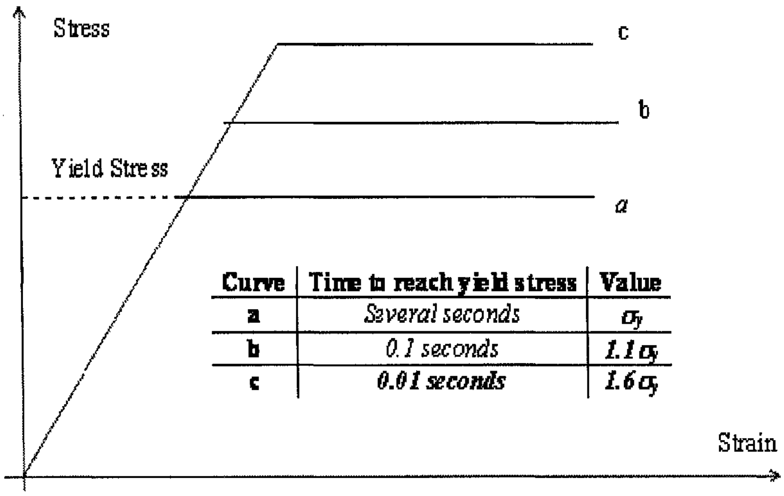

Curve	Time to reach yield stress	Value
a	Several seconds	σ_y
b	0.1 seconds	$1.1\sigma_y$
c	0.01 seconds	$1.6\sigma_y$

Fig. 2.2 Strain rate effect on yield strength

The delay time τ may be determined with iterative calculation (Henrych, 1979). In determining time τ the complex functions $\sigma(t)$ may be linearized in the subintervals $t_{i-1}<t<t_i$, $(i=1,2,\ldots n)$ where $t_n=\tau$. The function $\sigma(t)$ can then be expressed in the following form

$$\sigma(t)=\sigma(0)+\frac{t}{t_1}[\sigma(t_1)-\sigma(0)] \qquad 0\le t\le t_1$$

$$\sigma(t)=\sigma(t_1)+\frac{t-t_1}{t_2-t_1}[\sigma(t_2)-\sigma(t_1)] \qquad t_1\le t\le t_2$$

$$\sigma(t)=\sigma(t_{i-1})+\frac{t-t_{i-1}}{t_i-t_{i-1}}[\sigma(t_i)-\sigma(t_{i-1})] \qquad t_{i-1}\le t\le t_i$$

so that

$$\int_0^\tau \sigma^\alpha(t)dt=\sum_{i=1}^{n}\int_{t_{i-1}}^{t_i}\left[\sigma(t_{i-1})+\frac{t-t_{i-1}}{t_i-t_{i-1}}(\sigma(t_i)-\sigma(t_{i-1}))\right]^\alpha dt$$
$$=\frac{1}{\alpha+1}\sum_{i=1}^{n}\frac{\sigma^{\alpha+1}(t_i)-\sigma^{\alpha+1}(t_{i-1})}{\sigma(t_i)-\sigma(t_{i-1})}(t_i-t_{i-1})$$

Eq. (2.6) may then be written in the form

$$\sum_{i=1}^{n}\frac{\sigma^{\alpha+1}(t_i)-\sigma^{\alpha+1}(t_{i-1})}{\sigma(t_i)-\sigma(t_{i-1})}(t_i-t_{i-1})=(\alpha+1)t_0 f_y^\alpha \qquad (2.7)$$

With Eq. (2.7), an iterative calculation procedure can be derived to calculate the yielding delay time τ.

In TM 5-1300, the strain rate effects are taken into account with the calculation of the dynamic increase factor (DIF). DIF is equal to the ratio of the dynamic strength to the static strength, e.g.

$\frac{f_{dy}}{f_y}$, $\frac{f_{du}}{f_u}$ and $\frac{f'_{dc}}{f'_c}$

where

f_y	=	static yield stress of reinforcing steel
f_{dy}	=	dynamic yield stress of reinforcing steel
f'_c	=	static ultimate compressive strength of concrete
f'_{dc}	=	dynamic ultimate compressive strength of concrete
f_u	=	static ultimate stress of reinforcing steel
f_{du}	=	dynamic ultimate stress of reinforcing steel

The DIF depends upon the rate of strain of the element, increasing as the strain rate increases. The design curves and tables of DIF for concrete and steel reinforcement are given in the manual. The increase in capacity of flexural elements is primarily a function of the rate of strain of the reinforcement, in particular, the time to reach yield, τ, of the reinforcing steel. The average rate of strain for both concrete and steel may be obtained considering the strain in the materials at yield and the time to reach yield. The member is first designed using the DIF values given in the design table. The time to reach yield, τ, is then calculated using the response charts. For the values τ, the average strain rate in the materials can be obtained. The average strain rate in the concrete (based on f'_{dc} being reached at ε_c = 9,992 in./in.) is

$$\varepsilon'_c = \frac{0.002}{\tau} \tag{2.8}$$

while the average strain rate in the reinforcement is

$$\varepsilon'_s = \frac{f_{dy}}{E_s\,\tau} \tag{2.9}$$

where

τ = yielding delay time (time to reach yield of reinforcement)

E_s = modulus of elasticity for reinforcing steel

For the strain rates obtained from Eq. (2.8) and Eq. (2.9), the actual DIF is obtained for the concrete and reinforcement from the design curves in the manual. If the differences between the calculated DIF values and the design values of the design table are small, then the correct values of DIF are those calculated. If the differences are large, the calculated values of DIF are used as new estimates and the process is repeated until the differences between the "estimated" and "calculated" values of DIF are small.

For the elastic-plastic or plastic design of concrete elements, an equivalent elastic curve is considered rather than the actual elastic-plastic resistance-deflection function. The time to reach yield τ is computed based on this curve using the equivalent elastic deflection and stiffness. Actually, the reinforcement along the supports yields in less time than τ whereas the reinforcement at mid-span yields at a time greater than τ. These differences are compensating errors. Therefore, the time to reach yields τ for the equivalent curve when used in Eq. (2.8) and Eq. (2.9)produces an average DIF for the concrete and reinforcement at the critical section throughout a reinforced concrete element.

2.4 Structure strengthening

The FRP system, which employs the use of high-strength fibers in an epoxy matrix, provides a material with high-tension capacity along with an elasticity that is compatible with conventional materials. FRP has gained wide recognition as a primary strengthening measure to increase load carrying capacity of structural systems. These retrofit measures can be used to improve the performance of resisting blast loadings. Some tests done by fiber manufactures show that the fiber reinforced plastic sheet reinforcement is able to increase the explosion resistance of masonry by a factor of 5 to 10. (Design Guideline for S&P FRP system, 2002). Currently the design of FRP reinforced structures is based on test results and static capacity-based design principles to increase flexural and shear strength of beams, columns, slabs and walls. Many papers addressing the static design of new structures and the retrofit of existing structures to resist higher static loading have been published in the past 10 years.

Alsayed, et. al. (2000) gave some reviews of the basic mechanical properties of carbon, aramid and glass FRP composites. The major factors affecting the physical performance of an FRP composite are fiber orientation, length and shape of fibers, composition of the fibers, mechanical properties of the resin matrix, and adhesion of the fibers and the matrix. The principal mechanical properties are summarized as:

Tensile strength. The tensile strength of FRP is of the order of twice that of pre-stressing steel strands. However, FRP composites reach their ultimate tensile strength without exhibiting any yielding of the material. Typical values of tensile strength for glass FRP (GFRP), carbon FRP (CFRP) and aramid FRP (AFRP) reinforcements are shown in Table 2.1. The tensile strength fluctuation coefficient is 2-7%. Typical stress-strain relationships for different types of FRP and steel are shown in Fig. 2.3.

Table 2.1 Typical mechanical properties of S&P FRP systems and steel reinforcement (from Design Guideline for S&P System (2002)

Type of Fiber	Tensile strength: MPa	Modulus of Elasticity: GPa
GLASS	1700—3000	65—70
CARBON	2500—4000	240—640
ARAMID	3000—4000	124
STEEL	250—550	210

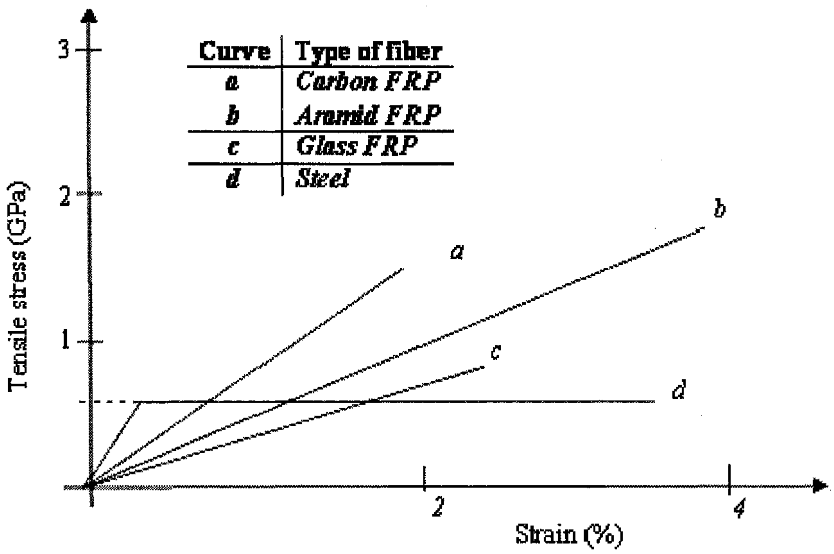

Fig. 2.3 Strong but brittle stress-strain relations for carbon, aramid and glass fiber reinforced polymer compared to steel

Specific gravity. FRP composites have a specific gravity ranging from 0.5 to 2.0, which is nearly four times lighter than steel. Typical values of specific gravity for GFRP, CFRP and AFRP are shown in Table 2.1.

Modulus of elasticity. The modulus of elasticity (E) of GFRP and AFRP is generally lower than that of steel, whereas for CFRP it ranges from a quarter to twice as much as that of steel. When GFRP and AFRP are used as main reinforcement, vertical deflection may control the design. The coefficient of variation of E is fairly low. Typical values for GFRP, CFRP and AFRP materials are shown in Table 2.1.

Ductility. In addition to structural strength, ductility is considered to be a major safety consideration in the design of plated reinforced concrete elements. It is characterized by the ability of the member to undergo excessive deflection or rotation while sustaining its strength.

Chapter 3

ANALYSIS OF BEAMS SUBJECTED TO AIR-BLAST LOADING

3.1 SDOF method for analysis of RC beam subjected to air-blast loading

The approach adopted here is essentially the Rayleigh-Ritz method of analysis. In this approach, it is assumed that both the solution of equilibrium equations and the load on the structure are of separation variable type. Further, the function in the solution concerned with geometric co-ordinates have the same form as that of the corresponding static problem of the same structure subjected to the loading of the same geometrical distribution as that of the blast load on the structure. Therefore, the procedure used in solving the problem includes two steps. The first step is to evaluate the static problem such that the solution concerned with the geometric co-ordinates can be obtained and the second step is to use the weight residual method to obtain an equation of the equivalent SDOF system.

3.1.1 Single span RC beam strengthened with FRP plate/sheet

Consider the beam with elastic supports and subjected to air-blast loading as shown in Fig. 3.1.

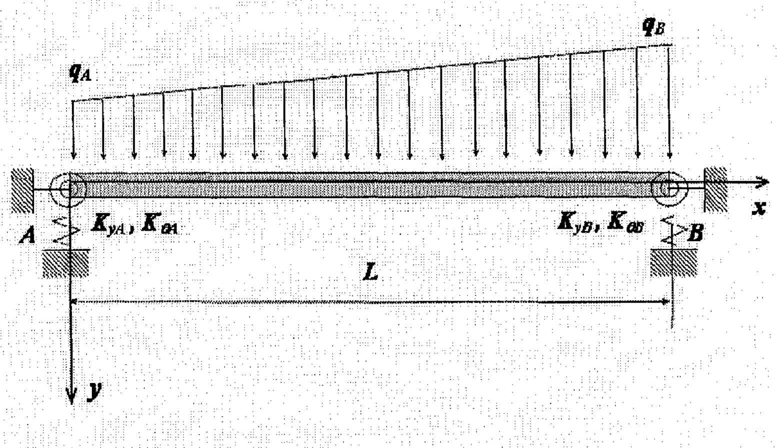

Fig. 3.1 Beam with elastic supports subjected to air-blast loading

The symbols used in Fig. 3.1 are defined as follows:

K_{yA} = vertical stiffness of elastic support at beam's left end

$K_{\theta A}$ = rotational stiffness of elastic support at beam's left end

K_{yB} = vertical stiffness of elastic support at beam's right end

$K_{\theta B}$ = rotational stiffness of elastic support at beam's right end

q_A = amplitude of the overpressure at beam's left end

q_B = amplitude of the overpressure at beam's right end

L = length of the beam

The equilibrium differential equation of a beam subjected to air-blast loading can be expressed as

$$EI\frac{\partial^4 w(x,t)}{\partial x^4}+m\frac{\partial^2 w(x,t)}{\partial t^2}=P(x,t) \tag{3.1}$$

where

EI = bending or flexural stiffness

m = distributed mass

$w(x,t)$ = dynamic beam deformation

$P(x,t)$ = dynamic loading function

The bending moment and shear force are calculated respectively from

$$M(x,t)=-EI\frac{\partial^2 w(x,t)}{\partial x^2} \tag{3.2}$$

$$V(x,t)=-EI\frac{\partial^3 w(x,t)}{\partial x^3} \tag{3.3}$$

The loading (on the beam) and the beam deflection can be described respectively as

$$P(x,t) = p\, f_1(x) f(t) \tag{3.4}$$

$$w(x,t) = p\, W(x) T(t) \tag{3.5}$$

where

p	=	amplitude of air-blast load
$f_1(x)$	=	distribution of air-blast load on beam
$f(t)$	=	time-varying loading
$W(x)$	=	deformation of the beam subjected to static load of $f_1(x)$
$T(t)$	=	dynamic function

In this thesis $f_1(x)$ is assumed to be a linear function. If the amplitude of the air-blast load, p, is set with an average value of $0.5(q_A + q_B)$, the linear function $f_1(x)$ can be represented in the following form

$$f_1(x) = 1 - \alpha + 2\alpha x/L \tag{3.6}$$

$$\alpha = (q_B - q_A)/(q_B + q_A) \tag{3.7}$$

The static deformation $W(x)$ satisfies the following equation

$$EI \frac{d^4 W(x)}{dx^4} = f_1(x) \tag{3.8}$$

and the supporting boundary conditions. The beam with elastic supports subjected to linearly distributed loading together with the definitions of loading and support stiffness (load variation q_A and q_B, the vertical and rotational stiffness $K_{yA}, K_{\theta A}, K_{yB}, K_{\theta B}$) is shown in Fig. 3.1.

Substituting Eqs. (3.4) and (3.5) into Eq. (3.1), the residual is obtained in the form

$$R(x,t) = p\left[T(t)f_1(x) + m\ddot{T}(t)W(x) - f_1(x)f(t)\right] \tag{3.9}$$

With the condition that $\int_0^L R(x,t)W(x)dx = 0$, one obtains

$$\ddot{T}(t) + \omega^2 T(t) = \omega^2 f(t) \tag{3.10}$$

where

$$\omega^2 = \frac{\int_0^L f_1(x)W(x)dx}{m\int_0^L W^2(x)dx} \tag{3.11}$$

Here, ω is the circular frequency of the equivalent SDOF system of the beam.

The shock wave from an external explosion causes an almost instantaneous increase in pressure on nearby objects to a maximum value. This is followed by a brief positive phase during which the pressure decays back to its ambient value, and a somewhat longer but much less intense negative phase during which the pressure reverse direction. For most structures this phenomenon can be approximated using a triangular impulse loading with zero rise time and linearly decay. The parameters of this equivalent load are calibrated to match the maximum reflected pressure (p) and total reflected impulse (i) of the actual load's positive phase, so that the design duration $t_d = 2i/p$. The negative phase is neglected because it usually has little effect to the maximum response. As shown in Fig. 3.2 the dynamic loading function can be expressed in the following form

$$f(t) = \begin{cases} 1 - \dfrac{t}{t_d} & 0 \le t \le t_d \\ 0 & t > t_d \end{cases} \tag{3.12}$$

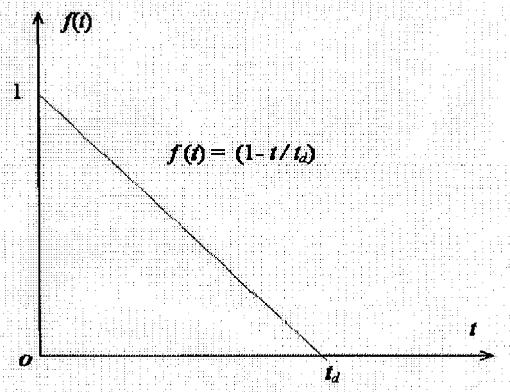

Fig. 3.2 Idealized air-blast load

The maximum reflected pressure (p) and total reflected impulse (i) can be estimated for a given combination of the standoff distance (R) and explosive charge (W) using the scaled distance parameter ($Z = R/\sqrt[3]{W}$) and published curves. Although the angle of incidence at which a blast wave strikes the building surface also influences these parameters, it is usually conservative to neglect this adjustment. The approximate value of the peak reflected overpressure may be calculated by interpolation from the values given in Table 3.1.

Table 3.1 Peak reflected overpressures (MPa) with different W-R combinations (TM5-1300, 1990)

R	100kg (TNT)	500kg(TNT)	1000kg(TNT)	2000kg(TNT)
1 m	165.8	354.5	464.5	602.9
2.5 m	34.2	89.4	130.8	188.4
5 m	6.65	24.8	39.5	60.19
10 m	0.85	4.25	8.15	14.7
15 m	0.27	1.25	2.53	5.01
20 m	0.14	0.54	1.06	2.13
25 m	0.09	0.29	0.55	1.08
30 m	0.06	0.19	0.33	0.63

Substituting Eq. (3.12) into Eq. (3.10), results in

$$\begin{cases} \omega^2 T(t) + \ddot{T}(t) = \omega^2 (1 - t/t_d) & 0 < t < t_d \\ \omega^2 T(t) + \ddot{T}(t) = 0 & t > t_d \end{cases} \qquad (3.13)$$

With initial conditions, $T(0)=0$, $\dot{T}(0)=0$, and the continuity conditions at time t_d, $T(t_d-0)=T(t_d+0)$, $\dot{T}(t_d-0)=\dot{T}(t_d+0)$, the solution of Eq. (3.13) can be determined as

$$T(t)=\begin{cases} 1-\cos\omega t-\dfrac{t}{t_d}+\dfrac{1}{\omega t_d}\sin\omega t & 0<t<t_d \\ \dfrac{1}{\omega t_d}[\sin\omega t-\sin\omega(t-t_d)]-\cos\omega t & t>t_d \end{cases} \tag{3.14}$$

The solution would be applicable until the end of elastic stage when the cross-section yields. It is known that the yield strength of mild steel depends on the strain rate. Campbell (Campbell, 1953) proposed the following relationship to express the dependence of the dynamic yield strength on the strain rate as

$$\sigma_{dy}=\sigma(\tau)$$

where σ_{dy} is the dynamic yield strength of steel and τ is called the yielding delay time which is determined from

$$\int_0^{\tau}\left[\sigma(t)\right]^{\alpha}dt=t_0 f_y^{\alpha} \tag{3.15}$$

where

t_0 = a parameter depending on temperature, which is determined from test

α = dimensionless constant, which can be determined from test

f_y = static yield strength of reinforcing steel

The constants α and t_0 in Eq. (3.15) are used to describe the mild steel property of how the yield strength of the reinforcing steel depends on the strain rate. They are also dependent on the temperature. Experiments performed by Kotlyarevskii(1961) with mild steels have shown that at normal temperature (20°C), t_0 and α take the following values

$$t_0=0.895,\quad \alpha=17 \tag{3.16}$$

In the elastic stage, the stress in the steel bar is $\sigma(t)= \sigma_p T(t)$, where σ_p is a constant and $T(t)$ is the dynamic function. With the dynamic function $T(t)$, Eq. (3.15) can be written as

$$\int_0^{\tau}\left[T(t)\right]^{17} dt = 0.895\left(f_y/\sigma_p\right)^{17} \tag{3.17}$$

Using a numerical method, the time τ (when the steel bar yields) can be calculated. The approximate formula to calculate τ is derived in Chapter 5 of this thesis.

During the period of the blast load acting on the beam, the elastic response will end at the time τ, when the steel bars yield. If the RC beam is not strengthened with FRP plates, then the plastic hinge will appear at the point where the bending moment is largest. If the RC beam is strengthened with FRP plates and the rupture strain of FRP plates is larger than the yield strain of the steel bar, the bending stiffness of the beam in the interval where the steel bar has yielded will reduce after the time τ. Therefore, the elastic response will continue but with a lower vibration frequency.

In the event of extreme blast load, the structural members exposed directly to air overpressure are expected to undergo large inelastic deformation. Key parameters that describe the full-range ductile behavior of reinforced concrete flexural members are: 1) rotational capacity of the plastic hinge, φ_u; 2) hinge length, l_y; and 3) softening slope parameter, a. Full-range analysis including post-peak behavior for the structural member without FRP reinforcement has been recommended in many seismic design guidelines such as FEMA 273/274, FEMA 356/357, FEMA 368/369, and FEMA 306/307/308. Since this study focuses on the mathematical aspects of the SDOF method, the analysis of plastic hinge is not carried out in detail and some assumptions are made to simplify the calculation of dynamic response of a structural member subjected to air-blast loading.

As shown in Fig. 3.3, it is assumed that the beam segment with yielded steel bar is considered as a rotational spring, and which joins two beam segments together.

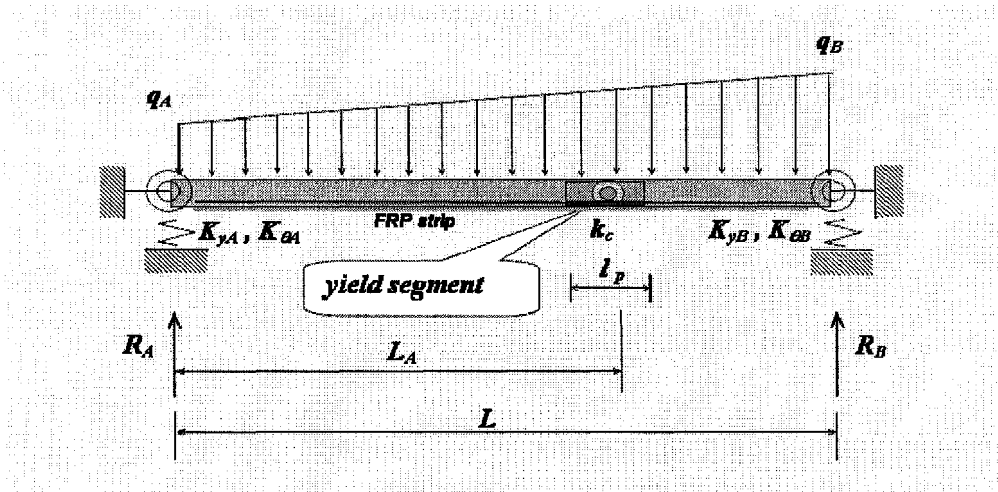

Fig. 3.3 Two beam segments joined with a rotational spring

The stiffness, k_c, of the rotation spring can be calculated with the residual bending stiffness of the cross-section and the length of yield zone in which the steel bar has yielded. It is known that FRP plate does not increase the bending stiffness of the beam significantly(refer to Sections 7.2 and 7.3 of this thesis). Therefore, the length of yield zone can be calculated from the empirical formulae of the equivalent length of the plastic hinge which were derived for the RC beam without FRP plate strengthening. Baker (Baker, 1956) proposed following two empirical formulae:

For members with unconfined concrete

$$l_p = k_1 k_2 k_3 \left(\frac{z}{d} \right)^{\frac{1}{4}} d \tag{3.18}$$

For members confined by transverse steel

$$l_p = 0.8 k_1 k_2 \left(\frac{z}{d} \right) c \tag{3.19}$$

where

k_1 = 0.7 for mild steel or 0.9 for cold-worked steel

k_2 = $1+0.5P_u/P_0$

P_u = axial compressive force in beam

P_0 = axial compressive strength of beam without bending moment

k_3 = 0.6 when $f'_c = 35.2\,N/mm^2$ or 0.9 when $f'_c = 11.7\,N/mm^2$, assuming $f'_c = 0.85\times(\text{cube strength of concrete})$

z = distance of critical section to the point of contra-flexure

d = effective depth of the beam's cross section

c = neutral axis depth at critical section

It is to be noted that l_p (in Eqs. (3.18) and (3.19)) is the equivalent plastic hinge length on the one side of the critical section. Thus a plastic hinge in the span of a symmetrically loaded beam will have a total equivalent length of $2\,l_p$.

Using the equivalent length of yield zone, the stiffness, k_c, may be calculated approximately from:

$$k_c = \begin{cases} (EI)_y/2l_p & \text{when the critical section in the span} \\ (EI)_y/l_p & \text{when the critical section at the support} \end{cases} \tag{3.20}$$

where $(EI)_y$ is the residual bending stiffness of the beam segment in the yield zone.

For convenience, we re-denote τ (the time interval between the instant of loading and the commencement of yielding, i.e., the duration of the first elastic stage of dynamic response of the beam subjected to air-blast loading) by τ_1. The dynamic deformation of the beam after time τ_1 can be written as

$$w(x,t) = pW_2(x)T_2(t) + pW_1(x)T_1(\tau_1) \tag{3.21}$$

where

$W_1(x)$ = deformation of the beam subjected to static load of $f_1(x)$

$W_2(x)$ = deformation of the two-segment beam (shown in Fig. 3.3) subjected to static load of $f_1(x)$

$T_1(t)$ = dynamic function for $t < \tau_1$

$T_2(t)$ = dynamic function for $t > \tau_1$

Substituting Eq. (3.21) into Eq. (3.1), the residual is obtained as

$$R(x,t) = p\ \left[T_2(t) f_1(x) + T_1(\tau_1) f_1(x) + m\ddot{T}_2(t) W_2(x) - f_1(x) f(t)\right]$$

With the condition that $\int_0^L R(x,t) W_2(x) dx = 0$, the following equation is obtained

$$\ddot{T}_2(t) + \omega_2^2 T_2(t) = \omega_2^2 [f(t) - T_1(\tau_1)] \qquad (3.22)$$

and

$$\omega_2^2 = \frac{\int_0^l f_1(x) W_2(x) dx}{\int m W_2^2(x) dx} \qquad (3.23)$$

with the initial conditions

$$T_2(\tau_1) = 0 \qquad (3.24)$$

and

$$\dot{T}_2(\tau_1) = \dot{T}_1(\tau_1) \int_0^L W_1(x) dx \Big/ \int_0^L W_2(x) dx \qquad (3.25)$$

where

τ_1 = duration of first elastic stage

ω_2 = vibration frequency of second elastic stage

Eq. (3.25) is derived from the condition of conservation of momentum.

From the deflection function $w_2(x,t)$, the dynamic bending moment in the beam can be calculated. When the bending moment at a cross-section increases to the value at which the steel reinforcement starts yielding or the FRP reinforcement ruptures, a new rotation spring or a plastic hinge will appear. The beam will then deform with a lower frequency. A similar procedure will continue until the beam is changed to a mechanism with three hinges, in which two are at the beam's ends and one is in the span of the beam.

It should be noted that if the $(i\text{-}1)^{th}$ ($i \geq 3$) phase of the dynamic deformation of the beam terminates due to rupture of the FRP reinforcement, the bending moment at the position where FRP reinforcement ruptures would be suddenly released. For simplicity, it is assumed that the strain energy corresponding to the dynamic deformation developed in $(i\text{-}1)^{th}$ phase is converted to the kinetic energy of the beam immediately at the time when the FRP reinforcement rupture. Therefore, with the conservation law of energy, the formula to calculate the initial value of the derivative of dynamic function, $\dot{T}_i(\tau_{i-1})$, can be derived as

$$\dot{T}_i(\tau_{i-1}) = \frac{\omega_i}{\omega_{i-1}}\sqrt{\dot{T}_{i-1}^2(\tau_{i-1}) + 2\omega_{i-1}^2 T_{i-1}^2(\tau_{i-1})}\sqrt{\int_0^L f_1(x)W_{i-1}(x)dx \Big/ \int_0^L f_1(x)W_i(x)dx}$$

The deformation of the beam in the i^{th} stage can be expressed as

$$w(x,t) = pW_i(x)T_i(t) + p\sum_{k=1}^{i-1} ik \ W_k(x)T_k(\tau_k) \tag{3.26}$$

where

$W_k(t)$ = deformation of the beam after the reinforcing steel yield at k^{th} cross-sections subjected to static load of $f_1(x)$, $k=1,2,\ldots i$

$T_k(t)$ = dynamic function of k^{th} phase of the dynamic deformation, $k=1,2,\ldots i$

ik = rupture index of k^{th} phase of the dynamic deformation

In the case that the k^{th} elastic phase of the dynamic deformation terminates due to external FRP reinforcement rupture ik takes the value of zero, while in the case that the k^{th} elastic stage terminates due to steel reinforcement yielding, then ik takes the value of 1, i.e.

$$ik = \begin{cases} 0, & \text{if } k^{th} \text{ elastic stage terminates due to FRP reinforcement rupture} \\ 1, & \text{if } k^{th} \text{ elastic stage terminates due to steel reinforcement yielding} \end{cases}$$

The frequency in the i^{th} stage can be calculated with the following formula

$$\omega_i^2 = \frac{\int_0^L f_1(x) W_i(x) dx}{\int_0^L m W_i^2(x) dx} \tag{3.27}$$

and $T_i(t)$ is determined from the equation

$$\ddot{T}_i(t) + \omega_i^2 T_i(t) = \omega_i^2 \left[f(t) - \sum_{k=1}^{i-1} ik \ T_k(\tau_k) \right] \tag{3.28}$$

with the initial conditions

$$T(\tau_{i-1}) = 0 \tag{3.29}$$

$$\dot{T}_i(\tau_{i-1}) = \dot{T}_{i-1}(\tau_{i-1}) \int_0^L W_{i-1}(x) dx \Big/ \int_0^L W_i(x) dx \tag{3.30}$$

if the i^{th} phase of the dynamic response terminates due to yielding of steel bars, or

$$\dot{T}_i(\tau_{i-1}) = \frac{\omega_i}{\omega_{i-1}} \sqrt{\frac{2\omega_{i-1}^2 U_{pi} + p^2 \left[\dot{T}_{i-1}^2(\tau_{i-1}) + 2\omega_{i-1}^2 T_{i-1}^2(\tau_{i-1}) \right] \int_0^L f_1(x) W_{i-1}(x) dx}{p^2 \int_0^L f_1(x) W_i(x) dx}} \tag{3.31}$$

if the i^{th} phase of the dynamic response terminates due to rupturing of FRP sheet. In Eq. (3.31), U_{pi} is the plastic energy dissipated during $(i-1)^{th}$ stage which can be calculated from

$$U_{pi} = pT_{i-1}(\tau_{i-1})\sum_{k=1}^{m_i} M_{pk} \left. \frac{dW_{i-1}(x)}{dx} \right|_{x=x_k-0}^{x=x_k+0} \tag{3.32}$$

where

m_i = total number of plastic hinges appeared in the beam before the time τ_{i-1} when i^{th} stage begins

M_{pk} = bending moment on k^{th} $(k=1,2,\cdots m_i)$ plastic hinge

$T_{i-1}(t)$ = dynamic function of $(i-1)^{th}$ stage of the dynamic deformation

x_k = location of k^{th} plastic hinge

The internal force in the beam in i^{th} phase of the dynamic deformation can be calculated from

$$M(x,t) = M_{pi}(x)T_i(t) + \sum_{k=1}^{i-1} ik \;\; M_{pk}(x)T_k(\tau_k) \tag{3.33}$$

$$V(x,t) = V_{pi}(x)T_i(t) + \sum_{k=1}^{i-1} ik \;\; V_{pk}(x)T_k(\tau_k) \tag{3.34}$$

where

$$M_{pk}(x) = -pEI\frac{d^2W_k(x)}{dx^2}, \quad k=1,2,\cdots i \tag{3.35}$$

$$V_{pk}(x) = -pEI\frac{d^3W_k(x)}{dx^3}, \quad k=1,2,\cdots i \tag{3.36}$$

Using the initial conditions of Eqs. (3.29) and (3.30) or (3.31), the solution of Eq. (3.28) can be obtained as

$$T_i(t) = 1 - \frac{t}{t_d} - \left(1 - \frac{\tau_{i-1}}{t_d}\right)\cos\omega_i(t-\tau_{i-1}) + \frac{1}{\omega_i}\left(\dot{T}_i(\tau_{i-1}) + \frac{1}{t_d}\right)\sin\omega_i(t-\tau_i) \tag{3.37}$$

When three plastic hinges developed in the span of the beam, the beam will be a free movable mechanism. In case that the vertical stiffness of the supports at both the beam's end are very large, the vertical displacements of the beam's ends would be very small compared to the plastic deformation of the beam. Thus the end displacement could be neglected. The beam in this plastic stage is shown in Fig. 3.4.

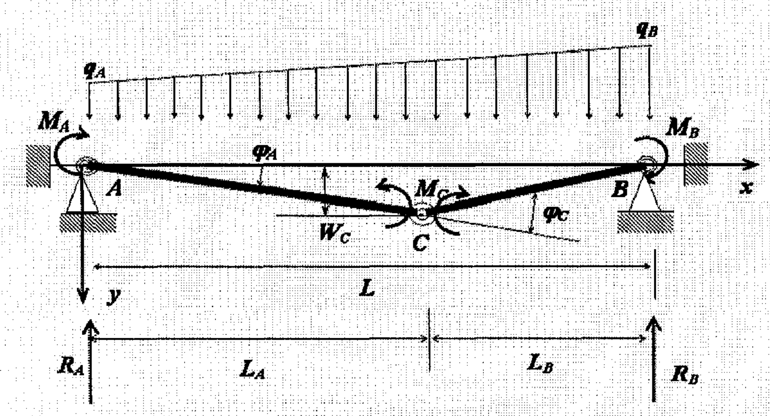

Fig. 3.4 Two beam segments joined with a plastic hinge

The deformation of the beam in the plastic stage can then be expressed as

$$w(x,t) = pW_p(x)T_p(t) + p\sum_{k=1}^{n} ik \; W_k(x)T_k(\tau_k) \tag{3.38}$$

where n is the total number of the elastic deformation stages before the plastic deformation stage and

$$W_p(x) = \begin{cases} x & 0 < x < L_A \\ \dfrac{L-x}{L-L_A} L_A & L_A < x < L \end{cases} \tag{3.39}$$

Substituting Eqs. (3.38) and (3.39) into Eq. (3.1), the residual is obtained in the form

$$R(x,t) = p\left[f_1(x)\sum_{k=1}^{n} ik \; T_k(\tau_k) + m\ddot{T}_p(t)W_p(x) - f_1(x)f(t) \right]$$

With the condition that $\int_0^L R(x,t)W_p(x)dx = 0$, the differential equation to determine dynamic function $T_p(t)$ of the plastic stage is obtained as

$$\ddot{T}_p(t) = \omega_p^2\left[f(t) - \sum_{k=1}^{n} ik\, T_k(\tau_k)\right], \qquad \tau_n < t < t_d \tag{3.40}$$

where

$$\omega_p^2 = \int_0^L f_1(x)W_p(x)dx \Big/ \int_0^L mW_p^2(x)dx = \frac{1}{m}\left(\frac{3-\alpha}{2L_A} + \frac{\alpha}{L}\right) \tag{3.41}$$

$$\alpha = \frac{q_B - q_A}{q_B + q_A}$$

Similar to Eqs. (3.29) and (3.30) or (3.31), the initial conditions can be expressed as

$$T_p(\tau_n) = 0 \tag{3.42}$$

and

$$\dot{T}_p(\tau_n) = \dot{T}_n(\tau_n)\frac{\int_0^L W_n(x)dx}{\int_0^L W_p(x)dx} = \frac{2\dot{T}_n(\tau_n)}{LL_A}\int_0^L W_n(x)dx \tag{3.43}$$

if last elastic stage terminates due to yielding of steel reinforcement or

$$\dot{T}_p(\tau_n) = \frac{\omega_p}{\omega_n}\sqrt{\frac{6}{L_A}}\sqrt{\frac{2\omega_n^2 U_{pp} + p^2\left[\dot{T}_n^2(\tau_n) + 2\omega_n^2 T_n^2(\tau_n)\right]\int_0^L f_1(x)W_n(x)dx}{p^2\left[3L + \alpha(L_A - L_B)\right]}} \tag{3.44}$$

if last elastic stage terminates due to rupturing of FRP plate. In Eq. (3.44), U_{pp} is the plastic energy dissipated during n^{th} stage which can be calculated from

$$U_{pp} = pT_n(\tau_n)\sum_{k=1}^{m_p} M_{pk}\left.\frac{dW_n(x)}{dx}\right|_{x=x_k-0}^{x=x_k+0} \tag{3.45}$$

where

m_p = total number of plastic hinges appeared in the beam before the time τ_n when plastic stage begins

M_{pk} = bending moment on k^{th} $(k=1,2,\cdots m_p)$ plastic hinge

$T_n(t)$ = dynamic function of n^{th} phase of the dynamic deformation

x_k = location of k^{th} plastic hinge

For $\tau_n < t < t_d$, substituting Eq. (3.12) into Eq. (3.40) and integrating twice with respect to t, the following results are obtained

$$\dot{T}_p(t) = -\frac{\omega_p^2(t-\tau_n)}{2t_d}\left((t-\tau_n)+2t_d\sum_{k=1}^{n} ik\ T_k(\tau_k)-2(t_d-\tau_n)\right)+\dot{T}_p(\tau_n) \quad (3.46)$$

$$T_p(t) = -\frac{\omega_p^2(t-\tau_n)^2}{6t_d}\left[(t-\tau_n)+3t_d\sum_{k=1}^{n} ik\ T_k(\tau_k)-3(t_d-\tau_n)\right]+\dot{T}_p(\tau_n)(t-\tau_n) \quad (3.47)$$

The time when $T_p(t)$ is a maximum value can be obtained by solving the following equation

$$-\frac{\omega_p^2(t-\tau_n)}{2t_d}\left((t-\tau_n)+2t_d\sum_{k=1}^{n} ik\ T_k(\tau_k)-2(t_d-\tau_n)\right)+\dot{T}_p(\tau_n)=0$$

That is

$$t_m = t_d\left\{1-\sum_{k=1}^{n} ik\ T_k(\tau_k)+\sqrt{\left(1-\frac{\tau_n}{t_d}-\sum_{k=1}^{n} ik\ T_k(\tau_k)\right)^2+\frac{2\dot{T}_p(\tau_n)}{t_d\omega_p^2}}\right\} \quad (3.48)$$

It is possible that t_m obtained from Eq. (3.48) is greater than t_d. For $t > t_d$ the dynamic function $T_p(t)$ can be determined from

$$\ddot{T}_{p1}(t) = -\omega_p^2\sum_{k=1}^{n} ik\ T_k(\tau_k), \qquad t > t_d \quad (3.49)$$

Integrating Eq. (3.49) the following equations are obtained

$$\dot{T}_{p1}(t) = -\omega_p^2 (t - t_d) \sum_{k=1}^{n} ik \;\; T_k(\tau_k) + \dot{T}_p(t_d), \qquad t > t_d \tag{3.50}$$

$$T_{p1}(t) = -\frac{\omega_p^2 (t - t_d)^2}{2} \sum_{k=1}^{n} ik \;\; T_k(\tau_k) + \dot{T}_p(t_d)(t - t_d) + T_p(t_d), \qquad t > t_d \tag{3.51}$$

where $\dot{T}_p(t_d)$ and $T_p(t_d)$ are calculated from Eq. (3.46) and (3.47) respectively.

With the condition $\dot{T}_{p1}(t) = 0$, the time when $T_{p1}(t)$ reaches its maximum value can be calculated from Eq. (3.50) as

$$t_m = t_d + \frac{\dot{T}_p(t_d)}{\omega_p^2 \sum_{k=1}^{n} ik \;\; T_k(\tau_k)} \tag{3.52}$$

The maximum open angle of the crack at point C (see Fig. 3.4) can then be calculated by

$$\varphi_C = \frac{w_p(L_A, t_m) L}{L_B L_A} = \frac{pL}{L_A L_B}\left[L_A T_p(t_m) + \sum_{k=1}^{n} ik \;\; W_k(L_A) T_k(\tau_k) \right] \tag{3.53}$$

3.1.2 Continuous RC beam loaded by static axial force

The analysis procedure can be generalized to the analysis of a continuous beam. As shown in Fig. 3.5, a continuous beam is subjected to combined static axial forces and air-blast loading.

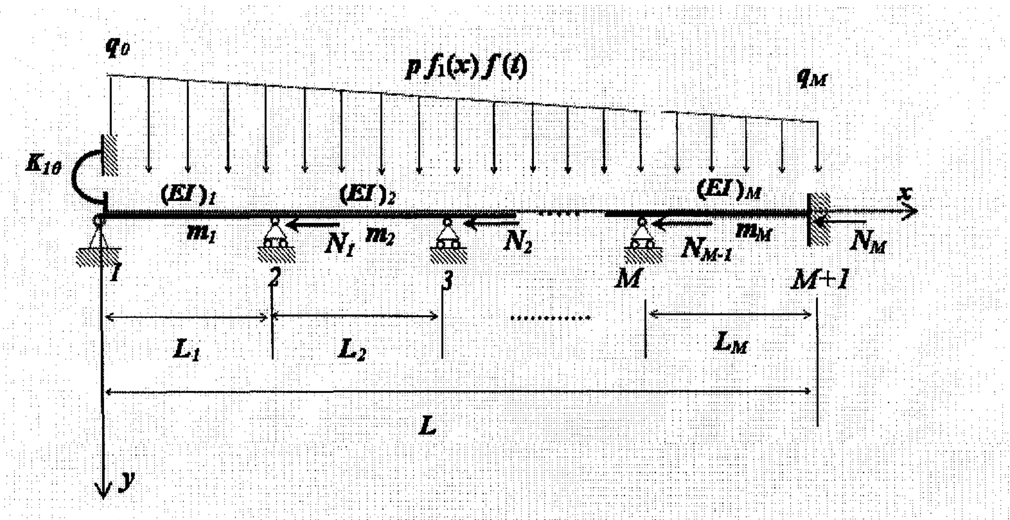

Fig. 3.5 Continuous beam loaded by both axial force and air-blast loading

The differential equation of this problem can be written as

$$EI(x)\frac{\partial^4 w(x,t)}{\partial x^4} + N(x)\frac{\partial^2 w(x,t)}{\partial x^2} + m(x)\frac{\partial^2 w(x,t)}{\partial t^2} = pf_1(x)f(t) \quad (3.54)$$

The initial and boundary conditions of this problem are

$$w(x,t)\big|_{t=0} = 0 \quad (3.55)$$

$$\left.\frac{dw(x,t)}{dt}\right|_{t=0} = 0 \quad (3.56)$$

$$w(x,t)\big|_{x=y_i} = 0 \quad i = 1,2,\cdots,M+1 \tag{3.57}$$

$$\left[K_{1\theta}\frac{\partial w(x,t)}{\partial x} + EI(x)\frac{\partial^2 w(x,t)}{\partial x^2}\right]_{x=0} = 0 \tag{3.58}$$

$$\frac{\partial w(x,t)}{\partial x}\bigg|_{x=L} = 0 \tag{3.59}$$

where $K_{1\theta}$ is the rotational supporting stiffness at joint 1 and M is the total number of spans of the continuous beam (See Fig. 3.5).

The dynamic deformation of this continuous beam can be expressed as

$$w(x,t) = pW(x)T(t) \tag{3.60}$$

$$p = \frac{1}{2}(q_0 + q_M) \tag{3.61}$$

Values of q_0 and q_M are the magnitudes of the overpressures of the blast loading at the continuous beam's left and right ends respectively. The function $W(x)$ is the deformation of the continuous beam subjected to the static load $f_1(x)$, which is assumed to be a linear function and can be expressed as

$$f_1(x) = \frac{1}{p}\left[q_M + \frac{L-x}{L}(q_0 - q_M)\right] = 1 - a + \frac{2x}{L}a \tag{3.62}$$

$$a = \frac{q_M - q_0}{q_M + q_0} \tag{3.63}$$

Substituting Eq. (3.60) into Eq. (3.54), the residual is obtained in the following form

$$R(x,t) = pT(t)\left[f_1(x) + N(x)\frac{dW(x)}{dx}\right] + pm(x)W(x)\ddot{T}(t) - pf_1(x)f(t)$$

With the condition $\int_0^L R(x,t)W(x)dx = 0$, the following equation is obtained

$$\omega^2 T(t) + \ddot{T}(t) = \gamma^2 f(t) \tag{3.64}$$

where

$$\omega^2 = \frac{\int_0^L W(x) f_1(x) dx - \sum_{k=1}^{M} \overline{N}_k \int_{y_{k-1}}^{y_k} \left(\frac{dW(x)}{dx} \right)^2 dx}{\int_0^L m W^2(x) dx} \tag{3.65}$$

$$\gamma^2 = \frac{\int_0^L W(x) f_1(x) dx}{\int_0^L m W^2(x) dx} \tag{3.66}$$

$$\overline{N}_i = \sum_{k=i}^{M} N_k$$

$$y_i = \sum_{k=1}^{i} L_k \quad , \quad i = 1, 2, \cdots, M$$

The initial conditions as shown in Eq. (3.56) is reduced to the following form

$$\begin{cases} T(0) = 0 \\ \dot{T}(0) = 0 \end{cases} \tag{3.67}$$

Solving Eq. (3.64), the dynamic function $T(t)$ can be obtained and then the dynamic deformation can be calculated from Eq. (3.60). If the loading function $f(t)$ is given by Eq. (3.12), the solution of Eq. (3.64) is

$$T(t) = \eta \begin{cases} 1 - \cos \omega t - \dfrac{t}{t_d} + \dfrac{1}{\omega t_d} \sin \omega t & 0 < t < t_d \\ \dfrac{1}{\omega t_d} \left[\sin \omega t - \sin \omega (t - t_d) \right] - \cos \omega t & t > t_d \end{cases} \tag{3.68}$$

where

$$\eta = \frac{\gamma^2}{\omega^2} = \frac{\int_0^L W(x) f_1(x) dx}{\int_0^L W(x) f_1(x) dx - \sum_{k=1}^{M} \bar{N}_k \int_{y_{k-1}}^{y_k} \left(\frac{dW(x)}{dx} \right)^2 dx} \tag{3.69}$$

The coefficient η is an amplification factor to take account of the static axial force effect. If the dynamic function is still expressed by Eq. (3.14), the dynamic response of the continuous beam should be represented as

$$w(x,t) = p\eta W(x) T(t) \tag{3.70}$$

As the dynamic deformation increase, the cross-section at some supporting joints will yield. Because the continuous beam is loaded with static axial forces, Eq. (3.17)should be modified to take account of the effect of these axial forces on the yielding delay time. The equation to determine the yielding delay time of the steel reinforcement in this problem may be written in the following form

$$\int_0^\tau T^{17}(t) dt = 0.895 \left(\frac{f_y + \sigma_N}{\sigma_p} \right)^{17} \tag{3.71}$$

where σ_N is the compressive stress in the steel reinforcement caused by the axial force, which can be calculated from:

$$\sigma_N = \frac{E_s}{E_c} \frac{N}{bh + \frac{E_s}{E_c} \bar{A}_s} \tag{3.72}$$

where

E_c = Young's modulus of concrete

E_s = Young's modulus of the steel reinforcement

N = axial force in the beam

h = height of cross-section

b = width of cross-section

$\bar{A}_s$ = the total area of the steel reinforcement

After the plastic hinges appear at the positions of some supporting joints, the continuous beam will be decomposed into several single span beams and a continuous beam with fewer spans. The response of these single span beams can then be calculated separately, while the continuous beam with fewer spans can be calculated with the formulae derived above. As shown in Fig. 3.6, after the plastic hinge appears at the supporting joint 2, the first span of the continuous beam can be analysed as a single span beam.

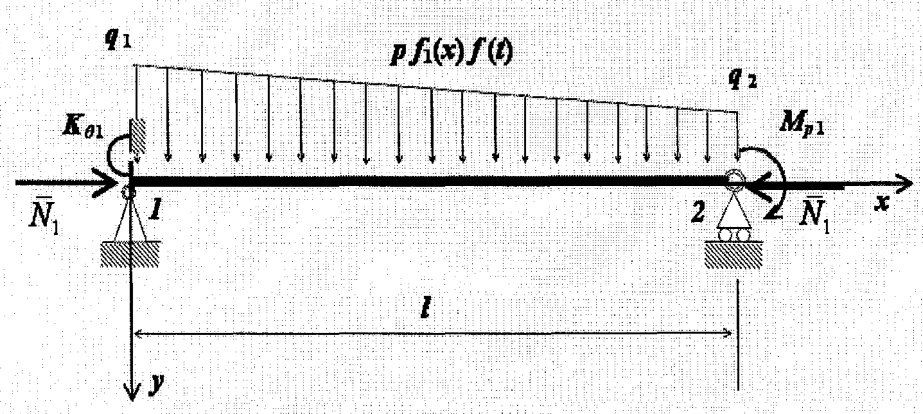

Fig. 3.6 Single span beam loaded by both axial force and air blast loading

The dynamic deformation of this single span beam can be expressed as

$$w(x,t) = p\eta_2 W_2(x) T_2(t) + p\eta_1 W_1(x) T_1(\tau_1) \tag{3.73}$$

The partial deferential equation of this single span beam can be written as

$$\begin{aligned} &\eta_2 T_2(t)\left[f_1(x) + \bar{N}_1 \frac{d^2 W_2(x)}{dx^2} \right] + \eta_2 m W_2(x) \ddot{T}_2(t) \\ &= f_1(x)\left[f(t) - \eta_1 T_1(\tau_1) \right] - \bar{N} \frac{dW_2(x)}{dx^2} \frac{dW_1(x)}{dx^2} \eta_1 T_1(\tau_1) \end{aligned} \tag{3.74}$$

With weighted residual method, one can obtain the govening equation of the SDOF system of this single span beam of the form

$$\eta_2\omega_2^2T_2(t)+\eta_2\ddot{T}_2(t)=\gamma_2^2\left[f(t)-\eta_1T_1(\tau_1)\left(1-\frac{c_{12}}{\gamma_2^2}\right)\right] \tag{3.75}$$

where $T_1(t)$ is the dynamic function of the first response stage of the continuous beam and τ_1 is the time when the plastic hinge appears at the supporting joint 2 of the continuous beam as shown in Fig. 3.5. The frequency ω_2 and the parameters γ_2 and c_{12} are calculated from

$$\omega_2^2=\frac{\int_0^l W_2(x)f_1(x)dx-\bar{N}_1\int_0^l\left(\frac{dW_2(x)}{dx}\right)^2dx}{\int_0^l m\ W_2^2(x)dx} \tag{3.76}$$

$$\gamma_2^2=\frac{\int_0^{L_1}W_2(x)f_1(x)dx}{\int_0^{L_1}mW_2^2(x)dx} \tag{3.77}$$

$$c_{12}=\bar{N}_1\int_0^l\frac{dW_1(x)}{dx}\frac{dW_2(x)}{dx}dx \tag{3.78}$$

where

$$\bar{N}_1=\sum_{k=1}^{M}N_k$$

In the elastic stage, the value of c_{12} is very small and negligible.

The initial values of the dynamic function $T_2(t)$ and its derivative can be calculated from the following equations

$$T_2(\tau_1)=0 \tag{3.79}$$

$$\dot{T}_2(\tau_1)=\dot{T}_1(\tau_1)\frac{\eta_1\int_0^l W_1(x)dx}{\eta_2\int_0^l W_2(x)dx} \tag{3.80}$$

where $W_1(x)$ is the static deformation of the continuous beam in the first span.

With the intial conditions given by Eq. (3.79) and Eq. (3.80), the differential equation (3.75) can be solved and the dynamic deformation can be calculated from Eq. (3.73). As the dynamic deformation increase, the steel reinforcement will yield at the cross-section where the bending moment is largest in the beam. The yielding delay time when a cross-section in the span yields can be obtained by solving Eq. (3.71).

After the plastic hinge appears in the span the beam is changed to a free movable mechanism as shown in Fig. 3.7.

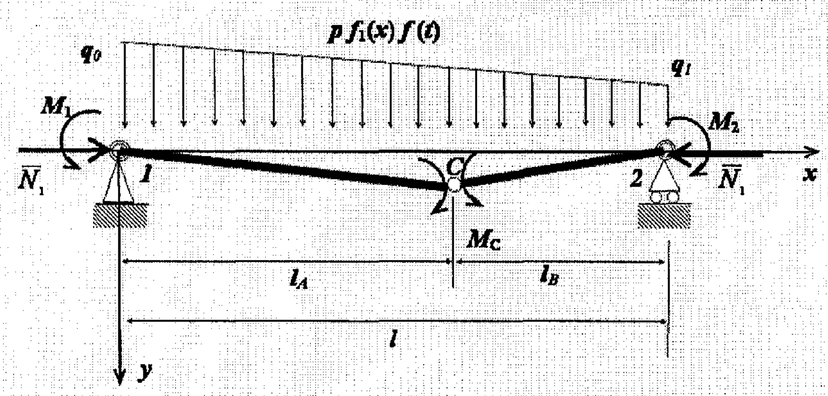

Fig. 3.7 Two beam segments joined with a plastic hinge and loaded by both axial force and air-blast loading

The differential equation of this problem can be written in the following form

$$EI\frac{\partial^4 w_p(x,t)}{\partial x^4}+\bar{N}_1\frac{\partial^2 w_p(x,t)}{\partial x^2}+m\frac{\partial^2 w_p(x,t)}{\partial t^2}=pf_1(x)f(t) \tag{3.81}$$

The deformation of the beam in the plastic stage can be expressed as

$$w_p(x,t)=pW_p(x)T_p(t)+p\sum_{i=1}^{n}W_i(x)\eta_i T_i(\tau_i) \tag{3.82}$$

where n is the total number of the dynamic deformation stages before the plastic hinge appears in the span and

$$\eta_i=\gamma_i^2/\omega_i^2$$

$$\omega_i^2=\frac{\int_0^l W_i(x)f_1(x)dx-\bar{N}_1\int_0^l\left(\frac{dW_i(x)}{dx}\right)^2dx}{\int_0^l m\ W_i^2(x)dx}$$

$$\gamma_i^2=\int_0^{L_1}W_i(x)f_1(x)dx\Big/\int_0^{L_1}mW_i^2(x)dx$$

$$W_p(x)=\begin{cases}x & 0<x<l_A\\ \dfrac{l-x}{l-l_A}l_A & l_A<x<l\end{cases} \tag{3.83}$$

Substituting Eqs. (3.82) and (3.83) into Eq. (3.81), the residual is obtained as:

$$R(x,t)=\Bigg[pf_1(x)\sum_{i=1}^{n}\eta_i T_i(\tau_i)$$
$$+\bar{N}_1\left(\frac{d^2W_p(x)}{dx^2}T_p(t)+\sum_{i=1}^{n}\frac{d^2W_i(x)}{dx^2}\eta_i T_i(\tau_i)\right)+m\ddot{T}_p(t)W_p(x)-f_1(x)f(t)\Bigg]$$

With the condition that $\int_0^l R(x,t)W_p(x)dx=0$, one obtains the differential equation to determine dynamic function $T_p(t)$ of the plastic stage

$$-\omega_p^2T_p(t)+\ddot{T}_p(t)=\gamma_p^2\left[f(t)-\sum_{i=1}^{n}\eta_i T_i(\tau_i)\right]+\bar{N}_1\sum_{i=1}^{n}\beta_i T_i(\tau_i),\qquad \tau_n<t<t_d \tag{3.84}$$

where

$$\omega_p^2 = \frac{\overline{N}_1 \int_0^l \left(\frac{dW_p(x)}{dx} \right)^2 dx}{\int_0^l mW_p^2(x)} = \frac{3\overline{N}_1}{ml_A l_B} \tag{3.85}$$

$$\gamma_p^2 = \frac{\int_0^l f_1(x) W_p(x) dx}{\int_0^l mW_p^2(x) dx} = \frac{1}{m}\left(\frac{3-\alpha}{2l_A} + \frac{\alpha_1}{l} \right) \tag{3.86}$$

$$\beta_i = -\frac{l}{l_B} \eta_i W(l_A) \tag{3.87}$$

$$\alpha_1 = (q_1 - q_0)/(q_1 + q_0)$$

The initial conditions can be expressed as

$$T_p(\tau_n) = 0 \tag{3.88}$$

and

$$\dot{T}_p(\tau_n) = \dot{T}_n(\tau_n) \frac{\eta_n \int_0^l W_n(x) dx}{\int_0^l W_p(x) dx} = \frac{2\eta_n \dot{T}_n(\tau_n)}{l_A l} \int_0^l W_n(x) dx \tag{3.89}$$

The solution of Eq. (3.84) is

$$T_p(t) = A\exp\left[\omega_p (t-\tau_n)\right] + B\exp\left[-\omega_p (t-\tau_n)\right]$$
$$-\frac{\gamma_p^2}{\omega_p^2}\left[1 - \frac{t}{t_d} - \sum_{i=1}^{n} \eta_i T_i(\tau_i)\right] - \frac{\overline{N}_1}{\omega_p^2}\sum_{i=1}^{n} \beta_i T_i(\tau_i), \qquad \tau_n < t < t_d \tag{3.90}$$

With the initial conditions of Eqs. (3.88) and (3.89) the constants A and B can be determined by solving the linear system consisting of

$$A + B = \frac{\gamma_p^2}{\omega_p^2}\left[1 - \frac{\tau_n}{t_d} - \sum_{i=1}^{n} \eta_i T_i(\tau_i)\right] + \frac{\overline{N}_1}{\omega_p^2}\sum_{i=1}^{n} \beta_i T_i(\tau_i)$$

and

$$A-B=\frac{1}{\omega_p}\left[\dot{T}_p(\tau_n)-\frac{\gamma_p^2}{t_d\omega_p^2}\right].$$

The formulae to calculate values of A and B are obtained as

$$A=\frac{1}{2}\frac{\gamma_p^2}{\omega_p^2}\left\{1-\frac{\tau_n}{t_d}-\sum_{i=1}^{n}\eta_i T_i(\tau_i)-\frac{1}{\omega_p t_d}+\frac{\bar{N}_1}{\gamma_p^2}\sum_{i=1}^{n}\beta_i T_i(\tau_i)+\frac{\omega_p}{\gamma_p^2}\dot{T}_p(\tau_n)\right\} \tag{3.91}$$

$$B=\frac{1}{2}\frac{\gamma_p^2}{\omega_p^2}\left\{1-\frac{\tau_n}{t_d}-\sum_{i=1}^{n}\eta_i T_i(\tau_i)+\frac{1}{\omega_p t_d}+\frac{\bar{N}_1}{\gamma_p^2}\sum_{i=1}^{n}\beta_i T_i(\tau_i)-\frac{\omega_p}{\gamma_p^2}\dot{T}_p(\tau_n)\right\} \tag{3.92}$$

The time when the plastic deformation reaches its maximum value can be obtained by solving

$$\dot{T}_p(t)=\omega_p\{A\exp[\omega_p(t-\tau_n)]-B\exp[-\omega_p(t-\tau_n)]\}+\frac{\gamma_p^2}{t_d\omega_p^2}=0 \tag{3.93}$$

i.e.

$$t_m=\tau_n+\frac{1}{\omega_p}\ln\left\{\frac{1}{2\omega_p A}\left[-\frac{1}{t_d}\frac{\gamma_p^2}{\omega_p^2}\pm\sqrt{\left(\frac{1}{t_d}\frac{\gamma_p^2}{\omega_p^2}\right)^2+4\omega_p^2 AB}\right]\right\} \tag{3.94}$$

It is possible that t_m, calculated from Eq. (3.94), is greater than t_d. It should be noticed that Eqs. (3.84) and (3.94) are applicable for $t>t_d$. For $t>t_d$ the dynamic function $T_p(t)$ shall be determined from the following equation

$$-\omega_p^2 T_p(t)+\ddot{T}_p(t)=-\gamma_p^2\sum_{i=1}^{n}\eta_i T_i(\tau_i)+\bar{N}_1\sum_{i=1}^{n}\beta_i T_i(\tau_i), \qquad t>t_d \tag{3.95}$$

The solution of Eq. (3.95) is

$$T_p(t)=C\exp[\omega_p(t-t_d)]+D\exp[-\omega_p(t-t_d)] +\frac{\gamma_p^2}{\omega_p^2}\sum_{i=1}^{n}\eta_i T_i(\tau_i)-\frac{\bar{N}_1}{\omega_p^2}\sum_{i=1}^{n}\beta_i T_i(\tau_i), \qquad t>t_d \tag{3.96}$$

where C and D are determined from the following equations

$$C+D=A\exp\left[\omega_p\left(t_d-\tau_n\right)\right]+B\exp\left[-\omega_p\left(t_d-\tau_n\right)\right] \tag{3.97}$$

$$C-D=A\exp\left[\omega_p\left(t_d-\tau_n\right)\right]-B\exp\left[-\omega_p\left(t_d-\tau_n\right)\right]+\gamma_p^2/t_d\omega_p^3 \tag{3.98}$$

Solving the linear system composed of Eqs. (3.97) and (3.98), the formulae to calculate the values of C and D are obtained as

$$C=A\exp\left[\omega_p\left(t_d-\tau_n\right)\right]+\gamma_p^2/2t_d\omega_p^3 \tag{3.99}$$

$$D=B\exp\left[-\omega_p\left(t_d-\tau_n\right)\right]-\gamma_p^2/2t_d\omega_p^3 \tag{3.100}$$

The time when the plastic deformation reaches its maximum value can be obtained by solving

$$C\exp\left[\omega_p\left(t-\tau_n\right)\right]-D\exp\left[-\omega_p\left(t-\tau_n\right)\right]=0 \tag{3.101}$$

i.e.

$$t_m=t_d+\frac{1}{2\omega_p}\ln\frac{D}{C} \tag{3.102}$$

The maximum plastic displacement can then be calculated from

$$w_p\left(l_A,t_{\mathrm{m}}\right)=pl_AT_p\left(t_{\mathrm{m}}\right)+p\sum_{i=1}^{n}\eta_iW_i\left(l_A\right)T_i\left(\tau_i\right) \tag{3.103}$$

and

$$\varphi_C=\frac{w_p\left(l_A,t_{\mathrm{m}}\right)l}{l_Bl_A}=\frac{pl}{l_Al_B}\left[l_AT_p\left(t_{\mathrm{m}}\right)+\sum_{i=1}^{n}\eta_iW_i\left(l_A\right)T_i\left(\tau_i\right)\right] \tag{3.104}$$

3.2 Deformation mode and frequency of the equivalent SDOF system of beams subjected to air-blast loading

As discussed in Section 3.1, the procedure to analyse and to design a blast resistant RC beam strengthened by FRP plate/sheet can be described as follows:

1. provide the initial design parameters for the beam and set $i = 1$.
2. calculate the deformation, $W_i(x)$, of the beam subjected to static load with the same distribution of the air overpressure on the beam.
3. calculate the circular frequency, ω_i, of the equivalent SDOF system of the beam from Eq. (3.27).
4. solve the Eq. (3.28) to obtain the dynamic function, $T_i(t)$ of the i^{th} elastic stage.
5. calculate the deformation and internal force of beam in i^{th} response stage.
6. with the predefined criteria (see Chapters 5 and 6), calculate the time when a cross-section in the beam fails or partially fails.
7. if the steel reinforcement yields while the FRP plate/sheet does not rupture in a cross-section, insert a rotational spring at the position of the cross-section. If the FRP plate has ruptured, insert a plastic hinge at the position of the cross-section.
8. determine whether the beam with the plastic hinge is a free movable mechanism or not. If it is a free movable mechanism, go to step 9. If it is not a free movable mechanism, set $i = i + 1$, go to step 2.
9. calculate plastic response.

10. if the requirements on design of the beam are satisfied, the analysis and design are completed, otherwise modify the design parameters, set $i=1$ and go to step 2.

This section focuses on the derivations of the formulae to calculate the static deformation and the related integrations for beams with different supporting conditions. The formulae relating to a continuous beam loaded with axial force are also derived in the section.

3.2.1 Single span RC beams strengthened with FRP plate/sheet

The static beam deformation can be obtained by solving the corresponding static problem shown in Fig. 3.1. In practice, the beam or one-way slab to be designed may have different boundary conditions and continuous supports as in multiple spans. In order to simplify the design of the computer routine, it is convenient to express the beam deformation in the following form (Clough, 1996)

$$W(x)=v_A\phi_1(s)+\theta_A L\phi_2(s)+v_B\phi_3(s)+\theta_B L\phi_4(s)+v_P\phi_5(s,a) \qquad (3.105)$$

where

$$\phi_1(s)=1-3s^2+2s^3$$

$$\phi_2(s)=-s+2s^2-s^3$$

$$\phi_3(s)=3s^2-2s^3$$

$$\phi_4(s)=s^2-s^3$$

$$\phi_5(s,a)=s^2(s-1)^2(2as+5-a)$$

$$a=(q_B-q_A)/(q_B+q_A)$$

$$s=x/L$$

$v_P = L^4/120EI$

and

v_A = vertical displacement of beam's left end

θ_A = rotational displacement of beam's left end

v_B = vertical displacement of beam's right end

θ_B = rotational displacement of beam's right end

The positive directions of the joint displacement v_A, θ_A, v_B, and θ_B are defined in Fig. 3.8.

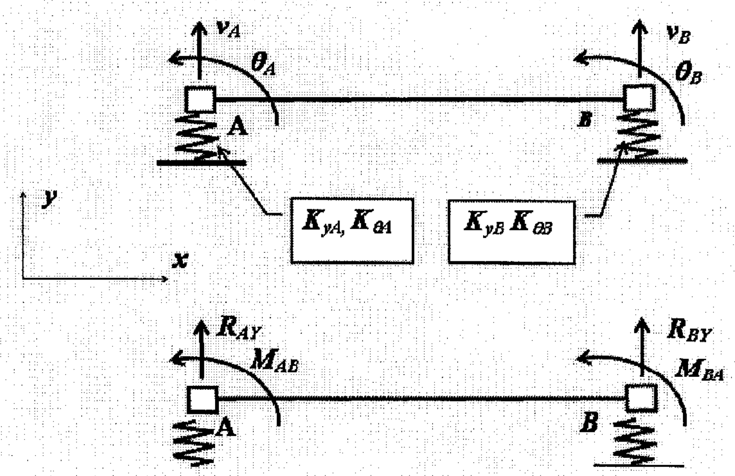

Fig. 3.8 Displacements and forces at ends of a beam

Functions $\phi_i(s),(i=1,2,3,4)$ in Eq. (3.105) are called shape functions corresponding to v_A, θ_A, v_B, and θ_B , respectively, the same as that used in finite element method (Klus-Jurgen Bathe, 1996), while $\phi_5(s)$ is the deflection of the beam with both ends fixed as shown in Fig. 3.9.

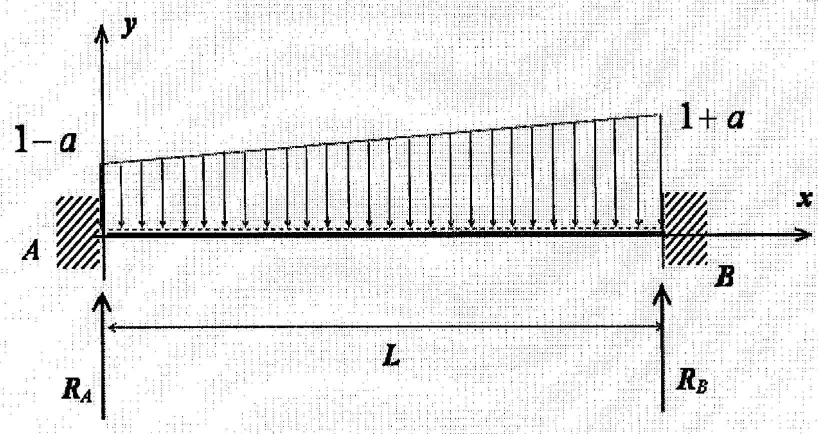

Fig. 3.9 Linearly distributed loading on a fixed beam

The equations to determine the values of v_A, θ_A, v_B, and θ_B can then be written in matrix form

$$\begin{bmatrix} 12+k_{ya} & -6 & -12 & 6 \\ -6 & 4+k_{a} & -6 & 2 \\ -12 & -6 & 12+k_{yb} & 6 \\ 6 & 2 & 6 & 4+k_{\theta b} \end{bmatrix} \begin{Bmatrix} v_A \\ L\theta_A \\ v_B \\ L\theta_B \end{Bmatrix} = -\frac{L^4}{120EI} \begin{Bmatrix} 12(5-a) \\ 10-a \\ 12(5+a) \\ -10-a \end{Bmatrix} \tag{3.106}$$

where

$$k_{\theta a} = \frac{L}{EI} K_{\theta A} \text{ , } k_{ya} = \frac{L^3}{EI} K_{yA} \text{ , } k_{\theta b} = \frac{L}{EI} K_{\theta B} \text{ , } k_{yb} = \frac{L^3}{EI} K_{yB}$$

and (see Fig. 3.8)

K_{yA} = vertical stiffness of elastic support at beam's left end

$K_{\theta A}$ = rotational stiffness of elastic support at beam's left end

K_{yB} = vertical stiffness of elastic support at beam's right end

$K_{\theta B}$ = rotational stiffness of elastic support at beam's right end

R_{AY} = vertical force acting at beam's left end

M_{AB} = moment acting at beam's left end

R_{BY} = vertical force acting at beam's left end

M_{BA} = moment acting at beam's right end

Solving Eq. (3.106), the displacements of the beam's ends can be obtained as

$$v_A = \frac{-L^4}{10EI\,D}\{[5(p_0+4s_0+d_0+12)-a(2p_0+7s_0+20)]k_{yb}+120(p_0+s_0)\} \quad (3.107)$$

$$\theta_A = \frac{-L^3}{60DEI}\{[5(p_y+12s_y+36d_y)-a(p_y-60s_y)](k_{\theta b}+2)+20(p_y-6s_y)\} \quad (3.108)$$

$$v_B = \frac{-L^4}{10DEI}\{[5(p_0+4s_0-d_0+12)+a(2p_0+7s_0+20)]k_{ya}+120(p_0+s_0)\} \quad (3.109)$$

$$\theta_B = \frac{-L^3}{60DEI}\{[-5(p_y+6s_y-36d_y)-a(p_y-60s_y)](k_{\theta a}+2)-20(p_y-6s_y)\} \quad (3.110)$$

where

$s_0 = k_{\theta a} + k_{\theta b}$

$d_0 = k_{\theta a} - k_{\theta b}$

$p_0 = k_{\theta a} k_{\theta b}$

$s_y = k_{ya} + k_{yb}$

$d_y = k_{ya} - k_{yb}$

$$p_y = k_{ya} k_{yb}$$

$$D = (p_0 + 4s_0 + 12)p_y + 12(p_0 + s_0)s_y$$

Substituting Eq. (3.105) into Eq. (3.27) and calculating the integrations, the formula of the frequency ω can be obtained as

$$\omega = \sqrt{\frac{33}{m}}\sqrt{\frac{D_1}{D_2}} \tag{3.111}$$

where

$$D_1 = 42(5-2a)v_A - 7(5-a)L\theta_A + 42(5+2a)v_B + 7(5+a)L\theta_B + 2(35+a^2)v_P$$

$$\begin{aligned} D_2 = &\left(132\theta_A^2 - 198\theta_A\theta_B + 132\theta_B^2\right)L^2 + [1452v_A + 858v_B + (495-11a)v_P]L\theta_A \\ &- [858v_A + 1452v_B + (495+11a)v_P]L\theta_B + \left(5148v_A^2 + 3564v_Av_B + 5148v_B^2\right) \\ &+ [(2310-88a)v_A + (2310+88a)v_B]v_P + \left(2a^2+550\right)v_P^2 \end{aligned}$$

The bending moment, M, and shear force, V, in the span of the beam can be calculated from the following equations

$$\begin{aligned} M(x) = -\frac{EI}{L^2}\{ &v_A(12s-6) + \theta_A L(6s-4) + v_B(6-12s) + \theta_B L(6s-2) \\ &+ v_p\left[40as^3 - 60(a-1)s^2 + 12(2a-5)s - 2(a-5)\right]\} \end{aligned} \tag{3.112}$$

$$V(x) = -\frac{6EI}{L^3}\{2v_A + L\theta_A - 2v_B + L\theta_B + 2v_p[10s(as-a+1) + 2a - 5]\} \tag{3.113}$$

where

$$s = x/L$$

The maximum bending moment in the beam span is at the position

$$x_m = \frac{L}{2}\left(1 - \frac{1}{a} \pm \sqrt{\frac{1}{5} + \frac{1}{a^2} - \frac{1}{5av_p}(\theta_A L + \theta_B L + 2v_A - 2v_B)}\right) \tag{3.114}$$

Especially, for $a = 0$

$$x_m = \frac{L}{2} - \frac{L}{20v_p}(\theta_A L + \theta_B L + 2v_A - 2v_B) \tag{3.115}$$

The maximum bending moment in span is

$$\begin{aligned} M_{\max} = &-\frac{EI}{L^2}\left[6(v_B - v_A)\left(1 - \frac{2x_m}{L}\right) + 6x_m(\theta_A + \theta_B) - 2L\theta_A - L\theta_B\right] \\ &-\frac{EI\, v_P}{L^2}\left[40a\frac{x_m^3}{L^3} + 5(1-a)\left(1 + 12\frac{x_m^2}{L^2}\right) + 12(2a-5)\frac{x_m}{L}\right] \end{aligned} \tag{3.116}$$

Using the results obtained in this section the formulae for the beams with conventional supports are given as follows:

(1) Clamped-Clamped:

The static deformation before the rotational spring appears in the span is:

$$W(x) = \frac{L^4}{120EI}\left[\frac{x^2}{L^2}\left(\frac{x}{L} - 1\right)^2\left(2a\frac{x}{L} + 5 - a\right)\right] \tag{3.117}$$

$$\int_0^L W(x)dx = \frac{L^5}{720EI} \tag{3.118}$$

$$\int_0^L W^2(x)dx = \frac{L^9}{126(120EI)^2}\left(\frac{\alpha^2}{55} + 5\right) \tag{3.119}$$

The internal forces before rotational spring appeared in the span are:

$$M(x) = \frac{pL^2}{6}\left[3\frac{x^2}{L^2} - 3\frac{x}{L} + \frac{1}{2} + a\left(2\frac{x}{L} - 1\right)\left(\frac{x^2}{L^2} - \frac{x}{L} + \frac{1}{10}\right)\right] \tag{3.120}$$

$$M_A = M(0) = \frac{pL^2}{60}(5 - a) \tag{3.121}$$

$$M_B = M(L) = \frac{pL^2}{60}(5 + a) \tag{3.122}$$

$$V(x) = pL\left[\frac{x}{L} - \frac{1}{2} + a\left(\frac{x^2}{L^2} - \frac{x}{L} + \frac{1}{5}\right)\right] \tag{3.123}$$

$$V_A = V(0) = \frac{1}{10}(5 - 2a) \tag{3.124}$$

$$V_B = V(L) = \frac{1}{10}(5 + 2a) \tag{3.125}$$

The frequency of the SDOF system before the rotational spring appears in the span is:

$$\omega = \sqrt{\frac{33}{m}}\sqrt{\frac{D_1}{D_2}} = \sqrt{\frac{33}{mv_p}}\sqrt{\frac{35 + a^2}{275 + a^2}} = \frac{62.93}{L^2}\sqrt{\frac{EI}{m}}\sqrt{\frac{35 + a^2}{275 + a^2}} \tag{3.126}$$

(2) Pinned-Clamped:

The static deformation before the rotational spring appears in the span is:

$$W(x) = \frac{L^4}{240EI}\frac{x}{L}\left(\frac{x}{L} - 1\right)^2\left[4a\frac{x^2}{L^2} + \left(2\frac{x}{L} + 1\right)(5 - a)\right] \tag{3.127}$$

$$\int_0^L W(x)dx = \frac{L^5}{2880EI}(9 - a) \tag{3.128}$$

$$\int_0^L W^2(x)dx = \frac{L^9}{(240EI)^2}\left(\frac{9a^2}{770} - \frac{11a}{63} + \frac{95}{126}\right) \tag{3.129}$$

The internal forces before rotational spring appears in the span are:

$$M(x) = pLx\left[\frac{a}{3}\frac{x^2}{L^2} + (1 - a)\frac{x}{2L} - \frac{1}{40}(15 - 7a)\right] \tag{3.130}$$

$$M_B = M(L) = \frac{pL^2}{120}(15 + a) \tag{3.131}$$

$$V(x) = pL\left[\frac{x}{L} - \frac{3}{8} + a\left(\frac{x^2}{L^2} - \frac{x}{L} + \frac{7}{40}\right)\right] \tag{3.132}$$

$$V_A = V(0) = \frac{pL}{40}(15 - 7a) \tag{3.133}$$

$$V_B = V(L) = \frac{pL}{40}(15 + 7a) \tag{3.134}$$

The frequency of the SDOF system:

$$\omega = \sqrt{\frac{33}{m}}\sqrt{\frac{D_1}{D_2}} = \frac{12\sqrt{55}}{L^2}\sqrt{\frac{175 - 7a + 4a^2}{10450 - 2420a + 162a^2}}\sqrt{\frac{EI}{m}} \tag{3.135}$$

(3) Pinned-Pinned:

The static deformation before the rotational spring appears in the span is:

$$W(x) = \frac{L^4}{120EI}\frac{x}{L}\left(1 - \frac{x}{L}\right)\left[5\left(1 + \frac{x}{L} - \frac{x^2}{L^2}\right) - 2a\left(\frac{x}{L} - \frac{1}{2}\right)\left(\frac{x^2}{L^2} - \frac{x}{L} + \frac{1}{3}\right)\right] \tag{3.136}$$

$$\int_0^L W(x)dx = \frac{L^5}{120EI} \tag{3.137}$$

$$\int_0^L W^2(x)dx = \frac{L^9}{126(120EI)^2}\left(\frac{a^2}{55} + 155\right) \tag{3.138}$$

The internal forces before rotational spring appears in the span are:

$$M(x) = \frac{pLx}{6}\left[2a\frac{x^2}{L^2} + 3(1 - a)\frac{x}{L} - (3 - a)\right] \tag{3.139}$$

$$V(x) = pL\left[\frac{x}{L} - \frac{1}{2} + a\left(\frac{x^2}{L^2} - \frac{x}{L} + \frac{1}{6}\right)\right] \tag{3.140}$$

$$V_A = V(0) = \frac{pL}{6}(3-a) \tag{3.141}$$

$$V_B = V(L) = \frac{pL}{6}(3+a) \tag{3.142}$$

The frequency of the SDOF system before the rotational spring appears in the span is:

$$\omega = \sqrt{\frac{33}{m}}\sqrt{\frac{D_1}{D_2}} = \frac{12\sqrt{11}}{L^2}\sqrt{\frac{63+a^2}{1023+a^2}}\sqrt{\frac{EI}{m}} \tag{3.143}$$

The position of the rotational spring which appears in the span is

$$x = \begin{cases} \frac{1}{2a}\left[-(1-a)\pm\sqrt{1+\frac{a^2}{5}-\frac{a(A+B)}{5C}}\right], & \text{for } a = \frac{q_B - q_A}{q_B + q_A} \neq 0 \\ \frac{1}{2} - \frac{A+B}{20C} & \text{for } a = \frac{q_B - q_A}{q_B + q_A} = 0 \end{cases} \tag{3.144}$$

where

$$A = L\sum_{k=1}^{i}\theta_{Ak}T_k(\tau_k)$$

$$B = L\sum_{k=1}^{i}\theta_{Bk}T_k(\tau_k)$$

$$C = v_P\sum_{k=1}^{i}T_k(\tau_k)$$

It should be noticed that the value of $T_i(\tau_i)$ and the time τ_i are dependent of x_m. Therefore the approximate value of x_m can only be calculated from an iteration procedure.

3.2.2 Single span RC beams strengthened with FRP plate/sheet after steel bars have yielded

As described in Section 3.1, for the RC beam strengthened with FRP plates, the beam segment in which the steel bars have yielded is modeled as a rotational spring. The static deformation $W(x)$ of the simply-supported beam composed of two beam segments joined by a rotational spring can be obtained by solving the corresponding static problem shown in Fig. 3.3. Similar to Eq. (3.105), the static deformation of the beam with rotational spring in the span can be expressed as

$$W(x)=\begin{cases} v_A\phi_1(s)+\theta_A L_A\phi_2(s)+v_C\phi_3(s)+ \\ \quad +\theta_{CA}L_A\phi_4(s)+v_{pA}\phi_5(s,a_A), & s=x/L_A, \quad x<L_A \\ v_C\phi_1(s)+\theta_{CB}L_B\phi_2(s)+v_B\phi_3(s)+ \\ \quad +\theta_B L_B\phi_4(s)+v_{pB}\phi_5(s,a_B), & s=\dfrac{x-L_A}{L_B}, \quad L_A<x<L \end{cases} \tag{3.145}$$

where

$$a_A=\frac{ay}{1-a(1-y)}$$

$$a_B=\frac{a(1-y)}{1+ay}$$

$$y=L_A/L$$

$$v_{pA}=\frac{L_A^4}{120EI}(1-a+ay)$$

$$v_{pB}=\frac{L_B^4}{120EI}(1+ay)$$

The positive orientations of the displacement θ_A, v_A, θ_{CA}, v_C, θ_{CB}, v_B and θ_B are defined in Fig. 3.10.

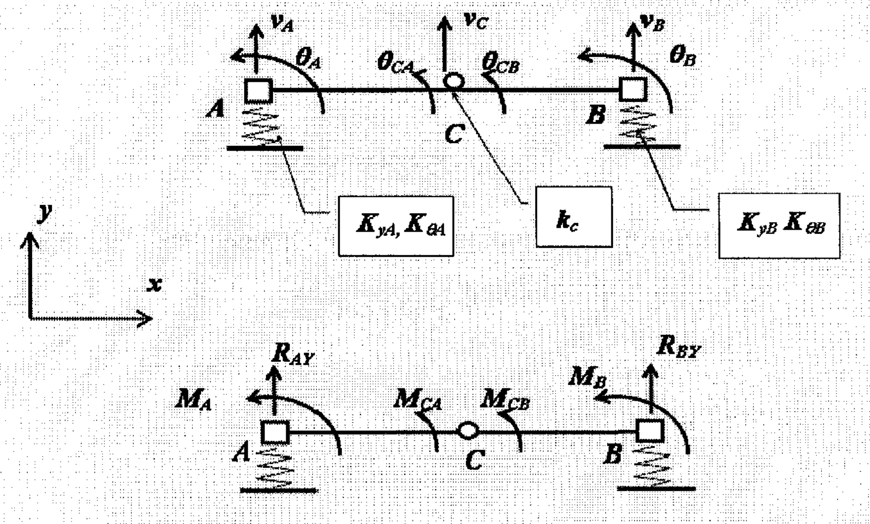

Fig. 3.10 Displacements and forces at ends of the two beam segments joined with a rotational spring

The meaning of the sympols to describe the displacement of the beam's ends are defined in Section 3.2.1, while the others are defined as follows

v_C = vertical displacement of the rotational spring in span of the beam

θ_{CA} = rotational displacement of cross-section on the left of rotational spring

θ_{CB} = rotational displacement of cross-section on the right of rotational spring

M_{CA} = bending moment in cross-section on the left of rotational spring

M_{CB} = bending moment in cross-section on the right of rotational spring

In an identical manner as the single span beam, we have the equilibrium equation to determine the joint displacement $\theta_A, v_A, \theta_{CA}, v_C, \theta_{CB}, v_B$ and θ_B,

$$K\,D = F \tag{3.146}$$

where

$$K = EI\begin{bmatrix} \frac{4}{L_A}+\frac{K_{\theta a}}{EI} & \frac{6}{L_A^2} & \frac{2}{L_A} & \frac{-6}{L_A^2} & 0 & 0 & 0 \\ \frac{6}{L_A^2} & \frac{12}{L_A^3}+\frac{K_{ya}}{EI} & \frac{6}{L_A^2} & \frac{-12}{L_A^3} & 0 & 0 & 0 \\ \frac{2}{L_A} & \frac{6}{L_A^2} & \frac{4}{L_A}+\frac{k_c}{EI} & \frac{-6}{L_A^2} & -\frac{k_c}{EI} & 0 & 0 \\ \frac{-6}{L_A^2} & \frac{-12}{L_A^3} & \frac{-6}{L_A^2} & \frac{12}{L_A^3}+\frac{12}{L_B^3} & \frac{6}{L_B^2} & \frac{-12}{L_B^3} & \frac{6}{L_B^2} \\ 0 & 0 & -\frac{k_c}{EI} & \frac{6}{L_B^2} & \frac{4}{L_B}+\frac{k_c}{EI} & \frac{-6}{L_B^2} & \frac{2}{L_B} \\ 0 & 0 & 0 & \frac{-12}{L_B^3} & \frac{-6}{L_B^2} & \frac{12}{L_B^3}+\frac{K_{yb}}{EI} & \frac{-6}{L_B^2} \\ 0 & 0 & 0 & \frac{6}{L_B^2} & \frac{2}{L_B} & \frac{-6}{L_B^2} & \frac{4}{L_B}+\frac{K_{\theta b}}{EI} \end{bmatrix}$$

$$F = \begin{Bmatrix} M_A \\ R_A \\ M_{CA} \\ R_C \\ M_{CB} \\ R_B \\ M_B \end{Bmatrix}, \qquad D = \begin{Bmatrix} \theta_A \\ v_A \\ \theta_{CA} \\ v_C \\ \theta_{CB} \\ v_B \\ \theta_B \end{Bmatrix}$$

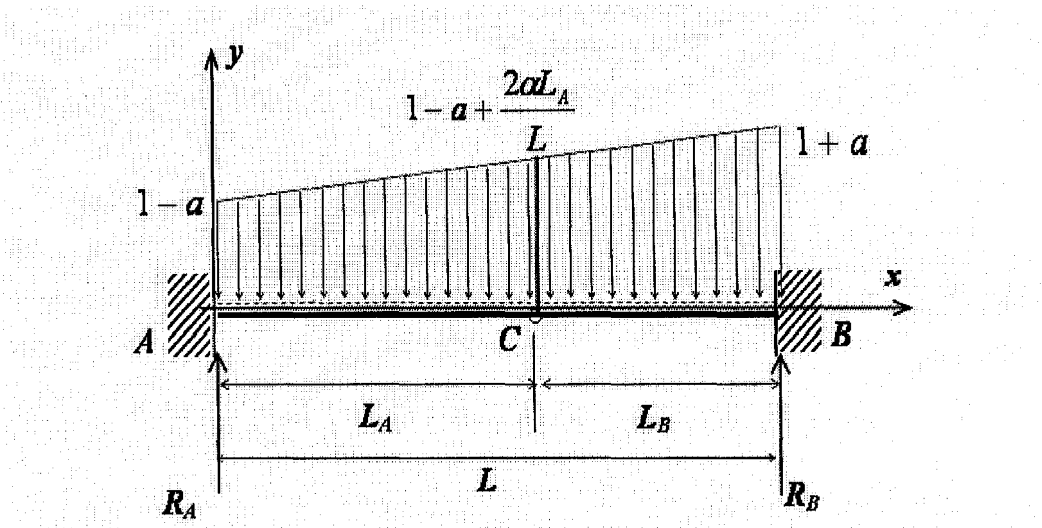

Fig. 3.11 Linearly distributed loading on two beam segments with their ends fixed

Solving the problem shown in Fig. 3.11, the components of the force vector $\{F\}$ can be obtained as follows

$$M_A = \frac{L_A^2}{60}[5(1-a)+4ay], \qquad R_A = \frac{L_A}{10}[5(1-a)+3ay]$$

$$M_{CA} = -\frac{L_A^2}{60}[5(1-a)+6ay], \qquad R_C = \frac{L}{10}[5+2a(2y-1)]$$

$$M_{CB} = \frac{L_B^2}{60}[5(1+a)-6a(1-y)], \qquad R_B = \frac{L_B}{10}[5(1+a)-4a(1-y)]$$

$$M_B = -\frac{L_B^2}{60}[5(1+a)-4a(1-y)]$$

Solving Eq. (3.146), the joint displacement $\theta_A, v_A, \theta_{CA}, v_C, \theta_{CB}, v_B$ and θ_B can be obtained. Substituting Eq. (3.145) into Eq. (3.27), the formula to calculate the frequency of the beam with rotational spring is obtained as

$$\omega = \sqrt{\frac{33}{m}}\sqrt{\frac{D_{1A}+D_{1B}}{D_{2A}+D_{2B}}} \tag{3.147}$$

where

$$D_{1A} = 42(5-2a_A)v_A + 7(5-a_A)L_A\theta_A + 42(5+2a_A)v_C - 7(5+a_A)L_A\theta_{CA} + 2(35+a_A^2)v_{AP}$$

$$\begin{aligned} D_{2A} = {} & (132\theta_A^2 - 198\theta_A\theta_{CA} + 132\theta_{CA}^2)L_A^2 + \left[1452v_A + 858v_C + (495-11a_A)v_{AP}\right]L_A\theta_A \\ & + \left[858v_A + 1452v_C - (495+11a_A)v_{AP}\right]L_A\theta_{CA} + (5148v_A^2 + 3564v_Av_C + 5184v_C^2) \\ & + \left[(2310-88a_A)v_A + (2310+88a_A)v_C\right]v_{AP} + (2a_A^2+550)v_{AP}^2 \end{aligned}$$

$$D_{1B} = 42(5-2a_B)v_C + 7(5-a_B)L_B\theta_{CB} + 42(5+2a_B)v_B - 7(5+a_B)L_B\theta_B + 2(35+a_B^2)v_{BP}$$

$$\begin{aligned} D_{2B} = {} & (132\theta_{CB}^2 - 198\theta_{CB}\theta_B + 132\theta_B^2)L_B^2 + \left[1452v_C + 858v_B + (495-11a_B)v_{BP}\right]L_B\theta_{CB} \\ & + \left[858v_C + 1452v_B - (495+11a_B)v_{BP}\right]L_B\theta_B + (5148v_C^2 + 3564v_Cv_B + 5184v_B^2) \\ & + \left[(2310-88a_B)v_C + (2310+88a_B)v_B\right]v_{BP} + (2a_B^2+550)v_{BP}^2 \end{aligned}$$

For simply-supported beam composed of two beam segments which are joined by a rotational spring as shown in Fig. 3.12, formulae to calculate the displacement and rotational angles of ends of the two beam segments can be obtained by solving Eq. (3.146).

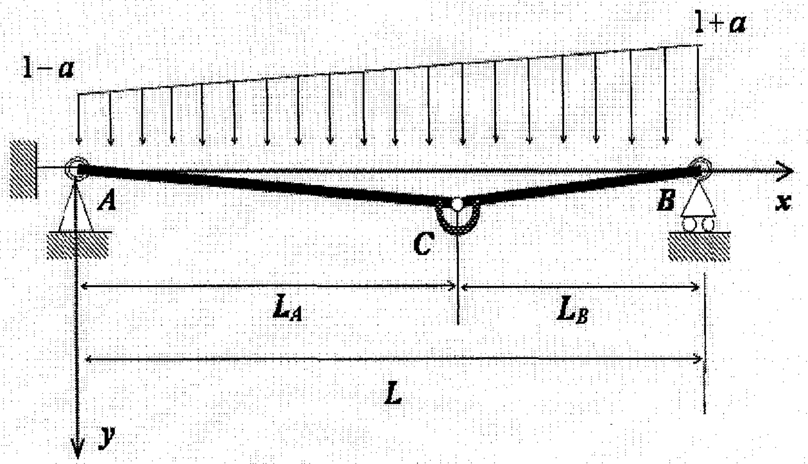

Fig. 3.12 Simply-supported beam with a rotational spring in the span

Setting $y = L_A/L$, the stiffness matrix K in Eq. (3.146) can be rewritten in the following form

$$K = \frac{EI}{L} G \begin{bmatrix} \frac{4}{y} & \frac{2}{y} & -\frac{6}{y^2} & 0 & 0 \\ \frac{2}{y} & \frac{4}{y} + \frac{Lk_C}{EI} & -\frac{6}{y^2} & -\frac{Lk_C}{EI} & 0 \\ -\frac{6}{y^2} & -\frac{6}{y^2} & \frac{12}{y^3} + \frac{12}{(1-y)^3} & \frac{6}{(1-y)^2} & \frac{6}{(1-y)^2} \\ 0 & -\frac{Lk_C}{EI} & \frac{6}{(1-y)^2} & \frac{4}{1-y} + \frac{Lk_C}{EI} & \frac{2}{1-y} \\ 0 & 0 & \frac{6}{(1-y)^2} & \frac{2}{1-y} & \frac{4}{1-y} \end{bmatrix} G$$

$$G=\begin{bmatrix}1&0&0&0&0\\0&1&0&0&0\\0&0&1/L&0&0\\0&0&0&1&0\\0&0&0&0&1\end{bmatrix}$$

The inverse of the stiffness matrix, K, can be obtained

$$K^{-1}=\frac{L}{EI}G^{-1}\left(\frac{1}{6}G_0+\frac{EI}{Lk_C}G_1\right)G^{-1} \tag{3.148}$$

where

$$G_0=\begin{bmatrix}2&2-6y+3y^2&2y-3y^2+y^3&2-6y+3y^2&-1\\2-6y+3y^2&2-6y+6y^2&2y-6y^2+6y^3&2-6y+6y^2&-1+3y^2\\2y-3y^2+y^3&2y-6y^2+6y^3&2y^2(1-y)^2&2y-6y^2+6y^3&-y+y^3\\2-6y+3y^2&2-6y+6y^2&2y-6y^2+6y^3&2-6y+6y^2&-1+3y^2\\-1&-1+3y^2&-y+y^3&-1+3y^2&2\end{bmatrix}$$

$$G_1=\begin{bmatrix}(1-y)^2&(1-y)^2&y(1-y)^2&-y(1-y)&-y(1-y)\\(1-y)^2&(1-y)^2&y(1-y)^2&-y(1-y)&-y(1-y)\\y(1-y)^2&y(1-y)^2&y^2(1-y)^2&-y^2(1-y)&-y^2(1-y)\\-y(1-y)&-y(1-y)&-y^2(1-y)&y^2&y^2\\-y(1-y)&-y(1-y)&-y^2(1-y)&y^2&y^2\end{bmatrix}$$

The force vector, F, in Eq. (3.146) can be written in the following form

$$F=\frac{L^2}{60}\begin{Bmatrix}\left[5-a(5-4y)\right]y^2\\-\left[5-a(5-6y)\right]y^2\\\frac{6}{L}\left[5+2a(2y-1)\right]\\\left[5-a(1-6y)\right](1-y)^2\\-\left[5+a(1+4y)\right](1-y)^2\end{Bmatrix}=\frac{L}{12}\begin{Bmatrix}y^2L\\-y^2L\\6\\(1-y)^2L\\-(1-y)^2L\end{Bmatrix}+\frac{aL}{60}\begin{Bmatrix}-(5-4y)y^2L\\(5-6y)y^2L\\12(2y-1)\\-(1-6y)(1-y)^2L\\-(1+4y)(1-y)^2L\end{Bmatrix}$$

Therefore the displacement can be calculated by

$$\begin{aligned} D = K^{-1}F &= \frac{L}{6EI}G^{-1}\left(G_0 + \frac{6EI}{Lk_c}G_1\right)G^{-1}F \\ &= \frac{L^3}{6}\left[\frac{15D_1 - aD_2}{60EI} + \frac{y-y^2}{Lk_c}[3+a(2y-1)]D_3\right] \end{aligned} \tag{3.149}$$

where

$$D = \begin{Bmatrix} \theta_A \\ \theta_{CA} \\ v_C \\ \theta_{CB} \\ \theta_B \end{Bmatrix}, D_1 = \begin{Bmatrix} 1 \\ 1-6y^2+4y^3 \\ (1-2y^2+y^3)Ly \\ 1-6y^2+4y^3 \\ -1 \end{Bmatrix}, D_2 = \begin{Bmatrix} 1 \\ 1-30y^2(1-y)^2 \\ (1-10y^2+15y^3-6y^4)Ly \\ 1-30y^2(1-y)^2 \\ 1 \end{Bmatrix}, D_3 = \begin{Bmatrix} 1-y \\ 1-y \\ y(1-y) \\ -y \\ -y \end{Bmatrix}$$

Particularly, for $a = 0$, the displacement vector D is reduced to

$$D = \frac{L^3}{24EI}\left\{\begin{Bmatrix} 1 \\ 4y^3-6y^2+1 \\ L(y^4-2y^3+y) \\ 4y^3-6y^2+1 \\ -1 \end{Bmatrix} + \frac{12EI}{Lk_C}y(1-y)\begin{Bmatrix} 1-y \\ 1-y \\ L(1-y)y \\ -y \\ -y \end{Bmatrix}\right\} \tag{3.150}$$

i.e.

$$\theta_A = \frac{L^3}{24EI}\left[1 + \frac{12EI}{Lk_C}y(1-y)^2\right]$$

$$\theta_{CA} = \frac{L^3}{24EI}\left[4y^3 - 6y^2 + 1 + \frac{12EI}{Lk_C}y(1-y)^2\right]$$

$$v_C = \frac{L^4}{24EI}y(1-y)\left[-y^2 + y + 1 + \frac{12EI}{Lk_C}y(1-y)\right]$$

$$\theta_{CB} = \frac{L^3}{24EI}\left[4y^3 - 6y^2 + 1 - \frac{12EI}{Lk_C}y^2(1-y)\right]$$

$$\theta_B = -\frac{L^3}{24EI}\left[1+\frac{12EI}{Lk_C}y^2(1-y)\right]$$

The static deformation is calculated from

$$W(x)=\begin{cases}\theta_A L_A\phi_2(s)+v_C\phi_3(s)+\theta_{CA}L_A\phi_4(s)+v_{pA}\phi_5(s,a_A), & s=x/L_A,\ x<L_A\\ v_C\phi_1(s)+\theta_{CB}L_B\phi_2(s)+\theta_B L_B\phi_4(s)+v_{pB}\phi_5(s,a_B), & s=\dfrac{x-L_A}{L_B},\ L_A<x<L\end{cases} \tag{3.151}$$

Using Eq. (3.151), the following integrations can be calculated

$$\int_0^L W(x)dx = \frac{L^5}{1440EI}\left\{\frac{12EI}{Lk_C}5y^2(y-1)(y^2+4y-6)+12\right\} \tag{3.152}$$

$$\int_0^L W^2(x)dx = \frac{L^9}{(24EI)^2}\frac{1}{630}\left\{24y^4(1-y)^2(35-45y-5y^2+16y^3)\left(\frac{6EI}{Lk_C}\right)^2+\right.$$
$$\left.+3y^2(1-y)(84-56y^2-56y^3+4y^4+66y^5-25y^6)\left(\frac{6EI}{Lk_C}\right)+31\right\} \tag{3.153}$$

The bending moment at the rotational spring can be calculated from

$$M_C = k_C(\theta_{BC}-\theta_{CA}) = \frac{L^2}{2}y(1-y) \tag{3.154}$$

The shear forces at beam's supports can be calculated from

$$V_A = -\frac{6EI}{L_A^3}\{L_A\theta_A - 2v_C + L_A\theta_{CA} + 2v_{pA}(2a_A-5)\} \tag{3.155}$$

$$V_B = -\frac{6EI}{L_B^3}\{2v_C + L_B\theta_{CB} + L_B\theta_B + 2v_{pB}(2a_B+5)\} \tag{3.156}$$

3.2.3 Continuous RC beam loaded by static axial force

The static deformation $W(x)$ of the continuous beam, as shown in Fig. 3.13, can be obtained from the finite element method. Each span of the continuous beam is selected as a element, the displacement vector $\{W\}$ consists of the rotational displacements of the cross-sections at each support of the continuous beam. That is

$$\{W\}^T = \{\theta_1, \theta_2, \theta_3, \cdots, \theta_{M-1}, \theta_M\} \tag{3.157}$$

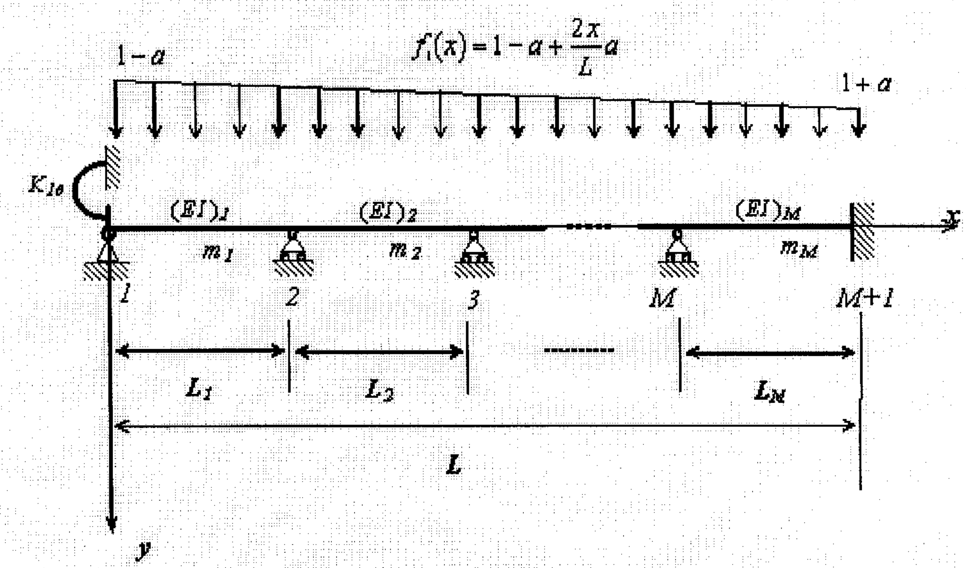

Fig. 3.13 Continuous beam subjected to static loading

The displacement vector $\{W\}$ can be obtained by solving the following linear system

$$[K]\{W\} = \{F\} \tag{3.158}$$

where

$$\{F\} = [F_1 \quad F_2 \quad \cdots \quad F_M]^T$$

$$F_1 = \frac{L_1^2}{12} f_1(0) + \frac{L_1^2}{30}\left(f_1(y_1) - f_1(0)\right)$$

$$F_k = -\frac{L_{k-1}^2}{12} f_1(y_{k-2}) - \frac{L_{k-1}^2}{20}\left[f_1(y_{k-1}) - f_1(y_{k-2})\right] + \frac{L_k^2}{12} f_1(y_{k-1}) + \frac{L_k^2}{30}\left[f_1(y_k) - f_1(y_{k-1})\right], \qquad k = 2, 3, \cdots, M$$

$$y_i = \sum_{k=1}^{i} L_k \quad , \quad i = 1, 2, \cdots, M$$

$$[K] = \begin{bmatrix} 4k_1 + K_{0\theta} & 2k_1 & 0 & \cdots & 0 & 0 \\ 2k_1 & 4k_1 + 4k_2 & 2k_2 & \cdots & 0 & 0 \\ 0 & 2k_2 & 4k_2 + 4k_3 & \cdots & 0 & 0 \\ \vdots & \vdots & \vdots & \ddots & \vdots & \vdots \\ 0 & 0 & 0 & \cdots & 4k_{M-2} + 4k_{M-1} & 2k_{M-2} \\ 0 & 0 & 0 & \cdots & 2k_{M-2} & 4k_{M-1} + 4k_M \end{bmatrix}$$

$$k_i = \frac{(EI)_i}{L_i}$$

The value of $f_1(y_k)$, $(k = 1, 2, \cdots, M)$ is calculated from Eq. (3.62). Solving the Eq. (3.158) the displacement vector $\{W\}$ can be obtained and the static deformation of the continuous beam can then be calculated from

$$W(x) = \begin{cases} L_1\left[\theta_1\phi_2(s) + \theta_2\phi_4(s) + v_{p1}\phi_5(s, a_1)\right] & s = \dfrac{x}{L_1} \quad 0 < x < y_1 \\ L_2\left[\theta_2\phi_2(s) + \theta_3\phi_4(s) + v_{p2}\phi_5(s, a_2)\right] & s = \dfrac{x - y_1}{L_2} \quad y_1 < x < y_2 \\ \vdots & \vdots \qquad \vdots \\ L_M\left[\theta_M\phi_2(s) + v_{pM}\phi_5(s, a_M)\right], & s = \dfrac{x - y_{M-1}}{L_M} \quad y_{M-1} < x < L \end{cases} \tag{3.159}$$

where

$$v_{pk} = \frac{L_k^3}{120EI}\left[1 - a + \frac{a}{L}(y_{k-1} + y_k)\right]$$

$$a_k = \frac{aL_k}{(1-a)L + a(y_{k-1} + y_k)}$$

Functions $\phi_2(s)$, $\phi_4(s)$ and $\phi_5(s,a)$ in Eq. (3.159) are the same as that in Eq. (3.105).

For the continuous beam with equal spans ($L_k = l,\ k = 1,2,\cdots,M$), the matrices $[K]$,$[G]$, $[M]$and $\{P\}$ can then be expressed in the following forms

$$[K] = \frac{2EI}{l}\begin{bmatrix} 2+k_0 & 1 & 0 & \cdots & 0 & 0 \\ 1 & 4 & 1 & \cdots & 0 & 0 \\ 0 & 1 & 4 & \cdots & 0 & 0 \\ \vdots & \vdots & \vdots & \ddots & \vdots & \vdots \\ 0 & 0 & 0 & \cdots & 4 & 1 \\ 0 & 0 & 0 & \cdots & 1 & 4 \end{bmatrix}_{M\times M}$$

$$[G] = \frac{l}{30}\begin{bmatrix} 4\overline{N}_1 & -\overline{N}_1 & 0 & \cdots & 0 & 0 \\ -\overline{N}_1 & 8\overline{N}_2 + 4N_1 & -\overline{N}_2 & \cdots & 0 & 0 \\ 0 & -\overline{N}_2 & 8\overline{N}_3 + 4N_2 & \cdots & 0 & 0 \\ \vdots & \vdots & \vdots & \ddots & \vdots & \vdots \\ 0 & 0 & 0 & \cdots & 8N_M + 4N_{M-1} & -N_M \\ 0 & 0 & 0 & \cdots & -N_M & 4N_M \end{bmatrix}_{M\times M}$$

$$[M] = \frac{ml^3}{420}\begin{bmatrix} 4 & -3 & 0 & \cdots & 0 & 0 \\ -3 & 8 & -3 & \cdots & 0 & 0 \\ 0 & -3 & 8 & \cdots & 0 & 0 \\ \vdots & \vdots & \vdots & \ddots & \vdots & \vdots \\ 0 & 0 & 0 & \cdots & 8 & -3 \\ 0 & 0 & 0 & \cdots & -3 & 8 \end{bmatrix}_{M\times M}$$

$$\{F\} = \frac{l^2}{60}\begin{bmatrix} 5(1-a) + \frac{4a}{M} & \frac{8a}{M} & \cdots & \frac{8a}{M} \end{bmatrix}^T$$

where

$$k_0 = \frac{K_{0\theta} l}{2EI} \tag{3.160}$$

Solving Eq. (3.158), the displacement vector $\{W\}$ can be obtained and static deformation of the continuous beam can then be expressed as

$$W(x) = \begin{cases} l\left[\theta_1\phi_2(s) + \theta_2\phi_4(s) + v_{p1}\phi_5(s, a_1)\right], & s = x/l, \quad 0 < x < y_1 \\ l\left[\theta_2\phi_2(s) + \theta_3\phi_4(s) + v_{p2}\phi_5(s, a_2)\right], & s = (x - y_1)/l, \quad y_1 < x < y_2 \\ \vdots & \vdots \qquad \vdots \\ l\left[\theta_M\phi_2(s) + v_{pM}\phi_5(s, a_M)\right], & s = (x - y_{M-1})/l, \quad y_{M-1} < x < L \end{cases} \tag{3.161}$$

where

$$v_{pk} = \frac{l^3 p_k}{120EI}, \quad k = 1,\ 2,\ \cdots, M$$

$$p_k = 1 - a + \frac{a}{M}(2k-1), \quad k = 1,\ 2,\ \cdots, M \tag{3.162}$$

$$a_k = \frac{a}{(1-a)M + a(2k-1)} \quad k = 1, 2, \cdots, M \tag{3.163}$$

Integrations in Eqs. (3.65) and (3.66) can be calculated from

$$\begin{aligned} \int_0^L W(x) f_1(x)\,dx = \frac{l^2}{25200M^2EI} \Big\{ & 2100M^2 EI(1-a)\sum_{k=1}^{M}(\theta_k - \theta_{k+1}) \\ & + 840M\ EI\ a\sum_{k=1}^{M}\left[(5k-3)\theta_k - (5k-2)\theta_{k+1}\right] + 35M^3 l^3 (1-a)^2 \\ & + 70M\ a\ l^3(1-a)\sum_{k=1}^{M}(2k-1) + 4\ a^2\ l^3\sum_{k=1}^{M}\left(35k^2 - 35k + 9\right) \Big\} \end{aligned} \tag{3.164}$$

$$\int_{(k-1)l}^{k\,l}\left(\frac{dW}{dx}\right)^2 dx=\frac{l}{70(180EI\ \ M)^2}\left\{42(60EI\ \ M)^2\left(2\theta_k^2+2\theta_{k+1}^2-\theta_k\theta_{k+1}\right)+\right.$$
$$+6300M^2EI\ \ (1-a)l^3(\theta_k-\theta_{k+1})+150Ma(1-a)(2k-1)l^6$$
$$+75M^2(1-a)^2l^6+360M\ \ EI\ \ al^3\left[(35k-19)\theta_k-(35k-16)\theta_{k+1}\right]$$
$$\left.+4a^2(2k-1)^2l^6\left(75k^2-75k+19\right)\right\} \tag{3.165}$$

$$\int_0^L W^2(x)\,dx=\frac{l^3}{770(360MEI)^2}\left\{66(120EIM)^2\sum_{k=1}^{M}\left(\theta_k^2+\theta_{k+1}^2-1.5\theta_k\theta_{k+1}\right)+\right.$$
$$+29700(1-a)M^2EIl^3\sum_{k=1}^{M}(\theta_k-\theta_{k+1})+275(1-a)^2M^3l^6+$$
$$+1320aMEIl^3\sum_{k=1}^{M}\left[(45k-23)\theta_k-(45k-22)\theta_{k+1}\right]$$
$$\left.+550a(1-a)M^2l^6\sum_{k=1}^{M}(2k-1)+4a^2l^6\sum_{k=1}^{M}\left(275k^2-275k+69\right)\right\} \tag{3.166}$$

As the dynamic deformation of the continuous beam increase, either cross-sections at the supporting joints 1 or 2 would yield. To calculate the dynamic response of the continuous beam after a plastic hinge appears at either the supporting joint 1 or 2, the following integrations should be calculated to obtain the initial value of the dynamic function of the next dynamic stages,

$$\int_0^L W(x)dx=\frac{l^2}{12}\sum_{k=1}^{M}\left[\theta_k-\theta_{k+1}+\frac{p_kl^3}{60EI}\left(1-a_k+\frac{a_k}{M}\right)\right] \tag{3.167}$$

$$\int_l^L W(x)dx=\frac{l^2}{12}\sum_{k=2}^{M}\left[\theta_k-\theta_{k+1}+\frac{p_kl^3}{60EI}\left(1-a_k+\frac{a_k}{M}\right)\right] \tag{3.168}$$

$$\int_0^l W(x)dx=\frac{l^2}{12}\left[\theta_1-\theta_2+\frac{p_1l^3}{60EI}\left(1-a_1+\frac{a_1}{M}\right)\right] \tag{3.169}$$

The bending moments and shear forces at joint k and joint $k+1$ in k^{th} span of the continuous beam can be calculated from

$$M_k = \frac{EI}{l}(4\theta_k + 2\theta_{k+1}) + \frac{(5-a)l^2}{60}\left[1 - a\left(1 - \frac{2k-1}{M}\right)\right] \tag{3.170}$$

$$V_k = -\frac{6EI}{l^2}(\theta_k + \theta_{k+1}) + \frac{(5-2a)l}{10}\left[1 - a\left(1 - \frac{2k-1}{M}\right)\right] \tag{3.171}$$

$$M_{k+1} = -\frac{EI}{l}(2\theta_k + 4\theta_{k+1}) - \frac{(5+a)l^2}{60}\left[1 - a\left(1 - \frac{2k-1}{M}\right)\right] \tag{3.172}$$

$$V_1 = -\frac{6EI}{l^2}(\theta_k + \theta_{k+1}) + \frac{(5+2a)l}{10}\left[1 - a\left(1 - \frac{2k-1}{M}\right)\right] \tag{3.173}$$

For continuous beams with 2, 3, 4, 5, and 6 spans, the rotational displacements of the cross-section at each joint and the bending moments and shear forces at joints 1 and 2 in the first span can be obtained as follows.

(1) Two-span continuous beam

a. Rotational displacements of the cross-section at each joint

$$\begin{Bmatrix} \theta_1 \\ \theta_2 \end{Bmatrix} = \frac{l^3}{120EI(7+4k_0)}\begin{Bmatrix} 20-16a \\ -5+11a+4ak_0 \end{Bmatrix} \tag{3.174}$$

b. The bending moments at supporting joints 1 and 2

$$M_1 = \frac{(5-4a)k_0}{15(7+4k_0)}l^2 \tag{3.175}$$

$$M_2 = \frac{45-8a+20k_0}{15(7+4k_0)}l^2 \tag{3.176}$$

c The shear forces at supporting joints 1 and 2

$$V_1 = \frac{-8(5-4a)k_0 + 44a - 55}{20(7+4k_0)}l \tag{3.177}$$

$$V_2 = \frac{8(5-a)k_0 - 26a + 85}{20(7+4k_0)}l \tag{3.178}$$

(2) Three-span continuous beam

a. Rotational displacements of the cross-section at each joint

$$\begin{Bmatrix} \theta_1 \\ \theta_2 \\ \theta_3 \end{Bmatrix} = \frac{l^3}{360EI(26+15k_0)} \begin{Bmatrix} 225-189a \\ -60+92a+24ak_0 \\ 15+29a+24ak_0 \end{Bmatrix} \tag{3.179}$$

b. The bending moments at supporting joints 1 and 2

$$M_1 = \frac{(225-189a)k_0}{180(26+15k_0)} l^2 \tag{3.180}$$

$$M_2 = \frac{495-239a+(225-87a)k_0}{180(26+15k_0)} l^2 \tag{3.181}$$

c. The shear forces at supporting joints 1 and 2

$$V_1 = \frac{-615+527a-(450-384a)k_0}{180(26+15k_0)} l \tag{3.182}$$

$$V_2 = \frac{945-513a+(450-216a)k_0}{30(26+15k_0)} l \tag{3.183}$$

(3). Four-span continuous beam

a. Rotational displacements of the cross-section at each joint

$$\begin{Bmatrix} \theta_1 \\ \theta_2 \\ \theta_3 \\ \theta_4 \end{Bmatrix} = \frac{l^3}{120EI(97+56k_0)} \begin{Bmatrix} 280-248a \\ -75+180a+24ak_0 \\ 20+10a+16ak_0 \\ -5+46a+24ak_0 \end{Bmatrix} \tag{3.184}$$

b. The bending moments at supporting joints 1 and 2

$$M_1 = \frac{(1680-1488a)k_0}{360(97+56k_0)} l^2 \tag{3.185}$$

$$M_2 = \frac{3690 - 2229a + (1680 - 888a)k_0}{360(97 + 56k_0)} l^2 \quad (3.186)$$

c. The shear forces at supporting joints 1 and 2

$$V_1 = \frac{-4590 + 4107a + (3360 - 3000a)k_0}{360(97 + 56k_0)} l \quad (3.187)$$

$$V_2 = \frac{7050 - 4623a + (3360 - 2040a)k_0}{360(97 + 56k_0)} l \quad (3.188)$$

(4). Five-span continuous beam

a. Rotational displacements of the cross-section at each joint

$$\begin{Bmatrix} \theta_1 \\ \theta_2 \\ \theta_3 \\ \theta_4 \\ \theta_5 \end{Bmatrix} = \frac{l^3}{600EI(362 + 209k_0)} \begin{Bmatrix} 5225 - 4741a \\ -1400 - 1880a + 352ak_0 \\ 375 + 375a + 246ak_0 \\ -100 + 548a + 246ak_0 \\ 25 + 587a + 352ak_0 \end{Bmatrix} \quad (3.189)$$

b. The bending moments at supporting joints 1 and 2

$$M_1 = \frac{(5225 - 4741a)k_0}{300(362 + 209k_0)} l^2 \quad (3.190)$$

$$M_2 = \frac{11475 - 7859a + (5225 - 4741a)k_0}{300(362 + 209k_0)} l^2 \quad (3.191)$$

c. The shear forces at supporting joints 1 and 2

$$V_1 = \frac{-14275 + 13609a - (10450 - 9548a)k_0}{300(362 + 209k_0)} l \quad (3.192)$$

$$V_2 = \frac{21925 - 15893a + (10450 - 7172a)k_0}{300(362 + 209k_0)} l \quad (3.193)$$

(5). Six-span continuous beam

a. Rotational displacements of the cross-section at each joint

$$\begin{Bmatrix} \theta_1 \\ \theta_2 \\ \theta_3 \\ \theta_4 \\ \theta_5 \\ \theta_6 \end{Bmatrix} = \frac{l^3}{180EI(1351+780k_0)} \begin{Bmatrix} 11700-10800a \\ -3135-4037a+660ak_0 \\ 840+56a+480ak_0 \\ -225+1143a+540ak_0 \\ 60+776a+480ak_0 \\ -15+1157a+660ak_0 \end{Bmatrix} \tag{3.194}$$

b. The bending moments at supporting joints 1 and 2

$$M_1 = \frac{(11700-10800a)k_0}{180(1351+780k_0)} l^2 \tag{3.195}$$

$$M_2 = \frac{25695-18938a+(11700-8040a)k_0}{180(1351+780k_0)} l^2 \tag{3.196}$$

c. The shear forces at supporting joints 1 and 2

$$V_1 = \frac{-31965+29714a-(23400-21720a)k_0}{180(1351+780k_0)} l \tag{3.197}$$

$$V_2 = \frac{49095-37836a+(23400-17280a)k_0}{180(1351+780k_0)} l \tag{3.198}$$

As the dynamic deformation increases, the cross-section at some supporting joints will yield. After the plastic hinges appear at the positions of some supporting joints the continuous beam will be decomposed into several single span beams and a continuous beam with fewer spans. The response of these single span beams can then be calculated separately, while the continuous beam with fewer spans can be calculated with the formulae given above.

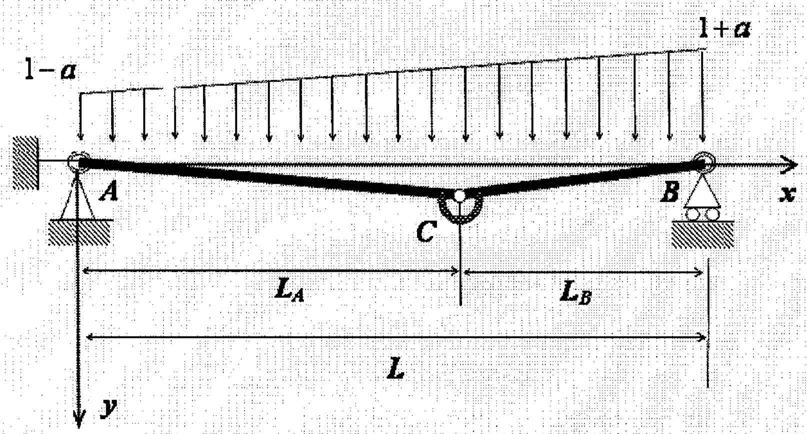

Fig. 3.14 Simply-supported beam loaded by both axis force and transverse loading

Consider the single span beam shown in Fig. 3.14, which may be any span of the continuous beam shown in Fig. 3.13 after a plastic hinge appears at right ends of the beams in $(k-1)^{th}$ and k^{th} spans of the continuous beam, where $K_{\theta k}$ is the rotation stiffness of the rotational spring which is joined up on the left end of the beam. The static deformation of this single span beam can be expressed in the form

$$W(x) = l\,\theta_k \phi_2\left(\frac{x}{l}\right) + l\,\theta_{k+1}\phi_4\left(\frac{x}{l}\right) + v_{pk}\phi_5\left(\frac{x}{l}, a_k\right) \qquad (3.199)$$

where

$$\theta_k = \frac{p_k l^3}{120EI}\frac{15-a_k}{3+k_0} \qquad (3.200)$$

$$\theta_{k+1} = -\frac{p_k l^3}{240EI}\frac{(5+a_k)(2+k_0)+20}{3+k_0} \qquad (3.201)$$

$$v_{pk} = \frac{p_k l^4}{120EI} \tag{3.202}$$

$$k_0 = \frac{lK_{\theta k}}{2EI} \tag{3.203}$$

$$p_k = 1 - a + \frac{2k-1}{M} a , \qquad k = 1,2,\cdots,M \tag{3.204}$$

$$a_k = \frac{a}{(1-a)M + a(2k-1)} , \qquad k = 1,2,\cdots,M \tag{3.205}$$

From Eq. (3.199) following integration formula can be obtained

$$\int_0^l W(x)dx = \frac{p_k l^5 \left[72 + (9 + a_k) k_0\right]}{2880EI(3 + k_0)} \tag{3.206}$$

The frequency ω_2 and the parameters γ_2 can be calculated from

$$\omega = \frac{2}{l^2}\sqrt{\frac{22EI}{m}}\sqrt{\frac{-g_1(k_0,a_k)\bar{N}_k^* + g_2(k_0,a_k)}{g_3(k_0,a_k)}} \tag{3.207}$$

$$\gamma^2 = \frac{88EI}{m\ l^4}\frac{g_2(k_0,a_k)}{g_3(k_0,a_k)} \tag{3.208}$$

where

$$g_1(k_0,a_k) = 135(255 + a_k^2) + 75(117 + 15.6a_k + a_k^2)k_0 + (675 + 180a_k + 17a_k^2)k_0^2$$

$$g_2(k_0,a_k) = 45(k_0 + 3)\left[40(63 + a_k^2) + (315 + 70a_k + 11a_k^2)k_0\right]$$

$$g_3(k_0,a_k) = 300(1023 + a_k^2) + (78375 + 8910a_k + 167a_k^2)k_0 + (5225 + 1210a_k + 81a_k^2)k_0^2$$

$$\bar{N}_k^* = \frac{l^2}{EI}\bar{N}_k$$

Chapter 4

ANALYSIS OF RC PLATES STRENGTHENED WITH FRP SHEET SUBJECTED TO AIR-BLAST LOADING

4.1 SDOF method for analysis of RC plates strengthened with FRP sheet subjected to air-blast loading

The dynamic analysis of a plate subjected to air-blast loading is more complex than the analysis of a beam. Even for the static problem, the solution of the equilibrium differential equation of an elastic plate can only be expressed by an infinite series. In order to simplify the dynamic analysis, the procedure to analyse a beam subjected to air-blast loading as described in Chapter 3, is also used to analyse a plate subjected to air-blast loading. Consider the flat but irregular concrete plate reinforced with both steel bars and FRP sheet subjected to air-blast loading shown in Fig. 4.1.

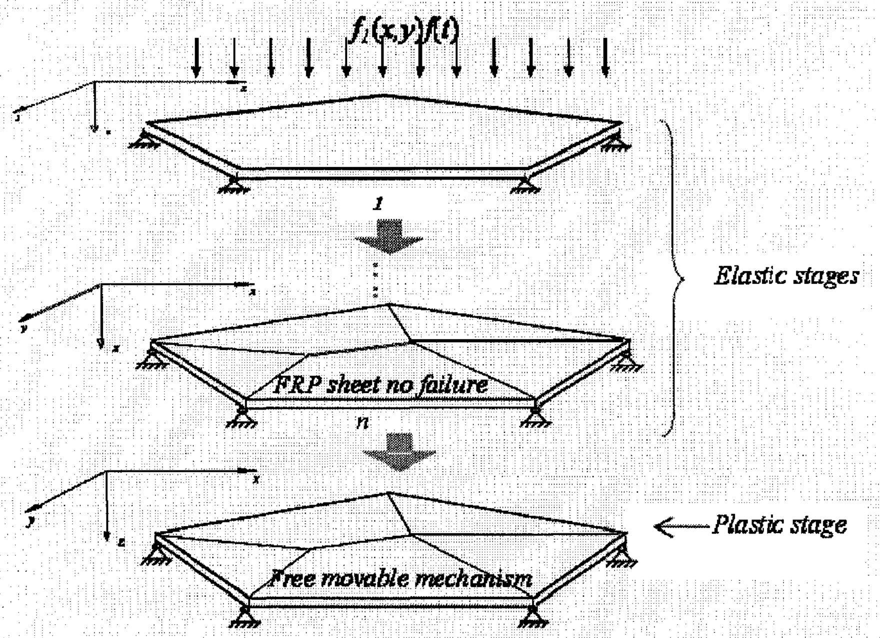

Fig. 4.1 Response stages of RC plate strengthened with FRP sheet subjected to air-blast load

The boundaries may be free, simply-supported or fixed. The analysis is similar to that of beams reinforced with combined steel bars and FRP sheet. As the dynamic deformation of the plate increases, either plastic yield lines (as the plate reinforced with steel bars only) or hinge lines with rotational stiffness (as the plate reinforced with both steel bars and FRP sheet) will appear on the boundaries or in the plate. After sufficient plastic yield lines appear both in the plate and on the fixed boundaries, the plate will be transformed to a free movable mechanism. In a similar manner as the beam's dynamic deformation described in Chapter 3, the dynamic deformation of a plate subjected to air-blast loading can be represented approximately as

$$w(x,y,t) = pW_i(x,y)T_i(t) + p\sum_{k=1}^{i-1} ik \; W_k(x,y)T_k(t_{yk}), \quad i = 1,2,... \tag{4.1}$$

where

p	=	amplitude of the blast load on plate
$W_i(x,y)$	=	plate deformation mode in i^{th} stage, which satisfies $D\nabla^4 W_i(x,y) = f_1(x,y)$ and supporting conditions
$T_i(t)$	=	dynamic function in i^{th} stage
ik	=	the rupture index
D	=	bending stiffness of plate

In the case when the k^{th} elastic stage terminates due to rupture of FRP sheet ik takes the value of zero, while in the case that the k^{th} elastic stage terminates due to yielding of steel reinforcement, ik takes the value of one, i.e.

$$ik = \begin{cases} 0 & \text{if } k^{th} \text{ stage terminates due to FRP mat rupturing} \\ 1 & \text{if } k^{th} \text{ stage terminates due to steel reinforcement yielding} \end{cases}$$

The differential equation of plate subjected to air-blast loading is

$$D\nabla^4 w(x,y,t) + m\frac{\partial^2 w(x,y,t)}{\partial t^2} = p\, f_1(x,y) f(t) \tag{4.2}$$

where

$$D = \frac{Eh^3}{12\left(1-\nu^2\right)} \tag{4.3}$$

E	=	Young's modulus
h	=	thickness of plate
ν	=	Poisson's ratio
m	=	distributed mass of plate
$f_1(x,y)$	=	distribution of air-blast load on plate
$f(t)$	=	dynamic function of air-blast load

Substituting Eq. (4.1) into (4.2), the residual is obtained as

$$R(x,y,t) = D\nabla^4 W_i(x,y)T_i(t) + mW_i(x,y)\ddot{T}_i(t) - f_1(x,y)\left[f(t) - \sum_{k=1}^{i-1} ik\, T_k(\tau_k)\right]$$

where

τ_k = time when k^{th} elastic stage ends

Using weighted residual method with $W_i(x,y)$ as the weighting function, and from the condition $\iint_\Omega R(x,y,t)W_i(x,y)\,dxdy = 0$, the following equation is obtained

$$\ddot{T}_i(t) + \omega^2 T_i(t) = \omega^2\left[f(t) - \sum_{k=1}^{i-1} ik\, T_k(\tau_k)\right] \tag{4.4}$$

If the plate is reinforced with steel bars only, yield lines will appear on the lines where the bending moment is largest, and if the plate is also reinforced with FRP sheet, the bending stiffness of the plate in the vicinity of the yield line will reduce after time τ_i. The elastic response will continue but with a lower vibration frequency. For simplicity, the vicinity of the yield line is modeled with a distributed rotational spring, which joins two plate segments together.

Fig. 4.2 shows a simply-supported rectangular plate after the steel bars in the vicinity of "yield lines" have yielded, while the FRP sheet remains elastic.

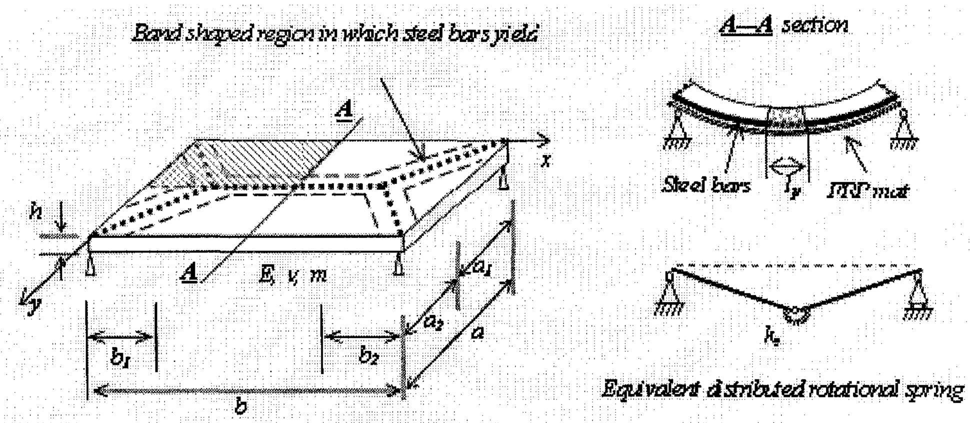

Fig. 4.2 Distributed rotational spring along yield lines of simply supported rectangular plate

The stiffness, k_c, of the distributed rotation spring can be calculated with the remaining stiffness of the cross-section and the width of the band shaped vicinity of the yield line in which the steel reinforcement has yielded. The width of the band shaped vicinity of the yield line can be calculated approximately from the formulae given by Eq. (3.18) or Eq. (3.19). The stiffness, k_c can then be calculated from

$$k_c = \begin{cases} B_y/2l_p & \text{when the critical section in the plate} \\ B_y/l_p & \text{when the critical section at the support} \end{cases} \tag{4.5}$$

where B_y is the remaining bending stiffness per unit length of the plate in the band shaped region and l_p is calculated from Eq. (3.18) or Eq. (3.19).

The frequency of the equivalent SDOF system of plate is calculated from

$$\omega_i^2 = \frac{\iint_\Omega f_1(x,y)W_i(x,y)dxdy}{m\iint_\Omega W_i^2(x,y)dxdy} \tag{4.6}$$

The initial value of the dynamic function, $T_i(t)$ is zero, i.e.

$$T_i(\tau_{i-1})=0 \tag{4.7}$$

The initial value of the derivative of the dynamic function is

$$\dot{T}_i(\tau_{i-1})=\dot{T}_{i-1}(\tau_{i-1})\,\frac{\iint_\Omega W_{i-1}dxdy}{\iint_\Omega W_i dxdy} \tag{4.8}$$

if the i^{th} response stage terminates due to steel reinforcement yields, or

$$\dot{T}_i(\tau_{i-1})=\frac{\omega_i}{\omega_{i-1}}\sqrt{\frac{2\omega_{i-1}^2 U_{pi}+p^2\left[\dot{T}_{i-1}^2(\tau_{i-1})+2\omega_{i-1}^2 T_{i-1}^2(\tau_{i-1})\right]\iint_\Omega f_1(x,y)W_{i-1}(x,y)\,dxdy}{p^2\iint_\Omega f_1(x,y)W_i(x,y)\,dxdy}} \tag{4.9}$$

if the i^{th} response stage terminates due to rupture of the FRP sheet.

In Eq. (4.9), U_{pi} is the plastic energy dissipated during $(i-1)^{th}$ stage which can be calculated from

$$U_{pi}=pT_{i-1}(\tau_{i-1})\sum_{k=1}^{m_{i-1}} l_{i-1k}M_{pi-1k}\theta_{i-1k} \tag{4.10}$$

where

$T_{i-1}(t)$ = dynamic function of $(i-1)^{th}$ stage of the dynamic deformation

m_{i-1} = total number of plastic hinges appeared in the plate in $(i-1)^{th}$ stage

l_{i-1k} = length of k^{th} $(k=1,2,\cdots m_{i-1})$ plastic hinge line

M_{pi-1k} = bending moment on k^{th} $(k=1,2,\cdots m_{i-1})$ plastic hinge line

θ_{i-1k} = relative rotation angle of the two cross sections joined by k^{th} $(k=1,2,\cdots m_{i-1})$ plastic hinge line in $(i-1)^{th}$ stage

If the blast load intensity is low relative to the resistance, then the structure will response elastically. With initial conditions, $T_1(0)=0, \dot{T}_1(0)=0$, and the continuity conditions at time t_d, $T_1(t_d-0)=T_1(t_d+0)$, $\dot{T}_1(t_d-0)=\dot{T}_1(t_d+0)$, the solution of Eq. (4.4) can be determined as

$$T_1(t)=\begin{cases} 1-\cos\omega t-\dfrac{t}{t_d}+\dfrac{1}{\omega\ t_d}\sin\omega t & 0<t<t_d \\ \dfrac{1}{\omega t_d}\left[\sin\omega t-\sin\omega(t-t_d)\right]-\cos\omega t & t>t_d \end{cases} \tag{4.11}$$

If the blast load intensity is high, the dynamic deformation increases and some cross-section will fail. The dynamic function in the first elastic stage is in the form shown by Eq. (4.11). Assuming there are a total of n elastic stages in the dynamic response of the structure, the dynamic function in k^{th} elastic stage can be represented as

$$T_k(t)=1-\cos\omega(t-\tau_{k-1})-\frac{t-\tau_{k-1}}{t_d}+\frac{1}{\omega\ t_d}\left(\dot{T}_k(\tau_{k-1})+\frac{1}{t_d}\right)\sin\omega(t-\tau_{k-1}) \tag{4.12}$$

After the dynamic function is obtained, the plate dynamic deformation can be calculated from Eq. (4.1). The dynamic internal forces in i^{th} stage can be calculated as follows:

$$\begin{aligned} M_{ix}(x,y,t)= & -pD\left(\frac{\partial^2 W_i(x,y)}{\partial x^2}+\nu\frac{\partial^2 W_i(x,y)}{\partial y^2}\right)T_i(t) \\ & -pD\sum_{k=1}^{i-1} ik\left(\frac{\partial^2 W_k(x,y)}{\partial x^2}+\nu\frac{\partial^2 W_k(x,y)}{\partial y^2}\right)T_k(\tau_k) \end{aligned} \tag{4.13}$$

$$\begin{aligned} M_{iy}(x,y,t)= & -pD\left(\frac{\partial^2 W_i(x,y)}{\partial y^2}+\nu\frac{\partial^2 W_i(x,y)}{\partial x^2}\right)T_i(t) \\ & -pD\sum_{k=1}^{i-1} ik\left(\frac{\partial^2 W_k(x,y)}{\partial y^2}+\nu\frac{\partial^2 W_k(x,y)}{\partial x^2}\right)T_k(\tau_k) \end{aligned} \tag{4.14}$$

$$M_{ixy}(x,y,t)=-pD(1-\nu)\left[\frac{\partial^2 W_i(x,y)}{\partial x\partial y}T_i(t)+\sum_{k=1}^{i-1} ik\ \frac{\partial^2 W_k(x,y)}{\partial x\partial y}T_k(\tau_k)\right] \tag{4.15}$$

$$Q_{ix}(x,y,t) = -pD\left[\frac{\partial}{\partial x}\nabla^2 W_i(x,y)T_i(t) + \sum_{k=1}^{i-1} ik\ \frac{\partial}{\partial x}\nabla^2 W_k(x,y)T_k(\tau_k)\right] \quad (4.16)$$

$$Q_{ix}(x,y,t) = -pD\left[\frac{\partial}{\partial y}\nabla^2 W_i(x,y)T_i(t) + \sum_{k=1}^{i-1} ik\ \frac{\partial}{\partial y}\nabla^2 W_k(x,y)T_k(\tau_k)\right] \quad (4.17)$$

The elastic response will end when there are sufficient yield lines in the plate and the plastic stage will start. In the plastic stage, the plate is divided into several rigid parts and joined together with the yield lines. For simplicity, it is assumed that the bending moments on the yield lines have the same value. Fig. 4.3 shows the yield mechanism of a simply-supported rectangular plate subjected to uniformly distributed air-blast load.

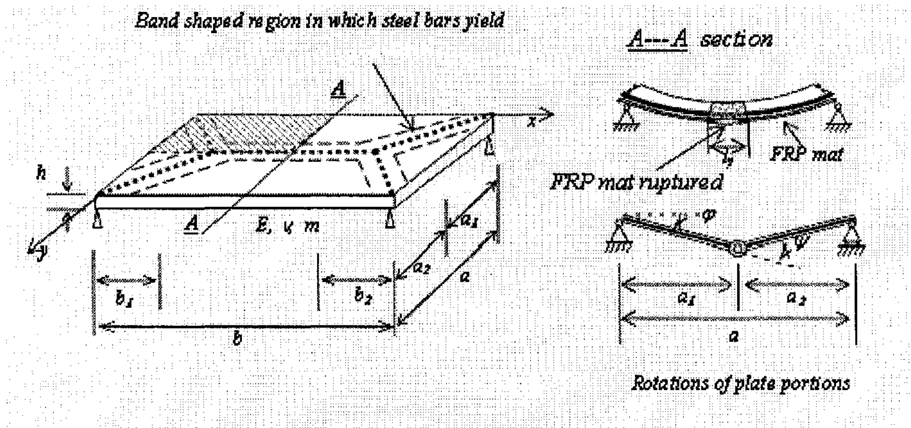

Fig. 4.3 Yield lines of simply supported rectangular plate

The dynamic deformation of simply-supported rectangular plate in plastic stage can be expressed in the following form

$$w(x,y,t) = pW_p(x,y)T_p(t) + p\sum_{i=1}^{n} ik\ W_i(x,y)T_i(\tau_i) \quad (4.18)$$

Where

$W_p(x,y)$ = deformation mode of the plate in the plastic stage

$T_p(t)$ = dynamic function of the plastic stage

The deformation mode in plastic stage can be obtained from the collapse mechanism of the plate. The collapse mechanism is governed by supporting conditions and the load on the plate, which is the mode of yield lines (or hinge lines) about which adjacent parts of the plate will experience exclusively a relative rotation. Most often, the yield lines will be straight because they will divide the slab into rigid parts hinged along the yield lines. It is known that the collapse mechanism is completely determined by the axes of rotation of various portions of the plate and the ratios of the angle of rotation. The method to determine the pattern of the yield lines of a collapse mechanism can be found in text books on limit analysis of concrete slabs (Save and Saxve, 1997). In the specification of a mechanism, one angle of rotation or one deflection, can be assigned an arbitrary value. This arbitrary value can be assigned as the dynamic function to form the expression of the dynamic deformation in plastic stage, and in general, the dynamic deformation in plastic stage is represented by Eq. (4.18). It is easy to find that the deformation mode in plastic stage, $W_p(x, y)$, is a linear function. Therefore, its derivatives of which the order higher than one are equal to zero.

Substituting Eq. (4.18) into Eq. (4.2) the residual is obtained as

$$R_p(x,y,t) = mW_p(x,y)\ddot{T}_p(t) - f_1(x,y)\left[f(t) - \sum_{k=1}^{n} ik\ T_k(\tau_k)\right]$$

where

n = total number of elastic stages before the plastic stage

With the condition $\iint_\Omega R_p(x,y,t)W_p(x,y)\,dxdy = 0$, the following equation is obtained

$$\ddot{T}_p(t) = \omega_p^2\left[f(t) - \sum_{i=1}^{n} ik\ T_i(\tau_i)\right] \tag{4.19}$$

where

$$\omega_p^2 = \iint_\Omega f_1(x,y)W_p(x,y)dxdy \Big/ \iint_\Omega mW_p^2(x,y)dxdy \tag{4.20}$$

If the final elastic stage is terminated due to rupturing of the FRP sheet, the elastic strain energy generated in the last elastic stage will be released when the FRP sheet ruptures. Similar to Eqs. (4.7), (4.8) and (4.9), the initial value of the dynamic function in the plastic stage can be calculated from

$$T_p(\tau_n) = 0 \tag{4.21}$$

The initial value of the derivative of the dynamic function, $\dot{T}_p(\tau_n)$ can be calculated from

$$\dot{T}_p(\tau_n) = \dot{T}_n(\tau_n) \iint_\Omega W_n(x,y)dxdy \Big/ \iint_\Omega W_p(x,y)dxdy \tag{4.22}$$

if the n^{th} elastic response stage terminates due to steel reinforcement yields, or

$$\dot{T}_p(\tau_n) = \frac{\omega_p}{\omega_n}\sqrt{\frac{2\omega_n^2 U_{pp} + p^2\left[\dot{T}_n^2(\tau_n) + 2\omega_n^2 T_n^2(\tau_n)\right]\iint_\Omega f_1(x,y)W_n(x,y)dxdy}{p^2\iint_\Omega f_1(x,y)W_p(x,y)dxdy}} \tag{4.23}$$

if the n^{th} elastic response stage terminates due to rupture of FRP sheet. In Eq. (4.9), U_{pp} is the plastic energy dissipated during n^{th} stage which can be calculated from

$$U_{pp} = pT_n(\tau_n)\sum_{k=1}^{m_n} l_{nk}M_{pnk}\theta_{nk} \tag{4.24}$$

where

$T_n(t)$	=	dynamic function of n^{th} stage of the dynamic deformation
m_n	=	total number of plastic hinges appeared in the plate in n^{th} stage

l_{nk} = length of k^{th} $(k = 1, 2, \cdots m_n)$ plastic hinge line

M_{pk} = bending moment on k^{th} $(k = 1, 2, \cdots m_n)$ plastic hinge line

θ_{nk} = relative rotation angle of the two cross sections joined by k^{th} $(k = 1, 2, \cdots m_n)$ plastic hinge line in n^{th} stage

For $\tau_n < t < t_d$, integrating Eq. (4.19) twice with respect to t results in

$$\dot{T}_p(t) = -\frac{\omega_p^2(t-\tau_n)}{2t_d}\left((t-\tau_n) + 2t_d\sum_{k=1}^{n} ik\, T_k(\tau_k) - 2(t_d - \tau_n)\right) + \dot{T}_p(\tau_n) \tag{4.25}$$

$$T_p(t) = -\frac{\omega_p^2(t-\tau_n)^2}{6t_d}\left[(t-\tau_n) + 3t_d\sum_{k=1}^{n} ik\, T_k(\tau_k) - 3(t_d - \tau_n)\right] + \dot{T}_p(\tau_n)(t-\tau_n) \tag{4.26}$$

The time, t_m, when $T_p(t)$ reached its maximum value can be obtained by solving the following equation

$$\dot{T}_p(t) = -\frac{\omega_p^2(t-\tau_n)}{2t_d}\left((t-\tau_n) + 2t_d\sum_{k=1}^{n} ik\, T_k(\tau_k) - 2(t_d - \tau_n)\right) + \dot{T}_p(\tau_n) = 0$$

That is

$$t_m = t_d\left\{\sqrt{\left(1 - \sum_{k=1}^{n} ik\, T_k(\tau_k) - \frac{\tau_n}{t_d}\right)^2 + \frac{2\dot{T}_p(\tau_n)}{t_d\omega_p^2}} + 1 - \sum_{k=1}^{n} ik\, T_k(\tau_k)\right\} \tag{4.27}$$

It is possible that t_m obtained from Eq. (4.27) is greater than t_d. For $t > t_d$ the dynamic function $T_{p1}(t)$ should be determined from

$$\ddot{T}_{p1}(t) = -\omega_p^2\sum_{k=1}^{n} ik\ T_k(\tau_k), \qquad t > t_d \tag{4.28}$$

Integrating Eq. (4.28), the following equations are obtained

$$\dot{T}_{p1}(t) = -\omega_p^2(t-t_d)\sum_{k=1}^{n} ik\ T_k(\tau_k) + \dot{T}_p(t_d), \qquad t > t_d \tag{4.29}$$

$$T_{p1}(t) = -\frac{\omega_p^2(t-t_d)^2}{2}\sum_{k=1}^{n} ik\ T_k(\tau_k) + \dot{T}_p(t_d)(t-t_d) + T_p(t_d), \qquad t > t_d \tag{4.30}$$

where $\dot{T}_p(t_d)$ and $T_p(t_d)$ are calculated from Eqs. (4.25) and (4.26), respectively.

With the condition $\dot{T}_{p1}(t) = 0$, the time when $T_{p1}(t)$ reaches its maximum value can be calculated from Eq. (4.29) as

$$t_m = t_d + \dot{T}_p(t_d) \Big/ \omega_p^2 \sum_{k=1}^{n} ik\ T_k(\tau_k) \tag{4.31}$$

The maximum plastic rotation angle of the band shape vicinity of yield lines can be calculated from the maximum deformation in the plastic stage. For example, for the plate shown in Fig. 4.3, the maximum plastic rotation angle can be calculated from

$$\psi_m = \frac{pa}{a_1 a_2}\left[W_p\left(\frac{b}{2}, a_1\right)T_p(t_m) + \sum_{k=1}^{n} ik\ W_k\left(\frac{b}{2}, a_1\right)T_k(\tau_k)\right] \tag{4.32}$$

where a_1 and a_2 are the widths of the two joined plate portions (see Fig. 4.3), while the formula to calculate the time, τ_k, when the k^{th} ($k=1,2,\ldots, n$) elastic response stage terminates are given in Chapter 5.

As shown in Fig. 4.3, for a simply-supported rectangular plate the dynamic deformation mode of the plastic stage, $W_p(x,y)$, in the shaded region may be represented by

$$W_p(x,y) = \frac{2}{a}\begin{cases} x & 0 \le x \le y \quad 0 \le y \le \dfrac{a}{2} \\ y & y \le x \le \dfrac{b}{2} \quad 0 \le y \le \dfrac{a}{2} \end{cases} \tag{4.33}$$

For $f_1(x,y)=1$, that is the air-blast load is uniformly distributed on the plate, calculating the integrations in Eq. (4.20) results in

$$\omega_p^2=\frac{\iint_\Omega W_p(x,y)dxdy}{m\iint_\Omega W_p^2(x,y)dxdy}=\frac{1}{m}\frac{3b-a}{2b-a} \tag{4.34}$$

The differential equation for this problem is

$$\ddot{T}_p(t)=\frac{1}{m}\frac{3b-a}{2b-a}\left[f(t)-\sum_{i=1}^{n}ik\,T_i(\tau_i)\right] \tag{4.35}$$

If the final elastic stage terminates due to the rupturing of the FRP sheet, the initial value of the derivative of the dynamic function, $\dot{T}_p(\tau_n)$, can be calculated from Eq. (4.23), i.e.

$$\dot{T}_p(\tau_n)=\frac{\omega_p}{\omega_n}\sqrt{\frac{12\omega_n^2U_{pp}+6p^2\left[\dot{T}_n^2(\tau_n)+2\omega_n^2T_n^2(\tau_n)\right]\iint_\Omega W_n(x,y)\,dxdy}{p^2a(3b-a)}} \tag{4.36}$$

If the last elastic stage terminates due to yielding of steel reinforcement, the initial value of the derivative of the dynamic function, $\dot{T}_p(\tau_n)$, can be calculate from Eq. (4.22), i.e.

$$\dot{T}_p(\tau_n)=\dot{T}_n(\tau_n)\frac{\iint_\Omega W_n(x,y)dxdy}{\iint_\Omega W_p(x,y)dxdy}=\frac{6\dot{T}_n(\tau_n)}{a(3b-a)}\iint_\Omega W_n(x,y)dxdy \tag{4.37}$$

If this simply-supported rectangular plate is only reinforced with steel bars, there will be only one elastic stage. The elastic deformation may be approximately represented as

$$W_n(x,y)=W_1(x,y)=16a^4\sin\frac{\pi}{b}x\sin\frac{\pi}{a}y\Big/\pi^6D\left(1+\frac{a^2}{b^2}\right)^2 \tag{4.38}$$

and

$$\int_0^a \int_0^b W_1(x,y)\,dxdy = \frac{64a^5b^5}{\pi^8 D\left(a^2+b^2\right)^2} \tag{4.39}$$

Substituting Eq. (4.39) into (4.37) results in

$$\dot{T}_p(\tau_1) = \frac{384a^4\dot{T}_1(\tau_1)}{\pi^8 D\left(1+a^2/b^2\right)^2(3-a/b)} \tag{4.40}$$

The dynamic function can be calculated from

$$T_p(t) = -\frac{\omega_p^2(t-\tau_1)^2}{6t_d}\left[(t-\tau_1)+3t_dT_1(\tau_1)-3(t_d-\tau_1)\right]+\dot{T}_p(\tau_1)(t-\tau_1) \tag{4.41}$$

The time, t_m, when $T_p(t)$ reached its maximum value is calculated from

$$t_m = \tau_1 + t_d\left\{\sqrt{\left(1-T_1(\tau_1)-\frac{\tau_1}{t_d}\right)^2+\frac{2\dot{T}_p(\tau_1)}{t_d\omega_p^2}}+1-T_1(\tau_1)-\frac{\tau_1}{t_d}\right\} \tag{4.42}$$

For $a_1 = a_2 = \frac{a}{2}$, calculating $W_p\left(\frac{b}{2},\frac{a}{2}\right)$ from Eq. (4.33) and then substituting it into Eq. (4.32), the maximum open angle can be obtained as

$$\psi_m = \frac{4p}{a}T_p(t_m)+64pa^3T(\tau_1)\Big/\pi^6D\left[1+(a/b)^2\right]^2 \tag{4.43}$$

The formula to calculate the time, τ_1, when the steel bar yield, is given in Chapter 5. The frequency corresponding to the elastic deformation represented by Eq. (4.38) is calculated from Eq.(4.6), i.e.

$$\omega_1 = \frac{\pi^2}{a^2}\left(1+\frac{a^2}{b^2}\right)\sqrt{\frac{D}{m}} \tag{4.44}$$

The maximum bending moments in $x-$ and $y-$directions in the plate can be calculated from (Боданский, 1974)

$$M_{xm} = q\,a^2 n_1 \tag{4.45}$$

and

$$M_{ym} = q\,a^2 n_2 \tag{4.46}$$

where

M_{xm}	=	maximum bending moments in x – directions in the plate
M_{ym}	=	maximum bending moments in y – directions in the plate
q	=	amplitude of uniformly distributed load on the plate.
a	=	width of the plate
n_1	=	bending parameter of M_{xm}
n_2		bending parameter of M_{ym}

The parameters n_1 and n_2 depend on the ratio of $\frac{b}{a}$, which can be found in Table 4.1.

Table 4.1 Bending coefficients of simply supported rectangular plate

b/a	1	1.1	1.2	1.3	1.4	1.5
n_1	0.0364	0.0433	0.0515	0.0587	0.0656	0.072
n_2	0.0364	0.0363	0.0357	0.0348	0.0336	0.032
b/a	1.6	1.7	1.8	1.9	2	
n_1	0.0776	0.0829	0.0874	0.0911	0.0946	
n_2	0.0303	0.0252	0.0266	0.0252	0.0236	

4.2 Deformation mode and frequency of the equivalent SDOF system of a rectangular RC plate strengthened with FRP sheet after steel bars have yielded

The SDOF method to analyze plates subjected to air-blast loading was illustrated in Section 4.1. If the RC plate is not strengthened with FRP sheet, the response of the simply-supported rectangular plate can be easily calculated with the derived formulae in Section 4.1. If the RC plate is strengthened with FRP sheet, the response of the plate will be different. Usually the rupture strain of FRP sheet is much larger than the yielding strain of steel. Therefore, after steel bars have yielded the FRP sheet will still deform elastically until the FRP sheet ruptures. As in the analysis of RC beams strengthened with FRP plate/sheet, the band shaped region in which reinforcing steel bars have yielded is modeled with the distributed rotational springs. To calculate the frequency of the equivalent SDOF system of such a plate after the steel bars have yielded, one needs to calculate the static deformation of the plate composed of several elastic plate portions, which may be in the shape of arbitrary triangles or arbitrary quadrilaterals, joined with distributed rotational springs.

It is almost impossible to determine a closed form expression for the deformation of the plate, which is composed of several plate portions joined with distributed rotational springs. It is assumed that the external FRP sheet reinforcement does not increase the bending stiffness of the RC plate before the steel bars have yielded. This implies that the band shaped region in which the steel bars yield would be the same as that of a plate without external FRP sheet reinforcement, provided that the loading on the plate is large enough. Therefore, it can be expected that the deformation of the plate be focused on the region where the steel bars have yielded. If the plate portions are assumed to be rigid, the static deformation of the plate after steel bars have yielded can be easily calculated by equating the work done by the loading on the plate and the strain energy stored in the rotational spring distributed along the "yield lines". With this static deformation, one can calculate the frequency of the equivalent SDOF system. Following the procedure outlined in Section 4.1 of this thesis the dynamic response can then be obtained. However, in this section a typical simply-supported rectangular plate, which is composed of four plate portions joined with distributed rotational springs, is analyzed. The frequencies and other parameters necessary for the analysis with the SDOF method are calculated.

Consider the simply-supported rectangular plate shown in Fig. 4.4. It is assumed that the position of the distributed rotational spring is the same as that of the yield lines of the plate, which is reinforced with steel bars only.

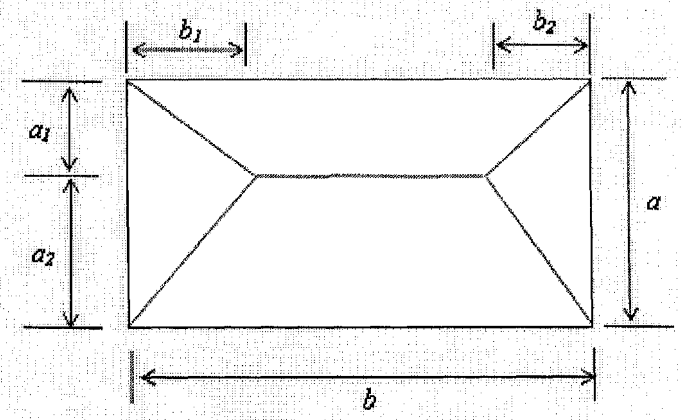

Fig. 4.4 Rectangular plate composed of four plate segments joined with distributed rotational spring

After the steel reinforcement has yielded, the deformation of the plate is assumed as the same shape of the plastic deformation of the plate, i.e. the elastic deformation of the plate is focused on the vicinity of the "yield lines" and the deformation of the plate can be expressed in the form

$$W(x,y) = \delta \, W_p(x,y) \tag{4.47}$$

where $W_p(x,y)$ is the mode of plastic deformation of the plate and δ is the maximum vertical displacement of the plate portions joined by distributed rotational springs subjected to the loading $f_1(x,y)=1$.

Equating the work done by the loading $f_1(x,y)=1$ on the plate and the strain energy stored in the distributed rotational springs, the formula to calculate the maximum displacement δ is obtained as

$$\delta=\frac{a(3b-b_1-b_2)}{3\Delta k_c} \tag{4.48}$$

where k_c is stiffness of the distributed rotational spring, and

$$\Delta=\frac{(a_1^2+b_1^2)^{\frac{3}{2}}}{a_1^2b_1^2}+\frac{(a_1^2+b_2^2)^{\frac{3}{2}}}{a_1^2b_2^2}+\frac{(a_2^2+b_1^2)^{\frac{3}{2}}}{a_2^2b_1^2}+\frac{(a_2^2+b_2^2)^{\frac{3}{2}}}{a_2^2b_2^2}+\frac{a^2}{a_1^2a_2^2}(b-b_1-b_2) \tag{4.49}$$

Using Eq. (4.47) the integrations in Eq. (4.6) can be calculated as

$$\iint_\Omega W(x,y)dxdy=\delta\iint_\Omega W_p(x,y)dxdy=\frac{a\delta}{6}[3b-(b_1+b_2)] \tag{4.50}$$

$$\iint_\Omega W^2(x,y)dxdy=\delta^2\iint_\Omega W_p^2(x,y)dxdy=\frac{a\delta^2}{6}[2b-(b_1+b_2)] \tag{4.51}$$

and,

$$\omega^2=\frac{1}{\delta}\frac{\iint_\Omega W_p(x,y)\,dxdy}{\iint_\Omega mW_p^2(x,y)\,dxdy}=\frac{1}{\delta}\frac{1}{m}\frac{3b-b_1-b_2}{2b-b_1-b_2} \tag{4.52}$$

The maximum bending moment in the plate can be calculated from

$$M_c=\frac{a_1+a_2}{a_1a_2}k_c\delta \tag{4.53}$$

For $a_i=b_i=\frac{a}{2}$, $(i=1,2)$, Eq. (4.48) is reduced to

$$\delta=\frac{a^3(3b-a)}{48k_c\left[b+\left(\sqrt{2}-1\right)a\right]}\approx\frac{a^3(3b-a)}{48k_c[b+0.414a]} \tag{4.54}$$

and Eq. (4.52) is reduced to

$$\omega^2 = \frac{48k_c(b+0.414a)}{ma^3(2b-a)} \tag{4.55}$$

and the bending moment is calculated from

$$M_c = \frac{a^2(3b-a)}{12[b+0.414a]} \tag{4.56}$$

Formulae to calculate the quantities related to the plate reinforced with combined steel bars and FRP sheet after the steel bars have yielded have been derived in this section. Following with the procedure described in Section 4.1 the plate reinforced with combined steel bars and FRP sheet can be analyzed. Numerical examples using these expressions are given in Chapter 7.

Chapter 5

FORMULAE TO CALCULATE THE TIME WHEN A DYNAMIC RESPONSE STAGE TERMINATES

As mentioned in Section 3.1 of this thesis, the time when a cross-section yields can be calculated from Eq. (3.17) on account of the strain rate effect. Eq. (3.17) can be solved with a numerical method (Henrych, 1979), but it is not convenient for a simplified design procedure. In this chapter, some approximate formulae will be derived for the calculation of the time when a cross-section yields. For analysis of concrete structures subjected to air-blast load it is convenient to replace f_y and σ_p by bending moments M_s and M_p in Eq. (3.17) for the analysis of frame and plate structures.

5.1 Static yielding bending moment of RC beams strengthened with FRP plate/sheet

The theory of bending of reinforced concrete assumes that the concrete will crack in the regions of tensile strains and that, after cracking, all the tension is carried by the tensile reinforcement. It is also assumed that plane sections of a structural member remain plane after straining, so that across the section there must be a linear distributed of strains. Fig. 5.1 shows the cross-section of a member subjected to bending, and the resultant strain diagram, together with two different types of stress distribution in the cross-section. The triangular stress distribution applies when stress vary nearly proportional to the strains, which generally occurs at the loading levels encountered under working conditions and is therefore used at serviceability limit state. The rectangular stress block represents the distribution at failure when the compressive strains are within the plastic range and it is associated with the design at ultimate limit state. The equivalent rectangular stress block is a simplified alternative to the rectangular-parabolic distribution. At the ultimate limit state it is assumed that member sections in flexure should be ductile and that failure should occur with the yielding of the tension steel and not by a sudden catastrophic compression failure of the concrete.

If the structure is designed to resist multiple blast loadings, the triangular stress distribution should apply. It should be noticed that the compressive strength of concrete increases by 20 to 30% of static strength at a very high strain rate (Боданский, etc., 1974). Thus, it ensures that the triangular stress distribution is well developed across the compressive zone of the cross-section. If the structure is designed to resist a blast loading once, which just requires that the structure should not collapse after the loading is applied on the structure, the rectangular-parabolic stress distribution should apply. For simplicity, the equivalent rectangular stress block can be used to calculate the static yielding bending moment of the cross-section.

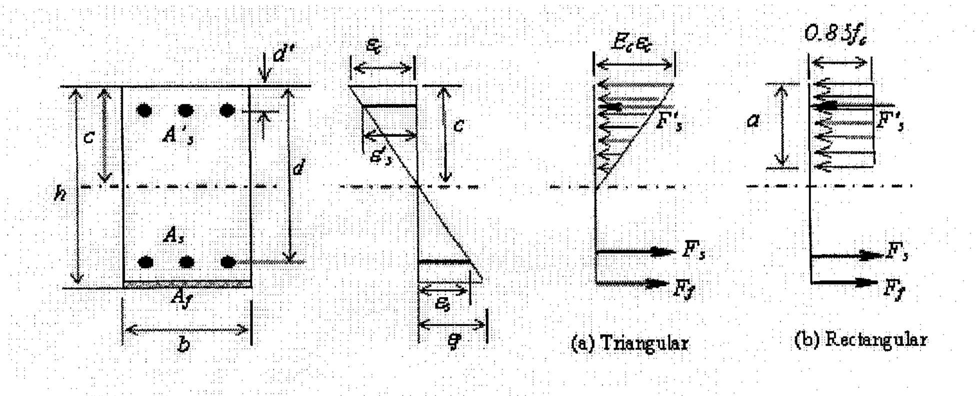

Fig. 5.1 Section with strain diagram and stress blocks

Referring to Fig. 5.1, for beams with mild steel reinforcement, Eq. (3.17) is changed into the form

$$\int_0^{\tau}\left[M_p T(t)\right]^{17} dt = 0.895\left(M_s - M_0\right)^{17} \tag{5.1}$$

where M_s and M_0 are the static yielding bending moment and initial static bending moment at the cross-section respectively, and M_p is the amplitude of the dynamic bending moment, which is calculated from

$$M_p = pEI\left[\partial^2 W/\partial x^2\right]\Big|_{x=x_m} \tag{5.2}$$

where

p = amplitude of air-blast load on the beam

EI = bending stiffness of beam

x_m = the location of the cross-section along the beam in which the tension reinforcing steel has yielded.

In blast analysis the cracked transformed moment of inertia is usually used to calculate the beam's bending stiffness. The bending stiffness of a cracked beam is

$$E_c I = E_c\left[\frac{1}{3}bc^3 + \alpha_s A_s (d-c)^2 + \alpha_s A'_s (c-d')^2 + \alpha_f A_f (h-c)^2\right] \tag{5.3}$$

where c is the depth to neutral axis and can be calculated from

$$c = \frac{\sqrt{[\alpha_s(A_s + A_s') + \alpha_f A_f]^2 + 2b(\alpha_s A_s d + \alpha_e A_s' d' + \alpha_f A_f h)} - [\alpha_s(A_s + A_s') + \alpha_f A_f]}{b} \tag{5.4}$$

and

α_s = E_s/E_c

α_f = E_f/E_c

h = height of cross-section

b = width of cross-section

d = depth to centroid of tension steel reinforcement

d' = depth to centroid of compression steel reinforcement

c = depth to neutral axis

E_c = Young's modulus of concrete

E_s = Young's modulus of the steel reinforcement

E_f = Young's modulus of the fiber material

f_y = static yield stress of steel

A_s = area of tension steel in the cross-section

A_f = total area of fiber contained in FRP laminate

For the triangular stress distribution, the static yielding bending moment is calculated from

$$M_{s1} = f_y \left[A_s \left(d - \frac{c}{3} \right) + A_f \frac{h-c}{d-c} \frac{E_f}{E_s} \left(h - \frac{c}{3} \right) + A'_s \frac{c-d'}{d-c} \left(\frac{c}{3} - d' \right) \right] \tag{5.5}$$

For the equivalent rectangular stress distribution, the static yielding bending moment is calculated from

$$M_{s2} = A_s f_y \left(d - \frac{a}{2} \right) + A_s' f_y \frac{ac - (a+2c)d' + 2d'^2}{2(d-c)} + A_f \alpha_{fs} f_y \frac{h-c}{d-c} \left(h - \frac{a}{2} \right) \tag{5.6}$$

where

$$c = \frac{f_y\left(A_s + A_s' + \alpha_{fs} A_f\right) + 0.85\beta_1 f_c b d}{1.7\beta_1 f_c b} - \frac{\sqrt{\left[f_y\left(A_s + A_s' + \alpha_{fs} A_f\right) + 0.85\beta_1 f_c b d\right]^2 - 3.4\beta_1 f_c f_y b\left(A_s d + A_s' d' + \alpha_{fs} A_f h\right)}}{1.7\beta_1 f_c b} \tag{5.7}$$

$$a = \beta_1 c \tag{5.8}$$

f_c = compressive strength of concrete

α_{fs} = E_f / E_s

a = depth of the rectangular compression block

$$\beta_1 = \begin{cases} 0.65 & if \quad (1.09-0.008f)_c < 0.65 \\ 0.85 & if \quad (1.09-0.008f_c) > 0.85 \\ 1.09-0.008f_c & if \quad (0.65 < 1.09-0.008f_c) < 0.85 \end{cases}$$

in which f_c is in unit MPa. (James, 1997)

5.2 Dynamic rupture bending moment and residual stiffness of the beam segment in which tensile steel bars have yielded

If, in a doubly reinforced beam, the tensile steel ratio is equal to or less than balanced steel ratio (the steel strain is exactly equal to the yielding strain when the strain in the concrete simultaneously reaches the crushing strain), the neutral axis is sufficiently high that the compression steel stress at failure is less than the yield stress, the strength of such a beam will be controlled by tensile yielding. It is known that compression failure in flexure, should it occur, gives little if any warning of distress, while a tension failure initiated by yielding of the steel is typically gradual. More importantly, in blast design, the blast overpressure on the beam is typically a very high amplitude loading but of very short duration and generally over one cycle. Blast-resistant design therefore relies on significant levels of allowable inelastic behavior. As a result, blast-resistant structures must have the ductile detailing necessary to withstand inelastic deformations and still perform acceptably. This can be done by requiring that the tension steel ratio be less than the balanced ratio. After the tensile steel bars have yielded, the bending moment corresponding to the rupture of FRP plate/sheet can be calculated as (Refer to Fig. (5.2))

$$M_r = A_s f_{dy}\left(d-\frac{a}{2}\right)+A'_s\frac{f_f}{\alpha_{fs}}\frac{c-d'}{h-c}\left(\frac{a}{2}-d'\right)+A_f f_f\left(h-\frac{a}{2}\right) \tag{5.9}$$

where

$$a = \beta_1 c \tag{5.10}$$

$$c = \frac{h}{2} + \frac{1}{1.7\beta_1 f_c b}\left\{A_s f_{dy} + \frac{A'_s}{\alpha_{fs}} f_f + A_f f_f - \sqrt{\left[A_s f_{dy} + \frac{A'_s}{\alpha_{fs}} f_f + A_f f_f + 0.85\beta_1 f_c bh\right]^2 - 3.4\beta_1 f_c f_f bh\left(\frac{A_s f_{dy}}{f_f} + \frac{A'_s d'}{\alpha_{fs} h} + A_f\right)}\right\} \quad (5.11)$$

$$f_{dy} = f_y\left(\frac{\sum_{k=1}^{i} M_{ipk} T_k(\tau_k)}{M_{is} - M_{i0}} + \frac{M_{i0}}{M_{is}}\right) \quad (5.12)$$

i = total number of dynamic stages before the time when the steel reinforcement yield at the cross-section where FRP plate/sheet ruptures.

M_{is} = static yield bending moment of the cross-section.

M_{i0} = bending moment due to the static load.

$$M_{ipk} = -pEI\left[d^2W_k/dx^2\right]\Big|_{x=x_i}, \quad k = 1, 2, \cdots i$$

x_i = coordinate of the cross-section.

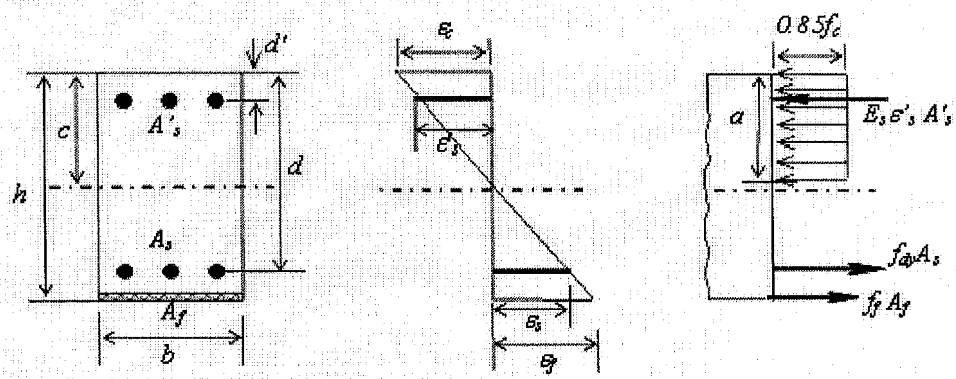

Fig. 5.2 Strain diagram and stress blocks after tensile steel bars have yielded

As shown in Fig. 5.3 (c), when the stress in FRP plate/sheet reaches the ultimate strength, only the concrete in the shaded area is remaining elastic. Therefore the remaining bending stiffness of the beam segment in which tensile steel bars have yielded can be calculated from

$$(E_c I)_y = E_c \left\{ (c_f - d')^2 \alpha_s A_s' + (h - c_f)^2 \alpha_f A_f + \frac{b(c-a_1)^3}{12} + \left[\frac{c+a_1}{2} - c_f \right]^2 (c-a_1) b \right\} \tag{5.13}$$

where c is calculated from Eq. (5.11), and

$$c_f = \frac{d'\alpha_s A'_s + h\,\alpha_f A_f + 0.5\left(c^2 - a_1^2\right)b}{\alpha_s A'_s + \alpha_f A_f + (c - a_1)b} \tag{5.14}$$

$$a_1 = \left(1 + \alpha_f \frac{f_c}{f_f}\right)c - \alpha_f \frac{f_c}{f_f} h \tag{5.15}$$

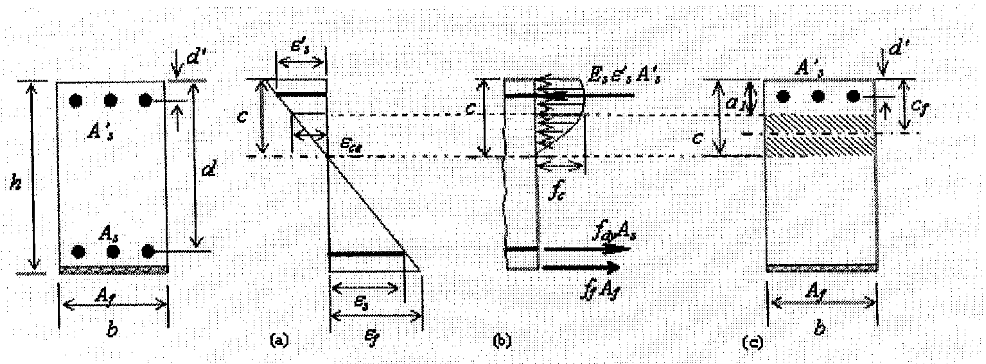

Fig. 5.3 Section to calculate residual bending stiffness after tensile steel bars have yielded

5.3 Formulae to calculate the time when first dynamic response stage terminates

To solve Eq. (5.1), the dynamic function $T(t)$ needs to be specified first. For a SDOF elastic system subjected to a blast load idealized as a triangular pulse, it is known that the dynamic function $T(t)$, with the initial conditions $T(0) = 0$ and $\dot{T}(0)=0$, has three different forms depending on the value of ωt_d (Smith and Hetherington, 1994).

In the case of $\omega t_d<0.4$, the load on the structure can be replace with the initial impulse and $T(t)$ can be expressed in the form

$$T(t)=A\sin\omega t \tag{5.16}$$

where A is calculated from

$$A=\frac{t_d}{2m\omega\int_0^L W(x)dx} \tag{5.17}$$

In the case of $\omega t_d>40$, the load on the structure can be considered as a suddenly applied constant load and $T(t)$ can be expressed in the following form

$$T(t)=1-\cos\omega t \qquad 0\le t\le t_d \tag{5.18}$$

In the case of $0.4<\omega t_d<40$

$$T(t)=1-\frac{t}{t_d}-\cos\omega t+\frac{\sin\omega t}{\omega t_d} \qquad 0\le t\le t_d \tag{5.19}$$

For RC beams strengthened with FRP plate/sheet and assuming that the steel bar yields before the FRP plate/sheet ruptures, the dynamic function $T(t)$ as shown in Eqs (5.16), (5.18) and (5.19) can be directly substituted into Eq. (5.1) and the yield delay time τ can be obtained by solving the resulting equation.

Substituting Eq. (5.16) into Eq. (5.1), the following equation is obtained

$$\left[\int_0^{\tau}\sin^{17}\omega t\ \ d(\omega t)\right]^{\frac{1}{17}}=(0.895\omega)^{\frac{1}{17}}\frac{M_s-M_0}{A\ \ M_p} \tag{5.20}$$

The function $T(t)$ and the integration in Eq. (5.20) are illustrated in Fig. 5.4.

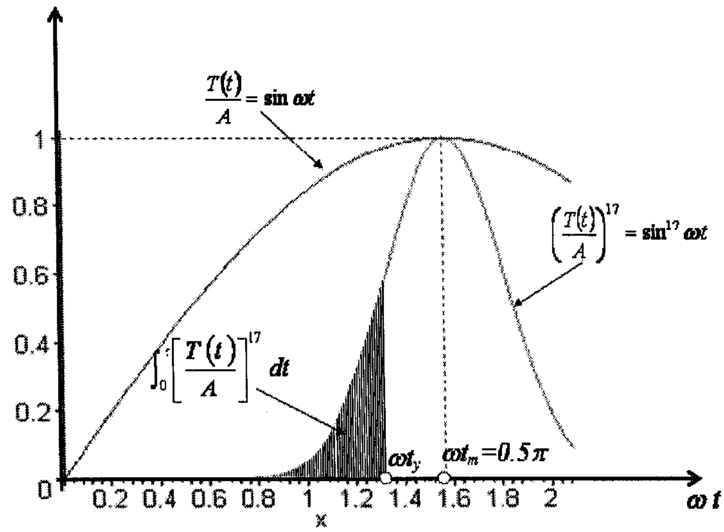

Fig. 5.4 Dynamic function, $T(t)$, for $\omega t_d<0.4$.

Integrating the left side of Eq. (5.20) directly and making some rearrangements, the following equation is obtained

$$\left[\frac{32768}{109395}-\cos\omega\tau+\frac{8}{3}\cos^3\omega\tau-\frac{28}{5}\cos^5\omega\tau+8\cos^7\omega\tau-\frac{70}{9}\cos^9\omega\tau+\frac{56}{11}\cos^{11}\omega\tau\right.$$
$$\left.-\frac{28}{13}\cos^{13}\omega\tau+\frac{8}{15}\cos^{15}\omega\tau-\frac{1}{17}\cos^{17}\omega\tau\right]^{\frac{1}{17}}=(0.895\omega)^{\frac{1}{17}}\frac{M_s-M_0}{AM_p}$$

(5.21)

The time τ when the steel reinforcement yields can be obtained by solving Eq. (5.21). The function $T(t)$ reaches its maximum value at $t_m=\pi/2$. It is assumed that τ is less than t_m. In the case of $\tau>t_m$, although there would be little plastic deformation developed in the steel reinforcement, the steel reinforcement would be considered elastic, because the stress in steel reduce very quickly for $t>t_m$.

On the other hand the inequality relation $AM_p \sin\omega\tau \geq M_s$ should hold, because dynamic strength of steel is larger than static strength. The function on the left side of Eq. (5.21) is a monotonic increasing function in the interval $0 \leq \omega\tau \leq \pi/2$ and can be accurately approximated in this interval by a rational function of which both the denominator and numerator are quadratic polynomials in the interval $[0.3, \pi/2]$. Approximating the function on the left side of Eq. (5.21) with the rational function results in

$$\frac{594+568\omega\tau+3026(\omega\tau)^2}{4826-2982\omega\tau+3862(\omega\tau)^2}=(0.895\omega)^{\frac{1}{17}}\frac{M_s-M_0}{AM_p} \tag{5.22}$$

The maximum relative error of the approximation is less than 0.3% in the interval $[0.3, \pi/2]$. Instead of solving Eq. (5.21), $\omega\tau$ may be obtained by solving Eq. (5.22)as:

$$\omega\tau=\frac{284+1491d\pm\sqrt{17744392d-1716788-16414931d^2}}{3862d-3026} \tag{5.23}$$

where

$$d=(0.895\omega)^{\frac{1}{17}}\frac{M_s-M_0}{AM_p} \tag{5.24}$$

and A is calculated from Eq. (5.17). For $\omega\tau<0.3$, i.e. $d<0.09$, $\sin\omega t$ is approximated by ωt and Eq. (5.20) reduces to

$$\omega\tau=(0.895\times18\omega)^{\frac{1}{18}}\left(\frac{M_s-M_0}{A\ M_p}\right)^{\frac{17}{18}} \tag{5.25}$$

Similarly, substituting Eq. (5.18) into Eq. (5.1) , the following equation is obtained

$$\left[\int_0^\tau(1-\cos\omega t\ )^{17}d(\omega t)\right]^{\frac{1}{17}}=(0.895\omega)^{\frac{1}{17}}\ \frac{M_s-M_0}{M_p} \tag{5.26}$$

The function $T(t)$ and the integration in Eq. (5.26) are illustrated in Fig. 5.5.

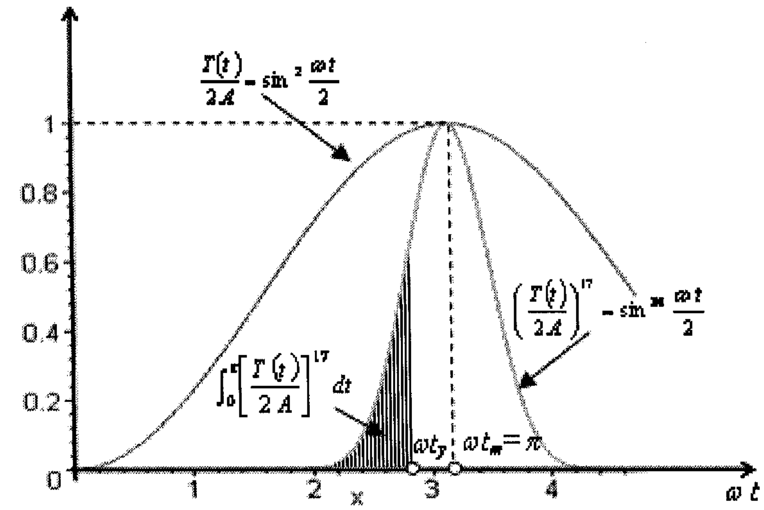

Fig. 5.5 Dynamic function, $T(t)$, for ωt_d>40.

Integrating the left side of Eq. (5.26) and making some rearrangements, the following equation is obtained

$$\left\{\left[-\frac{216320151}{7735}+\frac{583368787}{32768}\cos\omega\tau-\frac{108094328}{7735}\cos^2\omega\tau+\frac{193713521}{16384}\cos^3\omega\tau\right.\right.$$
$$-\frac{79755796}{7735}\cos^4\omega\tau+\frac{183965041}{20480}\cos^5\omega\tau-\frac{11697160}{1547}\cos^6\omega\tau+\frac{425164883}{71680}\cos^7\omega\tau$$
$$-\frac{924894}{221}\cos^8\omega\tau+\frac{23038587}{8960}\cos^9\omega\tau-\frac{1475768}{1105}\cos^{10}\omega\tau+\frac{510289}{896}\cos^{11}\omega\tau$$
$$\left.-\frac{213164}{1105}\cos^{12}\omega\tau+\frac{11135}{224}\cos^{13}\omega\tau-\frac{776}{85}\cos^{14}\omega\tau+\frac{17}{16}\cos^{15}\omega\tau-\frac{1}{17}\cos^{16}\omega\tau\right]\sin\omega\tau$$
$$\left.+\frac{583401555}{32768}\omega\tau\right\}^{\frac{1}{17}}=\left(0.895\omega\right)^{\frac{1}{17}}\frac{M_s-M_0}{M_p} \qquad (5.27)$$

Taking $\omega\tau$ as the unknown, the function on the left side of Eq. (5.27) is approximated with a rational function in the interval of $[0.5, \pi]$, as

$$\frac{-8678648+31009414\omega\tau+10196520(\omega\tau)^2}{124006493-51437644\omega\tau+13911386(\omega\tau)^2}=(0.895\omega)^{\frac{1}{17}}\frac{M_s-M_0}{M_p} \tag{5.28}$$

The maximum relative error of the approximation is less than 0.4% in the interval $[0.5, \pi]$. Solving Eq. (5.28), $\omega\tau$ may be obtained as

$$\omega\tau=\frac{257d+155\pm\sqrt{32889+194123d-106365d^2}}{139d-102} \tag{5.29}$$

where

$$d=(0.895\omega)^{\frac{1}{17}}(M_s-M_0)/M_p \tag{5.30}$$

For $\omega\tau<0.5$, i.e. $d<0.11$, $1-\cos\omega t$ is approximated by $\frac{1}{2}(\omega t)^2$ and Eq. (5.26) reduces to

$$\omega\tau=(0.895\times 70\omega)^{\frac{1}{35}}\left[(M_s-M_0)/M_p\right]^{\frac{17}{35}} \tag{5.31}$$

In the case of the dynamic function in the form of Eq. (5.18), the calculation of the integration in Eq. (5.1) would be more complicated than that of the two cases described above. Substituting Eq. (5.18) into Eq. (5.1), the following equation is obtained

$$\left[\int_0^\tau\left(1-\frac{t}{t_d}-\cos\omega t+\frac{\sin\omega t}{\omega t_d}\right)^{17}d(\omega t)\right]^{\frac{1}{17}}=(0.895\omega)^{\frac{1}{17}}\frac{M_s-M_0}{M_p} \tag{5.32}$$

The function $T(t)$ and the integration in Eq. (5.32) are illustrated in Fig. 5.6.

The maximum value of dynamic function $T(t)$ is

$$T(t_m)=2\left(1-\frac{1}{\omega t_d}\arctan\omega t_d\right) \tag{5.33}$$

where

$$t_m = \frac{2}{\omega}\arctan \omega t_d \tag{5.34}$$

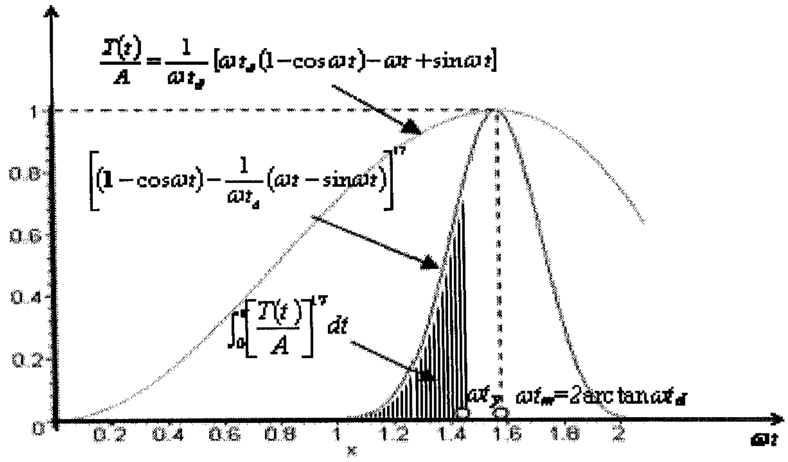

Fig. 5.6 Dynamic function, $T(t)$, for $0.4<\omega t_d<40$ (Assuming $\omega t_d = 1$).

Eq. (5.33) is applicable for $\omega t_d > 2.33$ for the condition $\omega\tau < \omega t_d$ to be satisfied. For $\omega t_d < 2.33$, the dynamic function, $T(t)$, should be expressed in the following form

$$T(t) = \begin{cases} 1 - \cos\omega t - t/t_d + \sin\omega t/\omega t_d & t \le t_d \\ \left[\sin\omega t - \sin\omega(t - t_d)\right]/\omega t_d - \cos\omega t & t > t_d \end{cases} \tag{5.35}$$

The maximum value of dynamic function $T(t)$ is

$$T(t_m) = \frac{1}{\omega t_d}\left[\sin\omega t_m - \sin\omega(t_m - t_d)\right] - \cos\omega t_m \tag{5.36}$$

where

$$\omega t_m = \pi - \arctan\left[\frac{1-\cos\omega t_d}{\omega t_d - \sin\omega t_d}\right] \tag{5.37}$$

In order to obtain similar approximate formula to calculate the yielding delay time τ, the rational function to approximate the integration on the left side of

Eq. (5.32) can be obtained by solving the following least square problem

$$\min\sum_{i=1}^{M}\sum_{j=1}^{N}\left[f\left(\omega\tau_i,\omega t_{dj}\right)-\frac{a_1\left(\omega t_{di}\right)^{c_1}+a_2\left(\omega t_{di}\right)^{c_2}\left(\omega\tau_j\right)^{e}+a_3\left(\omega t_{di}\right)^{c_3}\left(\omega\tau_j\right)^{2e}}{b_1\left(\omega t_{di}\right)^{d_1}+b_2\left(\omega t_{di}\right)^{d_2}\left(\omega\tau_j\right)^{e}+b_3\left(\omega t_{di}\right)^{d_3}\left(\omega\tau_j\right)^{2e}}\right]^2 \tag{5.38}$$

where a_k, b_k, c_k, d_k ($k=1,2,3$) and e are constants to be determined, and

$$f\left(\omega\tau,\omega t_d\right)=\left[\int_0^{\omega\tau}\left(T\left(u/\omega\right)\right)^{17}du\right]^{\frac{1}{17}} \tag{5.39}$$

and the points (ωt_{di} $\omega\tau_j$,) ($i=1\ldots M, j=1\ldots N$) may be the arbitrary points density distributed in the region of ($0<\omega\tau<\omega t_m$, $0.4<\omega t_d<40$). Using a numerical method, this least square problem is solved with a total number of 720 points in the region of ($0<\omega\tau<\omega t_m$, $0.4<\omega t_d<40$). The grid is set as

$$\left(\omega\tau_i,\omega t_{dj}\right)=\left(\frac{\omega t_m}{40}\times i,0.4+0.1165\times j\right),\quad i=6,\cdots,40;j=1,\cdots,16$$

in the region of ($0.4<\omega\tau<\omega t_m$, $0.4<\omega t_d<2.33$) where t_m is calculated from Eq. (5.37) and

$$\left(\omega\tau_i,\omega t_{dj}\right)=\left(\frac{\omega t_m}{40}\times i,\ 2.33+1.8835\times j\right),\quad i=6,\cdots,40;j=1,\cdots,20$$

in the region of ($0.5<\omega\tau<\omega t_m$, $0.4<\omega t_d<2.33$) where t_m is calculated from Eq. (5.33).

Replacing the left side of Eq. (5.32) with the obtained rational function, the following equation is obtained

$$\frac{-315\left(\omega t_d\right)^{-\frac{2}{33}}+3273\left(\omega t_d\right)^{\frac{8}{85}}\left(\omega\tau\right)^{\frac{11}{6}}-3.26\left(\omega t_d\right)^{\frac{1}{75}}\left(\omega\tau\right)^{\frac{11}{3}}}{7418\left(\omega t_d\right)^{\frac{3}{23}}+4127\left(\omega t_d\right)^{-\frac{13}{10}}\left(\omega\tau\right)^{\frac{11}{6}}+127\left(\omega t_d\right)^{-\frac{1}{75}}\left(\omega\tau\right)^{\frac{11}{3}}}=\left(0.895\omega\right)^{\frac{1}{17}}\frac{M_s-M_0}{M_p} \tag{5.40}$$

The difference between the specified set of data, $f\left(\omega\tau_i,\omega t_{dj}\right)$ (calculated from

Eq. (5.39)), and the simulated one, $\hat{f}\left(\omega\tau_i, \omega t_{dj}\right)$, is assessed by calculating the normalized error,

$$\sqrt{\sum_{i=6}^{40}\sum_{j=1}^{36}\left[f\left(\omega\tau_i, \omega t_{dj}\right)-\hat{f}\left(\omega\tau_i, \omega t_{dj}\right)\right]^2} \Bigg/ \sqrt{\sum_{i=6}^{40}\sum_{j=1}^{36}\left[f\left(\omega\tau_i, \omega t_{dj}\right)\right]^2} = 0.015$$

The maximum relative error of the approximation is less than 5% in the region of $(0.6 < \omega\tau < \omega t_m,\ 0.4 < \omega t_d < 2.33)$.

Solving Eq. (5.40) results in

$$\omega\tau = \frac{1}{\left(0.0652u^{\frac{1}{75}} + 2.54d\ u^{-\frac{1}{75}}\right)^{\frac{6}{11}}}\left\{32.73u^{\frac{8}{85}} - 41.27d\ u^{-\frac{13}{10}} \pm \sqrt{\left(1703u^{-\frac{13}{5}} - 377u^{\frac{1}{9}}\right)d^2 - \left(2702u^{-\frac{6}{5}} + 9.67u^{\frac{1}{7}} + 16u^{-\frac{1}{14}}\right)d + 1071u^{\frac{16}{85}} - 0.411u^{\frac{1}{21}}}\right\}^{\frac{6}{11}} \quad (5.41)$$

where

$$u = \omega t_d \quad (5.42)$$

and

$$d = \left(0.895\omega\right)^{\frac{1}{17}}\left(M_s - M_0\right)/M_p \quad (5.43)$$

For $\omega\tau < 0.6$, the dynamic function, $T(t)$, can be approximated by a linear function, as

$$T(t) \approx \frac{5\omega t}{3}T\left(0.6/\omega\right) \quad (5.44)$$

where the value of $T\left(0.6/\omega\right)$ is calculated from Eq. (5.35) and the equation to determine $\omega\tau$ is

$$\frac{5}{2}\times 18^{-\frac{1}{17}}T\left(\frac{0.6}{\omega}\right)(\omega\tau)^{\frac{18}{17}}=(0.895\omega\ )^{\frac{1}{17}}\frac{M_s-M_0}{M_p}$$

i.e.

$$\omega\tau=(18\times 0.895\omega)^{\frac{1}{18}}\left[3(M_s-M_0)/\left[5M_pT(0.6/\omega)\right]\right]^{\frac{17}{18}} \tag{5.45}$$

5.4 Formulae to calculate the time when k^{th} dynamic response stage terminates

5.4.1 Dynamic functions of k^{th} dynamic response stage

As mentioned in Section 3.1, the beam deforms firstly according to $w(x,t)=W_1(x)T_1(t)$ until the time τ_1 when steel reinforcement at the cross-section has yielded and a plastic hinge or an elastic hinge appears. After time τ_1, the beam will deform further in a new elastic stage if there are insufficient plastic hinges in the beam to make it a freely movable mechanism. Otherwise the beam will deform in the plastic stage. Following with the procedure discussed in Section 3.1, the static deformation $W_i(x)$ of the new elastic system, in which $(i-1)$ plastic/elastic hinges appeared, can be calculated and then the circular frequency of the equivalent SDOF system can be calculated.

For $t<t_d$, the dynamic function $T_i(t)$ would be in the following three possible forms:

- In the case of $\omega_i(t_d-\tau_{i-1})<0.4$, the load on the structure can be replaced with the initial impulse and $T_i(t)$ expressed in the form

$$T_i(t)=A_i\sin\omega_i(t-\tau_{i-1}) \tag{5.46}$$

where A_i is determined with the condition

$$\frac{1}{2t_d}(t_d-\tau_{i-1})^2+m\dot{T}_{i-1}(\tau_{i-1})\int_0^L W_{i-1}(x)dx=m\dot{T}_i(\tau_{i-1})\int_0^L W_i(x)dx$$

i.e.

$$A_i=\frac{1}{m\omega_i\int_0^L W_i(x)dx}\left[\frac{1}{2t_d}(t_d-\tau_{i-1})^2+m\dot{T}_{i-1}(\tau_{i-1})\int_0^L W_{i-1}(x)dx\right] \tag{5.47}$$

- In the case of $\omega(t_d-\tau_{i-1})>40$, the load on the structure can be considered as a suddenly applied constant load and $T_i(t)$ can be expressed in the following form

$$T_i(t)=1-\cos\omega_i(t-\tau_{i-1})+B_i\sin\omega_i(t-\tau_{i-1}),\quad t>\tau_{i-1} \tag{5.48}$$

where B_i is determined from

$$m\dot{T}_{i-1}(\tau_{i-1})\int_0^L W_{i-1}(x)dx=m\dot{T}_i(t_{i-1})\int_0^L W_i(x)dx$$

i.e.

$$B_i=\dot{T}_{i-1}(\tau_{i-1})\int_0^L W_{i-1}(x)dx\Big/\omega_i\int_0^L W_i(x)dx \tag{5.49}$$

In the case of $0.4<\omega(t_d-\omega\tau_{i-1})<40$ and for $t<t_d$

$$T_i(t)=1-t/t_d-\sum_{j=1}^{i-1}T_j(\tau_j)+C_i\,sin\,\omega_i(t-\tau_{i-1})-D_i\,cos\,\omega_i(t-\tau_{i-1}) \tag{5.50}$$

where C_i and D_i are calculated from

$$C_i=\frac{1}{\omega_i}\left(\frac{1}{t_d}+\dot{T}_{i-1}(\tau_{i-1})\int_0^L W_{i-1}(x)dx\Big/\int_0^L W_i(x)dx\right) \tag{5.51}$$

$$D_i=1-\tau_{i-1}/t_d-\sum_{j=1}^{i-1}T_j(\tau_j) \tag{5.52}$$

For $t>t_d$ the dynamic function, $T_i(t)$ is in the following form

$$T_i(t)=-\sum_{j=1}^{i-2}T_j(\tau_j)-T_{i-1}(t_d)+C_i\sin\omega_i(t-t_d)-D_i\cos\omega_i(t-t_d) \tag{5.53}$$

where C_i and D_i are calculated from

$$C_i = \dot{T}_{i-1}(t_d)/\omega_i \tag{5.54}$$

$$D_i = -\sum_{j=1}^{i-2} T_j(\tau_j) - T_{i-1}(t_d) \tag{5.55}$$

and the time when dynamic function, $T_i(t)$, reaches its maximum value can be calculated from

$$t_m = t_d - \frac{1}{\omega_i}\arctan\frac{C_i}{D_i}, \qquad t_m > t_d \tag{5.56}$$

5.4.2 Formulae to calculate the time when k^{th} dynamic response stage terminates due to the bending failure of the critical cross-section without strain rate effect

As the beam deforms further, the external FRP plate/sheet or the steel reinforcement at some cross-section will rupture or yield. The bending moment of a cross-section in the beam can be expressed as

$$M_i(t) = M_{i0} + \sum_{k=1}^{i-1} ik\, M_{ipk} T_k(\tau_k) + M_{ipi} T_i(t) \qquad i = 1, 2, \ldots \tag{5.57}$$

where M_{ipk} , $k = 1,\ 2\ ,\ \ldots\ ,\ i$ are the amplitudes of dynamic bending moments at the i^{th} cross-section during k^{th} stage and M_{i0} is the initial static bending moment at the i^{th} cross-section.

If the i^{th} deformation stage is terminated due to rupture of the FRP plate/sheet at i^{th} cross-section, the time τ_i can be obtained by solving the following equation

$$T_i(\tau_i) = \frac{1}{M_{ipi}}\left[M_{ir} - M_{i0} - \sum_{k=1}^{i-1} ik\, M_{ipk} T_k(\tau_k)\right] \tag{5.58}$$

where M_{ir} is the bending moment of the i^{th} cross-section corresponding to the rupture stress of FRP plate/sheet, which can be calculated from Eq. (5.9).

So that

- In the case of $\omega(t_d - \tau_{i-1})<0.4$, substituting Eq. (5.46) into Eq. (5.58), the equation to calculate the time τ_i can be easily derived as

$$\tau_i = \tau_{i-1} + \frac{1}{\omega_i}\arcsin\left\{\left(M_{ir} - M_{i0} - \sum_{k=1}^{i-1} M_{ipk} T_k(\tau_k)\right) \Big/ A_i M_{ipi}\right\} \tag{5.59}$$

where A_i is calculated from Eq. (5.47).

- In the case of $\omega(t_d - \tau_{i-1}) > 40$, substituting Eq. (5.48) into Eq. (5.58), the equation to calculate the time τ_i is obtained

$$\tau_i = \tau_{i-1} + \frac{1}{\omega_i}\left[\frac{\pi}{2} - \arctan\frac{1-c+B_i\sqrt{1+B_i^2-(1-c)^2}}{1+B_i^2}\right] \tag{5.60}$$

where B_i is calculated with Eq. (5.49) and

$$c = \frac{1}{M_{ipi}}\left[M_{ir} - M_{i0} - \sum_{j=1}^{i-1} ik\, M_{ipk} T_k(\tau_k)\right] \tag{5.61}$$

In the case of $0.4 < \omega(t_d - \tau_{i-1}) < 40$, substituting Eq. (5.50) into Eq. (5.58), the equation to determine the time τ_i is obtained as

$$D_i\left[1-\cos\omega_i(\tau_i - \tau_{i-1})\right] + C_i \sin\omega_i(\tau_i - \tau_{i-1}) - \frac{\tau_i - \tau_{i-1}}{t_d} = \frac{1}{M_{ipi}}\left[M_{ir} - M_{i0} - \sum_{j=1}^{i-1} ik\, M_{ipk} T_k(\tau_k)\right] \tag{5.62}$$

where C_i, D_i can be calculated from Eqs. (5.51) and (5.52).

Eq. (5.62) can be rewritten as

$$1 - \cos x + A \sin x - x/B = C \tag{5.63}$$

where $x = \omega_i(\tau_i - \tau_{i-1})$ is the unknown and

$$A = C_i/D_i \tag{5.64}$$
$$B = D_i\omega_i t_d \tag{5.65}$$
$$C = \frac{1}{D_i M_{ipi}}\left[M_{ir} - M_{i0} - \sum_{j=1}^{i-1} M_{ipj}T_j(\tau_j)\right] \tag{5.66}$$

Eq. (5.63) can only be solved using an approximate method. To calculate the approximate value of x in Eq. (5.63), the function on the left side of Eq. (5.63) is replaced with its *Pade* (Brezinski and Iseghem, 1994) approximation with both the numerator and denominator as quadratic polynomials. Thus, the approximate value of x is obtained as

$$x = \frac{1}{2a}\left(-b \pm \sqrt{b^2 - 4ac}\right) \tag{5.67}$$

where

(i) for $x < 1$

$$a = B^2(18 - 3C)(A^2 + 1) - A^2B^2C - 12AB - 6$$

$$b = 6\left[AB^2(4A^2 - C + 6) - B(8A^2 + C + 6) + 4A\right]$$

$$c = 12BC(2A - 2A^2B - 3B)$$

(ii) for $|x - \pi/2| < 1$

$$a = -360A^3B^2 + 36(2(1-C)B^2 - \pi B)A^2 + 48(6B - 7B^2 + 3)A + 96(1-C)B^2 - 48\pi B$$

$$\begin{aligned} b =\ & 360\pi A^3B^2 + \left[72(10 + \pi(C-1))B + 36(\pi^2 - 28)\right]BA^2 \\ & + 24\left[2(7\pi + 3C - 3)B^2 + 3(2C - 2 - 3\pi)B - 3\pi\right]A \\ & + 96\left[\pi(C-1) + 6\right]B^2 + 48(\pi^2 - 24)B + 576 \end{aligned}$$

$$\begin{aligned} c =\ & (864 - 90\pi^2)A^3B^2 + \left[\left((864 + 18\pi^2)(1-C) - 360\pi\right)B + 9\pi(8-\pi)\right]BA^2 \\ & + \left[(72\pi(1-C) + 576 - 84\pi^2)B + 72\pi(1-C) - 576 - 39\pi^2\right]AB \\ & + \left[24\pi^2 - 288\pi + 576 - (24\pi^2 + 576)C\right]B^2 - \left[576(1-C) - 288\pi + 12\pi^2\right]B^2 \end{aligned}$$

The formula to calculate the approximate value of x determined by Eq. (5.63) can also be obtained by expanding x as the power series of C for $C \ll 1$ in the following form

$$u_i = \omega_i\left(\tau_i - \tau_{i-1}\right) = \frac{BC}{(AB-1)}\left(1 - \frac{B^2C}{2(AB-1)^2} + \frac{B^3C^2\left(A^2B - A + 3B\right)}{6(AB-1)^4}\right) \tag{5.68}$$

The error of Eq. (5.68) is of the same order as C^4. After the value of x is determined, the time τ_i, when the FRP plate/sheet rupture, can be easily calculated from

$$\tau_i = \tau_{i-1} + x/\omega_i \tag{5.69}$$

If the maximum dynamic bending moment in the structure is not large enough to cause FRP plate/sheet rupture, Eq. (5.63) would have no positive solution. The time when the dynamic function $T_i(t)$ reaches its maximum value can be calculated as

$$t_m = \tau_{i-1} \pm \frac{1}{\omega_i}\left(\pm \arccos\frac{1}{B\sqrt{1+A^2}} + \arccos\frac{A}{\sqrt{1+A^2}}\right) \tag{5.70}$$

The maximum value of the dynamic function is $T_i(t_m)$ which can be calculated from Eq. (5.50).

5.4.3 Formulae to calculate the time when k^{th} dynamic response stage terminates due to the shear failure of the critical cross-section without strain rate effect

It is also possible that the i^{th} elastic deformation stage terminates with the shear failure of a cross-section. Calculation of the time of shear failure of a cross-section is similar to the formula for the calculation of the time when a cross-section fails caused by the rupture of the external FRP plate/sheet. The shear force of a cross-section in the beam can be expressed as

$$V_i(t) = V_{i0} + \sum_{k=1}^{i-1} V_{ipk} T_k(\tau_k) + V_{ipi} T_i(t) \qquad i = 1,\ 2,\ \ldots \tag{5.71}$$

where V_{ipk} , $k = 1,\ 2$, ... , i are the amplitudes of dynamic shear force at the i^{th} cross-section during k^{th} stage and V_{i0} is the initial static shear force.

If the i^{th} deformation stage is terminated due to shear failure at i^{th} cross-section, the time τ_i can be obtained by solving the following equation

$$T_i(\tau_i) = \frac{1}{V_{ipi}} \left[V_{is} - V_{i0} - \sum_{j=1}^{i-1} ik\, V_{ipj} T_j(\tau_j) \right] \tag{5.72}$$

where V_{is} is the failure shear force of the i^{th} cross-section.

So that

- In the case of $\omega(t_d - \tau_{i-1})<0.4$, the formula to calculate the time τ_i is

$$\tau_i = \tau_{i-1} + \frac{1}{\omega_i} \arcsin\left\{ \frac{1}{A_i V_{ipi}} \left[V_{is} - V_{i0} - \sum_{j=1}^{i-1} ik\ V_{ipk} T_k(\tau_k) \right] \right\} \tag{5.73}$$

where A_i is calculated from Eq. (5.47).

- In the case of $\omega(t_d - \tau_{i-1})>40$, the formula to calculate the time τ_i is

$$\tau_i = \tau_{i-1} + \frac{1}{\omega_i} \left[\frac{\pi}{2} - \arctan \frac{1 - c + B_i \sqrt{1 + B_i^2 - (1-c)^2}}{1 + B_i^2} \right] \tag{5.74}$$

where B_i is calculated from Eq. (5.49) and

$$c = \frac{1}{V_{ipi}} \left[V_{if} - V_{i0} - \sum_{j=1}^{i-1} V_{ipj} T_j(\tau_j) \right] \tag{5.75}$$

- In the case of $0.4<\omega(t_d - \tau_{i-1})<40$, the equation to determine the time τ_i is

$$C_i \sin \omega_i(\tau_i - \tau_{i-1}) + D_i\left[1 - \cos \omega_i(\tau_i - \tau_{i-1})\right] - \frac{\tau_i - \tau_{i-1}}{t_d} = \frac{1}{V_{ipi}} \left[V_{is} - V_{i0} - \sum_{j=1}^{i-1} ik\, V_{ipk} T_k(\tau_k) \right] \tag{5.76}$$

where C_i and D_i are calculated from Eq. (5.51) and (5.52).

Eq. (5.76) is in the same form of Eq. (5.63). Therefore τ_i can be calculated from Eq. (5.69) and x in Eq. (5.69) is calculated from Eq. (5.67) or Eq. (5.68), in which the value of C is calculated from

$$C = \frac{1}{D_i V_{ipi}} \left[V_{is} - V_{i0} - \sum_{k=1}^{i-1} V_{ipk} T_k(\tau_k) \right] \tag{5.77}$$

5.4.4 Formulae to calculate the time when k^{th} dynamic response stage terminates due to the yielding of tension steel bars at the critical cross-section with strain rate effect

If the i^{th} $(i>1)$ elastic deformation stage is terminated at the time when the steel reinforcement yield at a cross-section, the strain rate effect should be taken into account. The yielding delay time, τ_i, of the reinforcement at this cross-section is obtained by solving Eq. (5.1).

Substituting Eq. (5.57) into Eq. (5.1) results in

$$\begin{aligned} &\int_0^{\tau_1} \left[M_{ip1} T_1(t) \right]^{17} dt + \sum_{j=2}^{i-1} \int_{\tau_{j-1}}^{\tau_j} \left[\sum_{k=1}^{j-1} ik\, M_{ipk} T_k(\tau_k) + M_{ipj} T_j(t) \right]^{17} dt \\ &+ \int_{\tau_{i-1}}^{\tau_i} \left[\sum_{k=1}^{i-1} ik\, M_{ipk} T_k(\tau_k) + M_{ipi} T_i(t) \right]^{17} dt = 0.895 (M_{is} - M_{i0})^{17} \end{aligned} \tag{5.78}$$

For simplicity, the dynamic function, $(T_j(t), j = 2,3,...,i)$, is approximated with a linear function. Therefore, the integration on the time interval $[\tau_{j-1}, \tau_j]$ can be calculated as

$$\int_{\tau_{j-1}}^{\tau_j}\left[\sum_{k=1}^{j-1} M_{ipk}T_k(\tau_k)+M_{ipj}T_j(t)\right]^{17} dt=\frac{1}{\omega_j}\left[\sum_{k=1}^{j-1} ik\,M_{ipk}T_k(\tau_k)\right]^{17}\int_{\tau_{j-1}}^{\tau_j}\left[1+\frac{u}{u_j}\frac{M_{ipj}T_j(\tau_j)}{\sum_{k=1}^{j-1} ik\,M_{ipk}T_k(\tau_k)}\right]^{17} dt$$

$$=\frac{u_j}{18\omega_j M_{ipj}T_j(\tau_j)}\left[\sum_{k=1}^{j-1} ik\,M_{ipk}T_k(\tau_k)\right]^{18}\left[\left(1+\frac{M_{ipj}T_j(\tau_j)}{\sum_{k=1}^{j-1} M_{ipk}T_k(\tau_k)}\right)^{18}-1\right],\quad j=2,3,\ldots i$$

(5.79)

where

$$u_j=\omega_j\left(\tau_j-\tau_{j-1}\right)\qquad j=2,\ldots,i \tag{5.80}$$

Eq. (5.78) can be rewritten as

$$\frac{u_i\left[\sum_{k=1}^{i-1} ik\,M_{ipk}T_k(\tau_k)\right]^{18}}{18\omega_i M_{ipi}T_i(\tau_i)}\left[\left(1+\frac{M_{ipi}T_i(\tau_i)}{\sum_{k=1}^{i-1} ik\,M_{ipk}T_k(\tau_k)}\right)^{18}-1\right]=0.895\left(\frac{M_{is}-M_{i0}}{A_{ii}}\right)^{17}\times$$

$$\left[1-\left(\frac{M_{i1}M_{1s}}{M_{is}M_{11}}\right)^{17}\right]-\sum_{j=2}^{i-1}\left(\frac{M_{ipj}}{A_{ii}}\right)^{17}\frac{u_j\left[\sum_{k=1}^{j-1} ik\,M_{ipk}T_k(\tau_k)\right]^{18}}{18\omega_j M_{ipj}T_j(\tau_j)}\left[\left(1+\frac{M_{ipj}T_j(\tau_j)}{\sum_{k=1}^{j-1} ik\,M_{ipk}T_k(\tau_k)}\right)^{18}-1\right]$$

(5.81)

or simply as

$$\frac{u_i}{x}\left[(1+x)^{18}-1\right]=d \tag{5.82}$$

where

$$x=M_{ipi}T_i(\tau_i)\Big/\sum_{k=1}^{i-1} ik\,M_{ipk}T_k(\tau_k) \tag{5.83}$$

$$d = 0.895\times 18\omega_i \left(\frac{M_{is} - M_{i0}}{\sum_{k=1}^{i-1} ik\, M_{ipk} T_k(\tau_k)} \right)^{17} \left[1 - \left(\frac{M_{ip1}}{M_{1p1}} \frac{M_{1s}}{M_{is}} \right)^{17} \right] - \sum_{j=2}^{i-1} \frac{\omega_i u_j}{\omega_j} \frac{\sum_{k=1}^{j-1} ik\, M_{ipk} T_k(\tau_k)}{M_{ipj} T_j(\tau_j)} \left(\frac{\sum_{k=1}^{j-1} ik\, M_{ipk} T_k(\tau_k)}{\sum_{k=1}^{i-1} ik\, M_{ipk} T_k(\tau_k)} \right)^{17} \left[\left(1 + \frac{M_{ipj} T_j(\tau_j)}{\sum_{k=1}^{j-1} ik\, M_{ipk} T_k(\tau_k)} \right)^{18} - 1 \right] \tag{5.84}$$

If u_i is very small, it can be approximated by linear function of $T_i(\tau_i)$ as

$$u_i = \frac{\omega_i t_d}{(C_i \omega_i t_d - 1)} T_i(\tau_i) \tag{5.85}$$

Using Eq. (5.83), u_i is expressed as a linear function of x, as

$$u_i = \frac{\omega_i t_d \sum_{k=1}^{i-1} M_{ipk} T_k(\tau_k)}{(C_i \omega_i t_d - 1) M_{ipi}} x \tag{5.86}$$

Substituting Eq. (5.86) into Eq. (5.82), the following equation is obtained

$$\left[(1+x)^{18} - 1 \right] = d\,(C_i \omega_i t_d - 1) M_{ipi} \Big/ \omega_i t_d \sum_{k=1}^{i-1} M_{ipk} T_k(\tau_k) \tag{5.87}$$

Solving Eq. (5.87) results in

$$x = \left(d\,(C_i \omega_i t_d - 1) M_{ipi} \Big/ \omega_i t_d \sum_{k=1}^{i-1} M_{ipk} T_k(\tau_k) + 1 \right)^{\frac{1}{18}} - 1 \tag{5.88}$$

The dynamic function $T_i(\tau_i)$ can be calculated from

$$T_i(\tau_i) = \frac{x}{M_{ipi}} \sum_{k=1}^{i-1} M_{ipk} T_k(\tau_k) \tag{5.89}$$

and the time τ_i when steel bars yield can be calculated from

$$\tau_i = \tau_{i-1} + \frac{x\, t_d \sum_{k=1}^{i-1} M_{ipk} T_k(\tau_k)}{(C_i \omega_i t_d - 1) M_{ipi}} \left(1 - \frac{x\,(\omega_i t_d)^2 \sum_{k=1}^{i-1} M_{ipk} T_k(\tau_k)}{2 (C_i \omega_i t_d - 1)^2 M_{ipi}} \right) \tag{5.90}$$

It should be noticed that it is possible that i^{th} cross-section does not yield. The time when the dynamic function $T_i(t)$ reaches its maximum value is

$$t_m = \tau_{i-1} + \frac{1}{\omega_i}\left(\arccos\frac{1}{B\sqrt{A^2+1}} + \arccos\frac{A}{\sqrt{A^2+1}}\right) \tag{5.91}$$

where A and B are calculated from Eqs. (5.64) and (5.65) respectively.

The condition to determine whether the solution corresponds to the state of the i^{th} cross-section yielding is

$$\tau_i < t_m \tag{5.92}$$

If Eq. (5.92) is not satisfied, the i^{th} cross-section never yields and the structure will vibrate elastically from the time of τ_{i-1}.

Chapter 6

FAILURE CRITERIA FOR DESIGN OF REINFORCED CONCRETE MEMBERS

Reinforced concrete, when properly detailed, is generally preferred for blast-resistant structures. Usually it is expected that the concrete element is capable of undergoing large plastic deformation without suffering unacceptable damage. This requires careful detailing of members and connections. To ensure ductile behavior of concrete element subjected to blast loading, two changes in reinforcement layout when compared with 'conventional' design must be made (Smith and Hetherington, 1994). Firstly, the element should be reinforced symmetrically, which enables the compression reinforcement to carry all the compressive stresses once concrete in the compression zone has crushed and spalled. Secondly, the main flexural steel and enclosed concrete should be 'laced' together using an arrangement such as that shown in Fig. 6.1. This method allows the strain-hardening region of the steel stress/strain behavior to be fully developed and mobilizes the shear strength of the tensile steel and core concrete. It also has the effect of restraining the compression reinforcement from buckling and helps to spread out any effects of non-uniform loading.

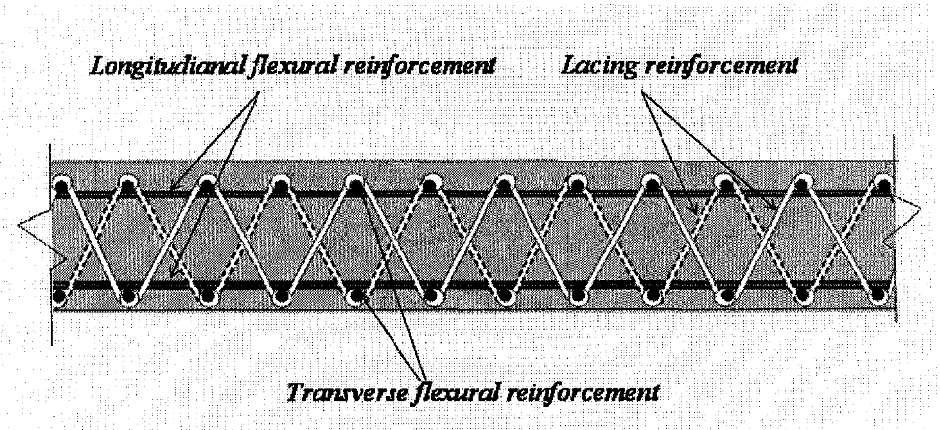

Fig. 6.1 Typical laced reinforcement arrangement

Failure modes of a reinforced beam subjected to blast loading can be illustrated by Fig. 6.2. Since the failure modes of the concrete element corresponding to shear, or FRP plate/sheet delamination or concrete debonding is relatively brittle, it is essential to provide appropriate reinforcement at and near supports to prevent shear failure. Some FRP plugs should be provided to prevent FRP plate/sheet delamination and concrete debonding. However, the shear stresses corresponding to the failure modes of shear, or FRP plate/sheet delamination or concrete debonding should be calculated and compared to the strengths of these failure modes in every dynamic response stage.

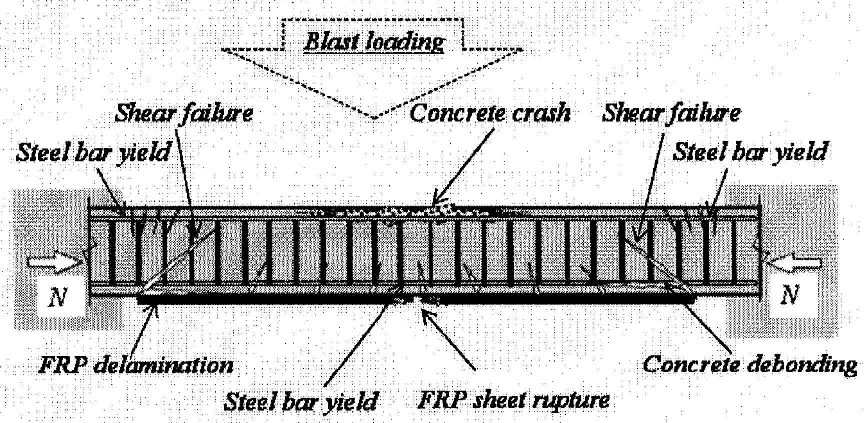

Fig. 6.2 Failure modes of RC beam strengthened with FRP plate/sheet

Concrete would fail in the compression zone of the cross-section before large plastic strain is developed in the steel reinforcement if the concrete beam is over-reinforced. In this case, the initial design should be modified to reduce the compressive stress in the cross-section. If the concrete beam is not over-reinforced, large cracks may appear in the vicinity of plastic hinges and the plastic strain in steel reinforcement in the vicinity of these plastic hinges would increase until the concrete in the compression zone fails due to the reduce area in the compression zone.

This thesis focuses on developing the algorithm and formulae to calculate the response of structures subjected to air-blast load using the SDOF method. The failure criteria of the structural member subjected to air-blast load should be specified before the analysis so that design could be carried out efficiently. For the convenience of describing the calculation and design procedure of structures subjected to air-blast load, some of the criteria based on the static analysis are listed in this chapter. A comprehensive review of loading rate effect on reinforcing steel by Malvar (Malver, 1990) indicated that the modulus of elasticity and ultimate strain remain nearly constant. Therefore, the criteria based on static theory may be used approximately in dynamic analysis and design of structures subjected to air-blast load.

6.1 Criteria for flexure failure

Fig. 6.3 shows the vicinity of a plastic hinge developed in a concrete beam. As mentioned in Section 3.1, the length of the plastic hinge at the yielded zone is assumed as $40d_s$, where d_s is the diameter of the steel bars. The relative rotation angle of two cross-sections at the ends of the plastic interval is defined as the rotation angle of the plastic hinge. This rotation angle of the plastic hinge in the bending concrete beam is usually taken as the control value to determine the plastic limit state. The condition to generate n plastic hinges in a beam is (Боданский, 1974)

$$\psi_i \le \psi_{di} \qquad i = 1,..,n \tag{6.1}$$

where ψ_i is the rotation angle of the i^{th} plastic hinge obtained from the dynamic analysis and ψ_{di} is the plastic rotation capacity of the i^{th} plastic hinge.

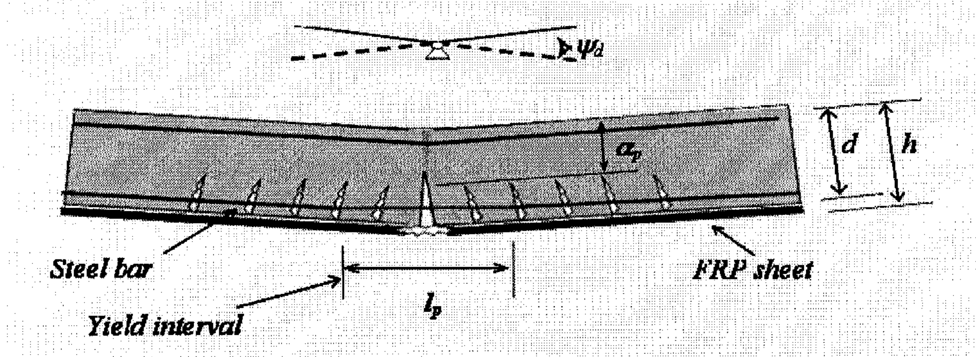

Fig. 6.3 Cracked cross-section after tensile steel bars have yielded

The plastic rotation capacity, ψ_{di} is determined by the relative height of the compression zone of the cross-section. It can be calculated approximately from the following empirical equation (Боданский, 1974)

$$\psi_d = 0.035 + \frac{0.003}{\alpha_p} \tag{6.2}$$

where

$$\psi_d = 0.035 + 0.003/\alpha_p \tag{6.3}$$

$$\alpha_p = \frac{f_s}{f_c}\rho \tag{6.4}$$

$$\rho = \frac{A_s}{bd} \tag{6.5}$$

d = effective depth of beam's cross-section

f_s = tensile strength of reinforcing steel

f_c = compression strength of concrete

A_s = area of tension steel

b = width of beam's cross-section

6.2 Criteria for shear failure

The shear failure of a concrete beam subjected to air blast loading usually results in instantaneous collapse. Therefore, the structural member in a blast resistant structure should be designed to guarantee that there is no plastic deformation developed in shear reinforcement during the period when the structure is subjected to air-blast loading. The criteria for shear failure may be written as:

$$V \le V_u \tag{6.6}$$

where V is the shear force due to blast load and V_u is the ultimate shear resistance of the beam.

Referring to Fig. 6.4, the formulae to calculate ultimate shear resistance is (Mosley and Bungey, 1990)

$$V_u = 0.87 f_{yv} A_{sv} + 1.23 f_{yv} A_{sb} \tag{6.7}$$

where

f_{yv} = characteristic strength of the stirrup reinforcement

A_{sv} = cross-sectional area of the two legs of stirrup

A_{sb} = Cross-sectional area of the bent-up bar

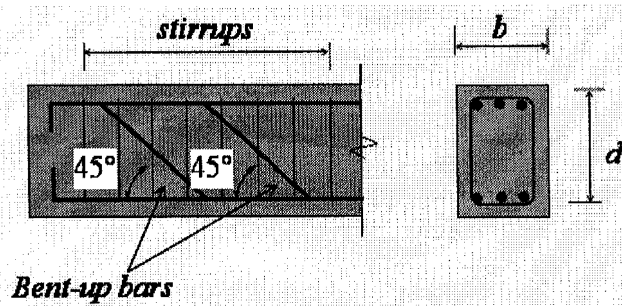

Fig. 6.4 Beam with stirrups and bent-up bars

6.3 Criteria for FRP plate delamination

Shear strength of the adhesive or interface between adhesive and concrete is critical for the success of the FRP plate strengthening technique. As shown in Fig. 6.5, it is assumed that the maximum shear stress occurred at the plate end or at the crack due to stress concentration. The criteria for FRP plate delamination can be written as:

$$\tau_0 < \tau_a \tag{6.8}$$

where τ_0 is the maximum shear stress in the adhesive layer and τ_a is the strength of FRP plate-adhesive-concrete surface, which can be determined by the double lap test (Sharif, et. al., 1994).

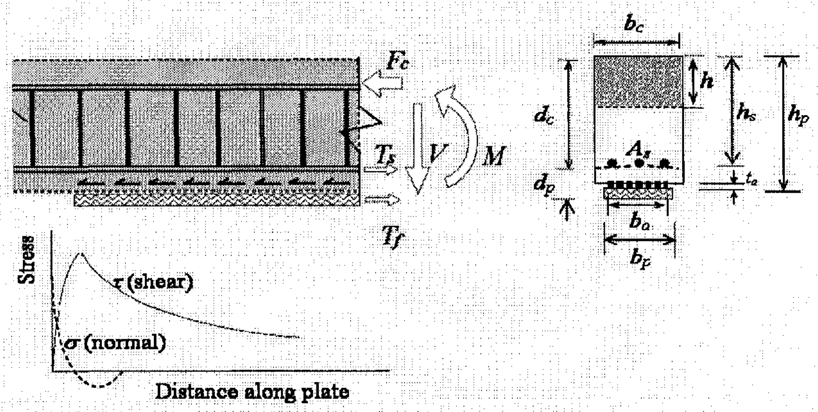

Fig. 6.5 Shear and normal stresses in adhesive joint

The maximum shear stress (τ_0) at the end of FRP plate can be calculated from (Nguyen, 2001):

$$\tau_0 = \frac{1}{l_p b_p}\frac{\beta^2}{\alpha^2}\left[V_0 + \left(\frac{2M_0}{l_p}\alpha - \frac{q\,l_p}{4\alpha}\right)\right] \tag{6.9}$$

where

b_p = width of the FRP plate

l_p = length of FRP plate

$$\alpha^2 = \frac{G_a}{4E_p}\frac{l_p^2}{t_p t_a}\left[1 + \rho_{p0}\frac{E_p}{E_c}\left(1 + \frac{A h_p h_c}{I}\right)\right] \tag{6.10}$$

$$\beta^2 = \frac{G_a}{4E_c}\frac{l_p^3 h_c b_a}{I\,t_a} \tag{6.11}$$

$$\rho_{p0} = \frac{b_p t_p}{A} \tag{6.12}$$

V_0 = shear force of the beam at the position at the end of FRP plate.

M_0 = bending moment at the position at the end of FRP plate.

h_p	=	distance from the center of FRP plate to the neutral axis of the reinforced concrete beam.
h_c	=	distance from concrete tension face to the neutral axis of the reinforced concrete beam.
G_a	=	shear modulus of adhesive.
I_e	=	second moment of area of equivalent cracked cross-section transformed to FRP material.
d_c	=	effective depth of beam's cross-section.
d_p	=	distance from steel bars to FRP plate.
b_a	=	width of the adhesive layer.
t_a	=	thickness of the adhesive layer.
t_p	=	thickness of the FRP plate.
E_c	=	Young's modulus of concrete
A	=	equivalent area of reinforced concrete section

Cracking is one of the major characteristics of concrete members that affect analysis and design procedures. Cracks play a significant role in the redistribution of interfacial shear stresses. A theoretical study shows that shear stresses at cracks are large and it may lead to local failure (Malek, et. al, 1998). Considering the interface shear stress between two adjacent cracks (Fig. 6.6), it is understandable that shear stress will increase if the tensile stress of FRP plate at cracks were to increase. When the interface stresses exceeds the bond strength of the specific adhesive, the bond between FRP plate and concrete will fail and the debonding of FRP plate will occur. This leads to an instant increase of tensile stress of the FRP plate nearby and results in further debonding. This bond failure is brittle, and if there are no extra anchorage (FRP plugs) between concrete and FRP plate, the FRP plate will delaminate from concrete surface. The beam loses load-carrying capacity suddenly. It should be noted that debonding of FRP plate usually occurs well before rupture of FRP plate if there is no extra anchorage (FRP plugs) besides the adhesive materials.

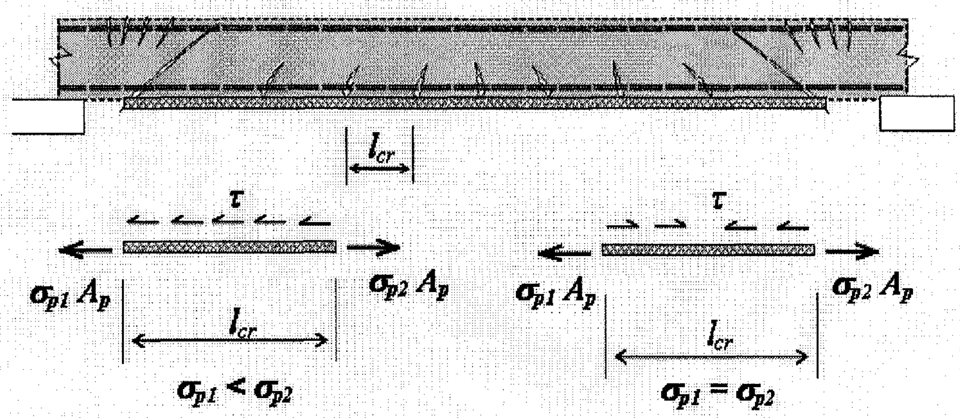

Fig. 6.6 Local tangential stresses due to initial cracking of concrete

The local tangential stress due to initial cracking of concrete can be calculated from (Malek, et. al, 1998)

$$\tau_m = \frac{b_p d_p}{b} \frac{V_m}{I}\left(h_p - h\right) + 2e^{-\gamma x_m}\left[\left(f_{20}\gamma + m_{20}\gamma^2\right)\cos\gamma x_m - m_{20}\gamma^2 \sin\gamma x_m\right] + 4\frac{T_{p0} - T_{pc}}{b_a l_{cr}} \quad (6.13)$$

where

b_p	=	width of the FRP plate
d_p	=	width of FRP plate.
V_m	=	shear force at the position where τ_m is maximum.
b	=	width of the beam reinforced with FRP plate.
x_m	=	the position where τ_m is maximum.
I	=	second moment of area of concrete cross-section.

$$\gamma^4 = \frac{1}{4I_p}\frac{E_a}{E_p}\frac{b_a}{d_a} \quad (6.14)$$

$$f_{20} = \frac{V_0}{1 + \frac{EI}{E_p I_p}} + \tau_0 \frac{d_p}{2} \quad (6.15)$$

$$m_{20} = \frac{M_0}{1+\frac{EI}{E_p I_p}} \tag{6.16}$$

$$\tau_0 = \left[V_0 + M_0\sqrt{\frac{K_s}{E_p b_p d_p}}\right]\frac{b_p d_p}{I_e b_a} \tag{6.17}$$

$$K_s = \frac{G_a b_a}{t_a} \tag{6.18}$$

$$T_{pc} = \sigma_{p1} A_p \tag{6.19}$$

$$T_{p0} = \frac{\sigma_{p2}+\sigma_{p2}}{2} A_p \tag{6.20}$$

l_{cr} = distance between two adjacent cracks

σ_{p1} = stress in FRP plate at left cracking point

σ_{p2} = stress in FRP plate at right cracking point

A_p = cross-sectional area of FRP plate

Therefore, in the case of including the effect of initial bending cracks in the concrete, the criteria for FRP plate delamination can be written as

$$\tau_{\mathrm{m}} \le \tau_a \tag{6.21}$$

where

τ_{m} = maximum shear stress in adhesive layer

τ_a = shear strength of adhesive material

6.4 Criteria for concrete ripping-off

Fig. 6.7 shows the concrete cover layer ripping-off. Ripping of concrete is determined by the tensile and shear stresses between the reinforcing steel bars and in the FRP plate end region.

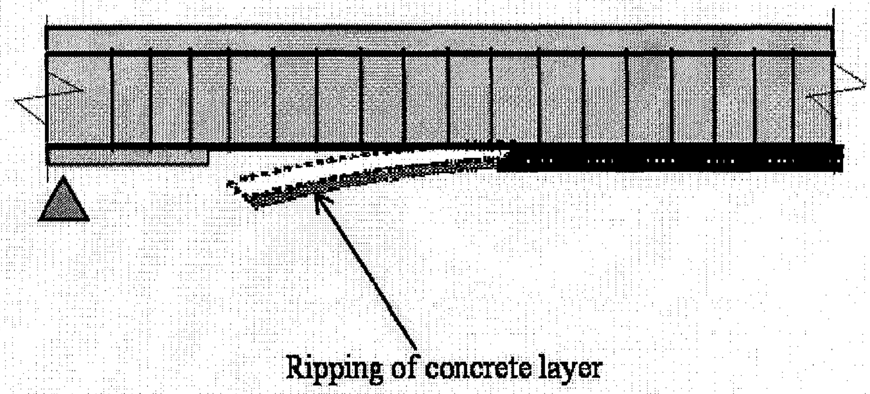

Fig. 6.7 Ripping of concrete layer between reinforcing steel and FRP plate

Nguyen et. al (Nguyen et. al, 2002) developed a simple approximated formulation to predict the ripping-off failure based on the full composite behavior of the strengthened beams and bending of the concrete "tooth". The criteria for ripping-off are

$$\sigma_c \leq f_t \tag{6.22}$$

and

$$\tau_c < \tau_u \tag{6.23}$$

where f_t is the tensile strength of concrete, which is taken about $\frac{1}{12}$ to $\frac{1}{8}$ of the concrete cube strength f_{cu} and τ_u is the shear strength of the concrete-steel bar interface.

Shear stress in the concrete cover (τ_c in Eq.(6.23)) is calculated form:

$$\tau_c = \frac{T_p}{l_{com} b} \tag{6.24}$$

where T_p is the tension force carried by the FRP plate at the full composite behavior position of the beam reinforced with FRP plate (at the distance of l_{dev} from the end of FRP plate) and l_{com} is the bond length (Fig. 6.8).

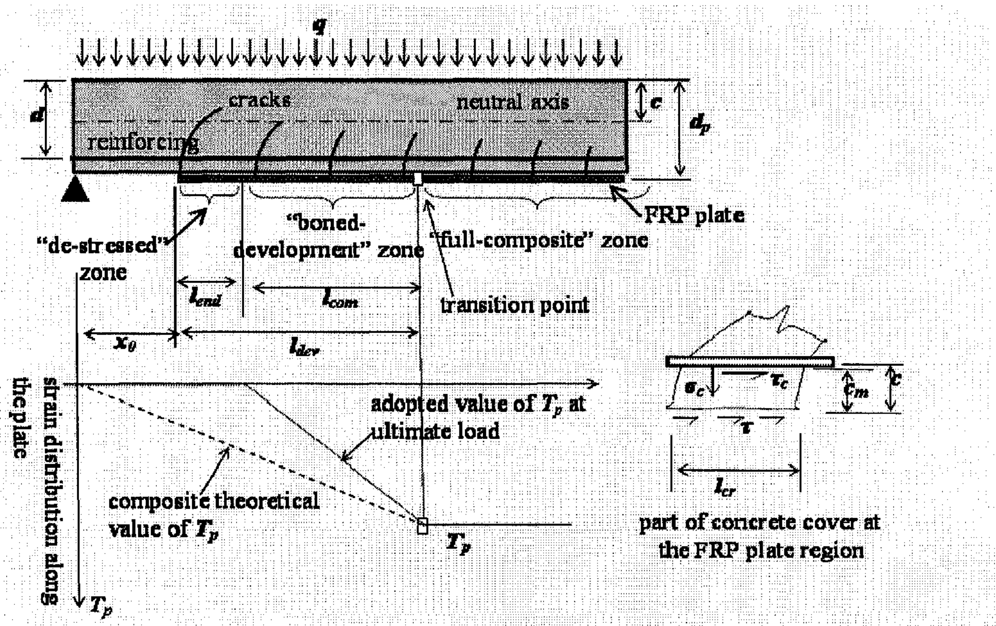

Fig. 6.8 Composite model of RC beam strengthened with FRP plate

Tension stress (σ_c in Eq. (6.22)) on the interface of the steel bar and concrete is determined by:

$$\sigma_c = 6\tau_c \frac{c_m}{l_{cr}} \tag{6.25}$$

where c_m is the thickness of concrete cover and l_{cr} is the crack spacing.

The value of T_p in Eq. (6.24) can be calculated from (Nguyen, 2001):

$$T_p = \frac{\beta^2}{\alpha^2}\left[\frac{M(x)}{l_p} - \frac{M(x)}{l_p}\frac{\cosh\alpha\frac{2x}{l_p}}{\cosh\alpha} - \frac{ql_p}{4\alpha^2}\left(1 - \frac{\cosh\alpha\frac{2x}{l_p}}{\cosh\alpha}\right)\right] \tag{6.26}$$

where

$$\alpha^2 = \frac{G_a}{4E_p}\frac{l_p^2}{t_p t_a}\left[1+\rho_{p0}\frac{E_p}{E_c}\left(1+\frac{Ah_p h_c}{I}\right)\right] \tag{6.27}$$

$$\beta^2 = \frac{G_a}{4E_c}\frac{l_p^3 h_c b_a}{I\, t_a} \tag{6.28}$$

$$\rho_{p0} = \frac{b_p t_p}{A} \tag{6.29}$$

$$x = \begin{cases} x_0 + l_{dev} & \text{for} \quad l_{cr} < l_{dev} \\ x_0 + l_{cr} & \text{for} \quad l_{cr} \geq l_{dev} \end{cases} \tag{6.30}$$

$M(x)$ = bending moment at the position of x.

l_p = length of FRP plate.

h_p = distance from the center of FRP plate to the neutral axis of the reinforced concrete beam.

h_c = distance from concrete tension face to the neutral axis of the reinforced concrete beam.

G_a = shear modulus of adhesive.

I_e = second moment of area of equivalent cracked cross-section transformed to FRP material.

d_c = effective depth of beam's cross-section.

d_p = distance from steel bars to FRP plate.

b_a = width of the adhesive layer.

t_a = thickness of the adhesive layer.

t_p = thickness of the FRP plate.

E_c = Young's modulus of concrete

A = equivalent area of reinforced concrete section

x_0 = distance from the support to end of FRP plate (Fig. 6.8).

In the design of a reinforced concrete member, flexure criteria is usually considered first, leading to the size of cross-section and arrangement of reinforcement to provide necessary moment resistance. Limits are placed on the amounts of flexural reinforcement to ensure that failure does not occur other than in flexural. Because shear failure, or FRP plate delamination or concrete debonding are frequently sudden and brittle, the design for failure modes must ensure that these shear strengths equal or exceed the flexural strength at all points in the concrete structure.

6.5 Design procedure for reinforced concrete structures strengthened with FRP strips/sheets subjected to air blast loading

With the initial size of the cross-section and the initial reinforcement the dynamic response of the structural member to the given blast load can be calculated from the formulae described in the Chapters 3, 4, and 5. If some of the criteria described in this section were not satisfied, the initial design should be modified and the calculation procedure as described Chapter 3 and Chapter 4 should be repeated again, until all the criteria are satisfied. The design procedure is described in the following flow chat:

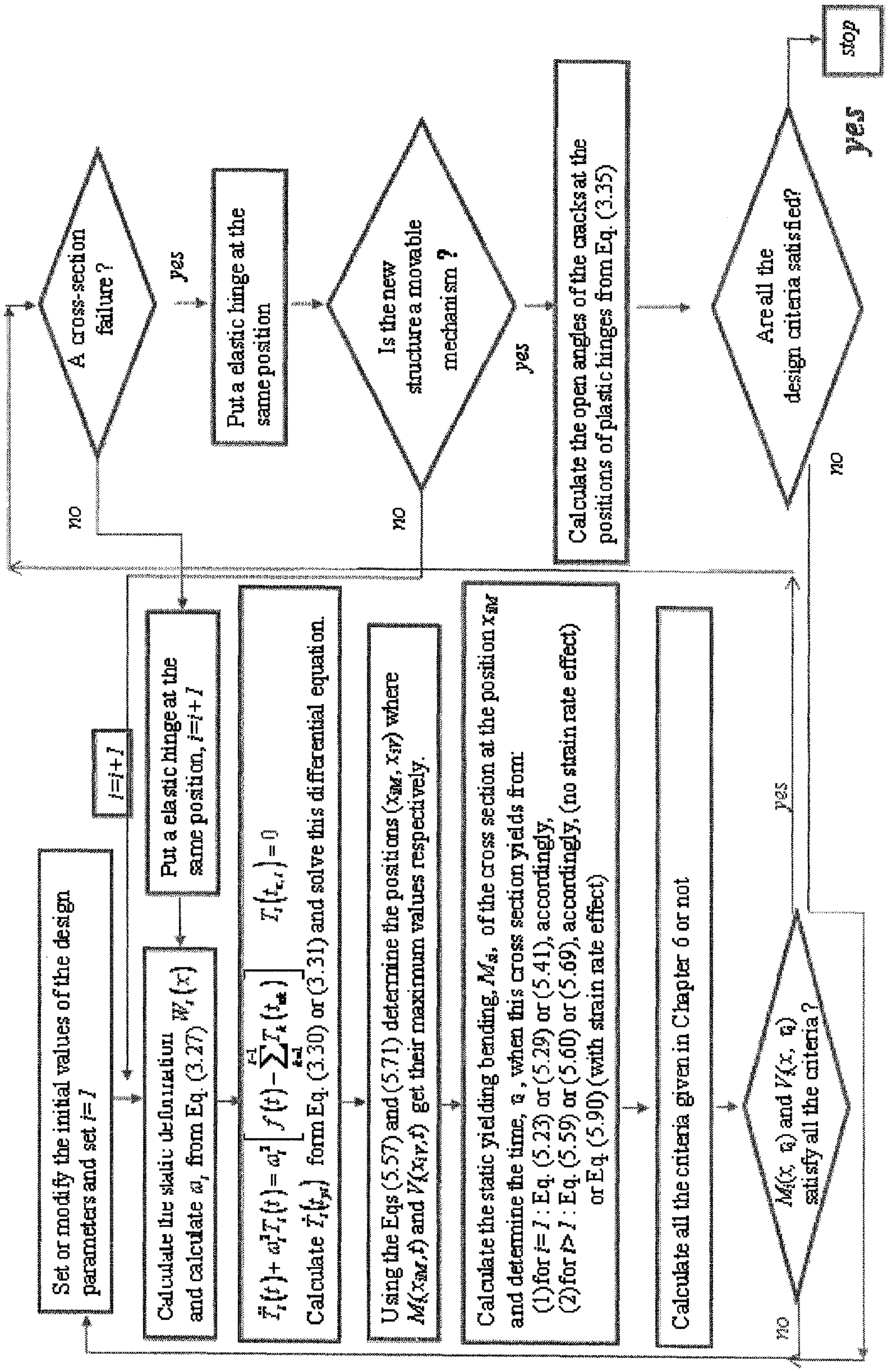
Set or modify the initial values of the design parameters and set $i=1$
Calculate the static deformation $W_i(x)$ and calculate ω_i from Eq. (3.27)
$i=i+1$
Put a elastic hinge at the same position, $i=i+1$
$\ddot{T}_i(t)+\omega_i^2T_i(t)=\omega_i^2\left[f(t)-\sum_{k=1}^{i-1}T_k(t_{sk})\right]$ $T_i(t_{s,i})=0$
Calculate $\dot{T}_i(t_{yi})$ form Eq. (3.30) or (3.31) and solve this differential equation.
Using the Eqs (5.57) and (5.71) determine the positions (x_{iM}, x_{iV}) where $M_i(x_{iM},t)$ and $V_i(x_{iV},t)$ get their maximum values respectively.
Calculate the static yielding bending, M_{si}, of the cross section at the position x_{iM} and determine the time, t_i, when this cross section yields from:
(1) for $i=1$: Eq. (5.23) or (5.29) or (5.41), accordingly,
(2) for $i>1$: Eq. (5.59) or (5.60) or (5.69), accordingly, (no strain rate effect) or Eq. (5.90) (with strain rate effect)
Calculate all the criteria given in Chapter 6 or not
$M_i(x, t_i)$ and $V_i(x, t_i)$ satisfy all the criteria ?
no
yes
A cross-section failure ?
no
yes
Put a elastic hinge at the same position
Is the new structure a movable mechanism ?
no
yes
Calculate the open angles of the cracks at the positions of plastic hinges from Eq. (3.35)
Are all the design criteria satisfied?
no
yes
stop

Chapter 7

EXAMPLES

This Chapter presents a series of worked examples to illustrate the procedures of the analysis of different structures using the formulas derived in this thesis. Sections 7.1 and 7.2 present examples of simply-supported concrete beams subjected to air-blast loading. In the example of Section 7.1, the beam is reinforced with steel bars only, while in the example of Section 7.2 the beam is reinforced with both steel bars and FRP mat. Section 7.3 presents the example of a concrete building subjected to blast loading generated by a vehicle bomb. Sections 7.4 and 7.5 present examples of simply-supported square concrete plates subjected to air-blast loading. In the example of Section 7.4, the plate is reinforced with steel bars only, while in the example of Section 7.5 the plate is reinforced with both steel bars and FRP mat.

7.1 Simply supported RC beam subjected to air-blast loading

To validate the formulas derived in this thesis, the example in this section is cited from Боданский's book (Боданский, 1974) and the results are compared. Fig. 7.1 shows a buried concrete shelter structure.

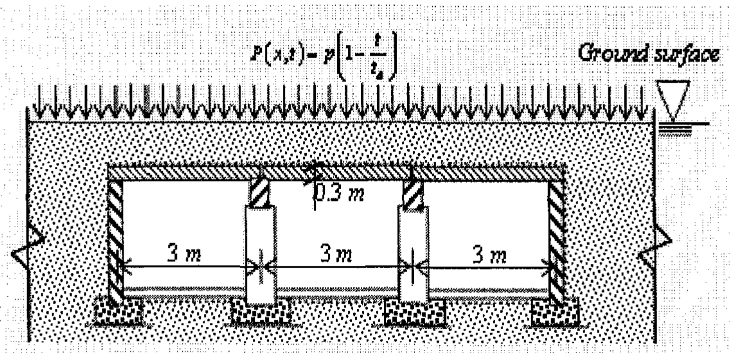

Fig. 7.1 Buried pre-cast concrete structure subjected to blast loading on ground surface generated by a nuclear explosion

The roof of this structure is composed of pre-cast concrete slabs of 300mm depth by 800mm width and 3000mm span. The blast load generated by a 1.0×10^6 tons equivalent TNT nuclear bomb explosion is idealized as a triangular load pulse with amplitude of $p = 2.2 \times 10^5 \, N/m^2$ and duration of $t_d = 0.54 \sec$.

The simply-supported one-way slab and the air-blast loading are shown in Fig. 7.2.

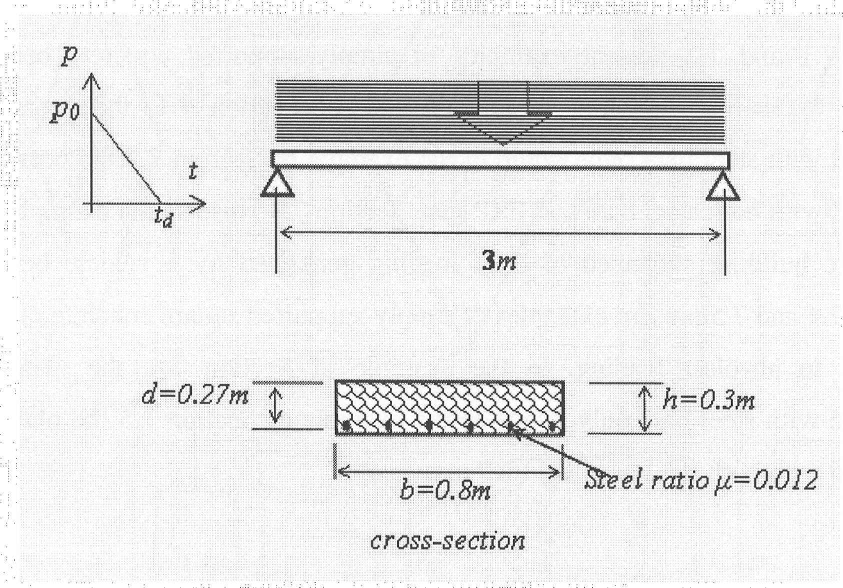

Fig. 7.2 Simply supported RC beam subjected to air-blast loading

A. Initial design parameters

1. length of beam

   $l = 3m$

2. height of the beam's cross-section

   $h = 0.3\, m$

3. width of the beam's cross-section

   $b = 0.8\, m$

4. effective height of the beam's cross-section

$d=$ 0.27 m

5. distributed mass including the self weight and the attached mass (soil) on the beam

   $m=$ 1630 kg/m

6. Young's modulus of concrete

   $E_c=$ 3.00E+10 N/m^2

7. Young's modulus of steel bar

   $E_s=$ 2.10E+11 N/m^2

8. area of reinforcement (tension)

   $A_s=$ 2592 mm^2

9. static yield strength of the steel reinforcement (tension)

   $f_y=$ 2.70E+08 N/m^2

10. static yield strength of concrete (compression)

    $f_c=$ 1.88E+07 N/m^2

11. static load including the self-weight of the slab and soil above the slab

    $q=$ 16000 N/m

12. blast load on the beam

    $p=$ 176000 N/m

    $t_d=$ 0.54 $sec.$

B. Calculation

1. calculate bending stiffness of the cross-section

a. calculate depth of neutral axis from Eq. (5.4) ($A'_s = 0$ and $A_f = 0$)

$c = 0.0903\ m$

b. calculate bending stiffness from Eq. (5.3)

$$E_c I = 3\times10^{10}\left[\frac{0.8\times0.0903^3}{3}+\frac{2.1\times10^{11}}{3\times10^{10}}\times0.002592(0.27-0.0903)^2\right]$$
$$= 2.35\times10^7 \quad Nm^2$$

2. calculate the frequency of equivalent SDOF system from Eq. (3.143)

$\omega = 132$ rad/sec

3. $\omega t_d = 71.1 > 40$

4. dynamic function (for $\omega t_d > 40$, use Eq. 5.18)

$T(t) = 1 - \cos 132\, t$

5. calculate the static yield bending moment M_s from Eq. (5.6)

$M_s = 169825 Nm$ ($A'_s = 0$ and $A_f = 0$)

6. calculate the bending moment M_0 at mid-span due to self-weight and weight of soil above the beam (uniform distributed static load on the beam)

$$M_0 = \frac{q\, l^2}{8} = \frac{16000\times3^2}{8}$$
$$= 18000 \quad Nm$$

7. calculate the bending moment M_p at mid-span from Eq. (5.2)

$$M_p = \frac{p\, l^2}{8} = \frac{176000\times9}{8} = 198000 \quad Nm$$

8. calculate the time when steel bar yield

a. calculate the value of d from Eq. (5.30)

$$d = (0.895\omega)^{\frac{1}{17}} \frac{M_s - M_0}{M_p} = 1.01513$$

b. calculate $\omega\tau$ from Eq. (5.29)

$$\omega\tau = \frac{257d + 155 - \sqrt{32889 + 194123d - 106365d^2}}{139d - 102} = 1.764$$

c. $$\tau = \frac{\omega\tau}{\omega} = \frac{1.764}{132} = 0.0134\,\text{sec.}$$

9. calculate the value of $T(\tau)$ from Eq. (5.18)

$$T(\tau) = 1 - \cos\omega\tau = 1.192$$

and the value of $\dot{T}(\tau)$

$$\dot{T}(\tau) = \omega \sin\omega\tau = 129$$

10. calculate the dynamic displacement of the beam's mid-span at time τ

a. calculate the value of deformation mode at the beam's mid-span from Eq. (3.136)

$$W(1.5) = \frac{1.5}{24 \times 2.35 \times 10^7} \times \left(1.5^3 - 2 \times 3 \times 1.5^2 + 3^3\right) = 4.494 \times 10^{-8}\ m$$

b. calculate the dynamic displacement of the beam's mid-span at time τ from Eq. (3.5)

$$w(1.5, 0.0133) = 176000 \times 1.192 \times 4.494 \times 10^{-8} = 0.00943\ m$$

11. calculate the integration in Eq. (3.134)

$$\int_0^l W(x)dx = \frac{l^5}{120EI} = 0.863 \times 10^{-7}\ m^2$$

12. calculate $\dot{T}_p(\tau)$ from Eq. (3.43)

$$\dot{T}_p(\tau)=\frac{4\dot{T}(\tau)}{L^2}\int_0^l W(x)dx=4.96\times10^{-6}$$

13. calculate ω_p^2 from Eq. (3.41)

$$\omega_p^2=\frac{3}{2mL_A}=\frac{1}{1630}$$

14. calculate the time when relative rotation angle of the plastic hinge reaches its maximum value t_m from Eq. (3.48)

$$t_m=t_d\left\{\sqrt{\left(1-T(\tau)-\frac{\tau}{t_d}\right)^2+\frac{2\dot{T}_p(\tau)}{t_d\omega_p^2}}+1-T(\tau)\right\}=0.0461\,\text{sec}.$$

15. calculate the value of $T_p(t_m)$ from Eq. (3.47)

$$T_p(t_m)=-\frac{\omega_p^2(t_m-\tau)^2}{6t_d}\left[(t_m-\tau)+3t_dT(\tau)-3(t_d-\tau)\right]+\dot{T}_p(\tau)(t_m-\tau)$$
$$=8.42\times10^{-8}$$

16. calculate maximum plastic displacement at mid-span from Eq. (3.38)

$$w\left(\frac{L}{2},t_m\right)=p\left[T_p(t_m)W_p(1.5)+T(\tau_1)W_1(1.5)\right]=0.0317\quad m$$

17. maximum open angle of the plastic hinge from Eq. (3.53)

$$\varphi_{c\max}=\frac{4}{L}w\left(\frac{L}{2},t_m\right)=0.0422\quad\text{rad.}$$

18. calculate the limit open angle of the plastic hinge from Eq. (6.2)

$$\psi_d=0.035+0.003\frac{f_c}{f_s}\frac{bd}{A_s}=0.0498\quad\text{rad.}$$

19. $\varphi_{c\,max}<\psi_d$, i.e. the slab is capable to resist the design blast load.

The maximum open angle of the plastic hinge given by Боданский (Боданский, 1974) is

$$\varphi_{c\max} = 0.0473 \quad \text{rad.}$$

The relative error is

$$\frac{0.0473 - 0.0422}{0.0473} = 11\%$$

The error is due to Боданский (Боданский, 1974) obtaining his result from a design chart which was constructed using an approximate method.

This example can also be calculated by using Biggs' method. The strain rate effect has been calculated in this example and the increase factor of the yielding bending moment can be calculated using the result of step 9 in above calculations:

$$f_d = \frac{1.192 M_p}{M_s - M_0} = 1.5545$$

The calculation procedure is as follows:

Initial data:

L	=	3	m	:bean length
m	=	1630	kg/m	:distributed mass
EI	=	2.354e7	Nm^2	:bending stiffness
Mt	=	4890	kg	:total mass of the beam
td	=	0.54	$sec.$	:duration of the blast load
P	=	176000	N/m^2	:amplitude of the uniformly distributed blast load
Ft	=	528000	N	:amplitude of the total force on the beam

Transformation factors for simply supported beam

Elastic		Plastic	
Load factor	Mass factor	Load factor	Mass factor
$K_{eL}=0.64$	$K_{eM}=0.5$	$K_{pL}=0.5$	$K_{pM}=0.33$

(Notes: the factors are obtained from Table 5.1 in Biggs' book (Biggs, 1964))

The maximum spring constant (k) and maximum resistance (R_m) are:

$$k=\frac{384EI}{5L^3}=6.696\times10^7\ N/m$$

$$R_m=\frac{8f_d\left(M_s-M_0\right)}{L^2}=\frac{8\times1.555\times151825}{3^2}=629378\ N$$

$$F_e=K_LF_t=0.64\times528000=337920\,N\,,\qquad M_e=K_{eM}M_t=0.5\times4890=1445\,kg$$

$$R_{em}=K_{el}R_m=0.64\times629378=402802N$$

$$\omega=\sqrt{\frac{k_e}{M_e}}=132\,,\qquad y_{el}=\frac{R_{em}}{k_e}=0.0094\,m\,,\qquad y_{st}=\frac{F_e}{k_e}=0.00789\,m$$

$$t_{el}=\frac{1}{\omega}\arccos\left(1-\frac{y_{el}}{y_{st}}\right)=0.0133\sec.$$

$$M_{pe}=K_{pL}M_t=0.333\times4890=1630\,kg$$

$$F_{pe}=K_{pL}F_t=0.5\times528000=264000\,N$$

$$R_{pm}=K_{pL}R_{em}=0.5\times629378=314659\,N$$

$$\ddot{y}_p\left(t_1\right)=\frac{F_{pe}}{M_{pe}}\left(1-\frac{t_1+t_{el}}{t_d}\right)-\frac{R_{pm}}{M_{pe}}\,,\qquad \ddot{y}_p\left(t_1\right)=-300t_1-35.1$$

$$\dot{y}_p(t_1) = -150t_1^2 - 35.1t_1 + \frac{K_{eL}}{K_{pL}} y_{st}\omega \sin \omega t_{el}$$,

$$\dot{y}_p(t_1) = -149.966t_1^2 - 35.094t_1 + 1.31$$

The time when the dynamic formation reaches its maximum value is determined by solving the following equation:

$$\dot{y}_p(t_{1m}) = -149.966t_{1m}^2 - 35.094t_{1m} + 1.31 = 0$$

The solution of this equation is: $t_{1m} = 0.03278$ sec.

$$y_p(t_1) = -49.99t_1^3 - 17.547t_1^2 + 1.311t + y_{el}$$

The maximum displacement in plastic stage is then obtained as:

$$y_p(t_{1m}) = y_p(0.03278) = 0.03177\ m$$

The result obtained by using Biggs' method is very close to that obtained by using the formulae derived in this thesis.

7.2 Simply-supported RC beam strengthened with FRP sheet subjected to air-blast loading

The size and type of steel reinforcement of the slab and blast loading on the slab are the same as that of the slab in Section 7.1. This example is designed to show the procedure to calculate the dynamic response of a one-way slab subjected to blast loading and how the external FRP reinforcement improves the blast resistant capability of a steel reinforced concrete one-way slab.

The simply-supported one-way slab and the air-blast loading are shown in Fig. 7.3.

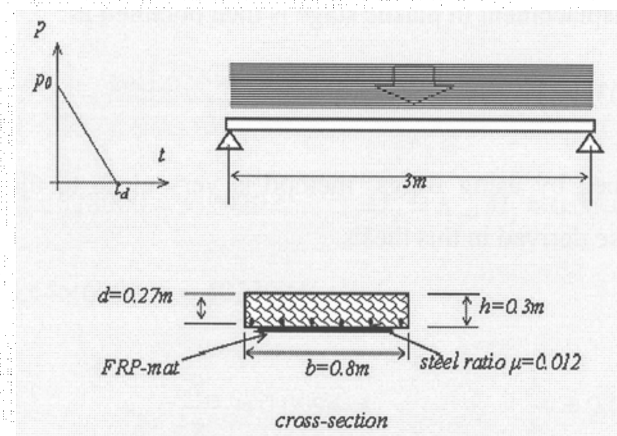

Fig. 7.3 Simply-supported RC beam strengthened with FRP sheet subjected to air-blast loading

A. initial design parameters

1. length of beam

   $L=3m$

2. height of the beam's cross-section

   $h=300mm$

3. width of the beam's cross-section

   b=800mm

4. effective height of the beam's cross-section

   d=270mm

5. distributed mass including the self weight & the attached mass on the beam
   m_0=1600 kg/m

6. Young's modulus of concrete

   E_c=3.00E+10 N/m^2

7. Young's modulus of steel bar

   E_s=2.10E+11N/m^2

8. area of reinforcement (tension)

   A_s=2592 mm^2

9. static yield strength of the steel reinforcement (tension)

   f_y=2.70E+08 N/m^2

10. static yield strength of concrete (compression)

    f_c=1.88E+07 N/m^2

11. parameters of S&P G-Sheet E 5050 A

    a. modulus of elasticity

       E_f=7.3×10^{10} N/m^2

    b. tensile strength

       f_f=3.4×10^{9} N/m^2

c. fiber cross-section area per meter in both two orthogonal directions

$A_f = 6.7 \times 10^{-5}\ m^2$

12. static load including the self-weight of the slab and soil above the slab

$q = 16000\ N/m$

13. blast load on the beam

$p_0 = 176000\ N/m$

$t_d = 0.54\ sec.$

B. calculation

1. calculate bending stiffness of the cross-section

a. calculate the total area of fiber cross-section on the tension face of the beam
$A_f = 0.8 \times 6.7 \times 10^{-5} = 5.36 \times 10^{-5}\ \mathrm{m}^2$

b. calculate depth of the neutral axis of cross-section from Eq. (5.4)

$c = 0.0906\ m$

c. calculate the bending stiffness of the beam from Eq. (5.3)

$E_c I = 2.37 \times 10^7 \quad Nm^2$

2. calculate vibration frequency from Eq. (3.142)

$\omega_1 = 132\ \ \mathrm{rad/sec}$

3. $\omega_1\ t_d = 71.4 > 40$

4. dynamic function (for $\omega\, t_d > 40$, use Eq. 5.15)

$T(t) = 1 - \cos 132t$

5. calculate the static yield bending moment M_s from Eq. (5.6)

   a. determine the value of β_1 and calculate α_{fs}

   $$1.09 - 0.008 \times f'_c = 1.09 - 0.008 \times 18.8 = 0.94 > 0.85$$

   $$\beta_1 = 0.85,\quad \alpha_{fs} = \frac{E_f}{E_s} = 0.3476$$

   b. calculate c from Eq. (5.7)

   $$c = 0.0649\, m$$

   c. calculate a from Eq. (5.8)

   $$a = 0.0551 m$$

   d. calculate the static yield bending moment M_s from Eq. (5.6)

   $$M_s = 1.71 \times 10^5 \ \ Nm$$

6. calculate the bending moment M_s at mid-span due to the static load (self-weight and the weight of soil above the beam) on the beam

   $$M_s = \frac{q\, l^2}{8} = 18000 \ \ Nm$$

7. calculate the bending moment M_{p1} at mid-span from Eq. (5.2)

   $$M_{p1} = \frac{p\, l^2}{8} = 198000 \ \ Nm$$

8. calculate the time when steel bar yield

   a. calculate the value of d from Eq. (5.30)

   $$d = (0.895\omega_1)^{\frac{1}{17}} \frac{M_s - M_0}{M_{p1}} = 1.025$$

   b. calculate $\omega_1 \tau_1$ from Eq. (5.29)

   $$\omega_1 \tau_1 = \frac{257d + 155 - \sqrt{32889 + 194123d - 106365d^2}}{139d - 102} = 1.775$$

c. $\tau_1 = \frac{\omega_1 \tau_1}{\omega_1} = 0.0134 \text{ sec}$

9. calculate the value of $T(\tau)$ from Eq. (5.18)

$$T_1(\tau) = 1 - \cos \omega_1 \tau_1 = 1.2$$

and the value of $\dot{T}(\tau)$

$$\dot{T}_1(\tau) = \omega_1 \sin \omega_1 \tau_1 = 129$$

10. calculate the dynamic displacement of the beam's mid-span at time τ

a. calculate value of deformation mode at the beam's mid-span from Eq. (3.136)

$$W(1.5) = \frac{1.5}{24 \times 2.35 \times 10^7} \times \left(1.5^3 - 2 \times 3 \times 1.5^2 + 3^3\right) = 4.488 \times 10^{-8} \ m$$

b. calculate dynamic displacement of beam's mid-span at time τ from Eq. (3.5)

$$w(1.5, \tau_1) = 0.009443 \, m$$

11. calculate the integration in Eq. (3.138)

$$\int_0^l W_1(x) dx = \frac{l^5}{120EI} = \frac{3^5}{120 \times 2.37 \times 10^7} = 0.857 \times 10^{-7} \, m^2$$

12. calculate stiffness of the equivalent rotational spring from Eq. (3.20)

a. calculate f_{dy} form Eq. (5.12)

$$f_{dy} = f_y \left(\frac{M_{p1} T_1(\tau_1)}{M_s - M_0} + \frac{M_0}{M_s} \right) = 4.48 \times 10^8 \ N/m^2$$

b. calculate c from Eq. (5.11)

$$c = 0.123 \ m$$

c. calculate a_1 from Eq. (5.15)

$$a_1 = \left(1+\alpha_f \frac{f_c}{f_f}\right)c - \alpha_f \frac{f_c}{f_f} h = 0.121\, m$$

d. calculate c_f from Eq. (5.14)

$$c_f = \frac{\alpha_f h A_f + 0.5\left(c^2 - a_1^2\right)b}{\alpha_f A_f + \left(c - a_1\right)b} = 0.134\, m$$

e. calculate remaining bending stiffness of the beam segment in which steel bars yield from (5.13)

$$\left(E_c I\right)_y = E_c\left[\left(h-c_f\right)^2 \alpha_f A_f + \frac{b\left(c-a_1\right)^3}{12} + \left(\frac{c+a_1}{2} - c_f\right)^2 \left(c-a_1\right)b\right]$$

$$= 1.16\times10^5 \;\; Nm^2$$

f. calculate the length of the yield zone from Eq. (3.18)

$$l_p = k_1 k_2 k_3 \left(\frac{z}{d}\right)^{\frac{1}{4}} d$$

$$k_1 = 0.7,\; k_2 = 1,\; k_3 = 0.9, z = 1.5,\; d = 0.27$$

$$l_p = 0.7\times1\times0.9\times\left(\frac{1.5}{0.27}\right)^{\frac{1}{4}} \times 0.27 = 0.26\, m$$

g. calculate stiffness of the equivalent rotational spring from Eq. (3.20)

$$k_c = \frac{\left(E_c I\right)_y}{2 l_p} = \frac{1.16\times10^5}{2\times0.26} = 2.21\times10^5 \;\; Nm$$

13. calculate the frequency of the equivalent SDOF system

a. calculate $\int_0^L W_2(x)\,dx$ from Eq. (3.152)

$$\int_0^L W_2(x)\,dx = 7.23\times10^{-6}\; m^2$$

b. calculate $\int_0^L W_2^2(x)dx$ from Eq. (3.153)

$$\int_0^L W_2^2(x)\,dx = 1.07\times10^{-11}\; m^3$$

c. calculate the frequency from Eq. (3.27)

$$\omega_2 = \sqrt{\frac{7.23\times10^{-6}}{1600\times1.07\times10^{-11}}} = 20.32 \ \text{rad/sec}$$

14. determine the form of the dynamic function $T_2(t)$

a. $\omega_2(t_d - \tau_1) = 20.32\times(0.54-0.0132) = 10.7 < 40$

For $0.4<\omega(t_d - \tau_1)<40$, dynamic function is in the form given by Eq. (5.50), i.e.

$$T_2(t) = 1 - \frac{t}{t_d} - T_1(\tau_1) + C_2 \sin\omega_2(t-\tau_1) - D_2\cos\omega_2(t-\tau_1)$$

b. calculate C_2 from (5.51)

$$C_2 = \frac{1}{\omega_2}\left(\frac{1}{t_d} + \dot{T}_1(\tau_1)\frac{\int_0^L W_1(x)\,dx}{\int_0^L W_2(x)\,dx}\right) = 0.167$$

c. calculate D_2 from (5.52)

$$D_2 = 1 - \frac{\tau_1}{t_d} - T_1(\tau_1) = -0.228$$

therefore the dynamic function is

$$T_2(t) = -0.2 - \frac{t}{0.54} + 0.167\sin 20(t-0.0134) + 0.228\cos 20(t-0.0134)$$

and the derivative of the dynamic function is

$$\dot{T}_2(t) = -\frac{1}{0.54} - 4.62\sin\left[20(t-0.0134)\right] + 3.4\cos\left[20(t-0.0134)\right]$$

15. calculate the maximum value of the dynamic function of $T_2(t)$

a. calculate A and B from Eqs. (5.64) and (5.65) respectively

$$A = \frac{C_2}{D_2} = -0.732\ , \quad B = D_2\omega_2 t_d \approx -2.5$$

b. calculate the time t_m from Eq. (5.70)

$$t_m = 0.0134 + \frac{1}{20.32}\left[-\arccos\frac{1}{-2.5\sqrt{1+0.732^2}} + \arccos\frac{-0.732}{\sqrt{1+0.732^2}}\right]$$
$$= 0.0283 \text{ sec}$$

c. calculate the value of $T_2(t_m)$ from the expression obtained in step 14.

$$T_2(t_m) = T_2(0.0283) = 0.0117$$

16. calculate the bending moment M_{p2} at mid-span

a. calculate the bending moment M_c at mid-span from Eq. (3.154)

$$M_C = \frac{L^2}{2}y(1-y) = \frac{3^2}{2}\times 0.5\times(1-0.5) = \frac{9}{8}$$

b. calculate $M_{p2} = pM_C$

$$M_{p2} = 176000\times\frac{9}{8} = 198000 \quad Nm$$

17. determine whether the external FRP reinforcement ruptures

a. calculate the maximum bending moment from Eq. (3.33)

$$M\left(\frac{L}{2}, t_m\right) = M_{p2}T_2(t_m) + M_{p1}T_1(\tau_1) = 2.4\times10^5 \quad Nm$$

b. calculate the rupture bending moment M_r, at which the external FRP reinforcement rupture from Eq. (5.9)
$c_f = 0.146\, m$ (obtained in step (12))

$$f_{dy} = f_y\left(\frac{M_pT_1(\tau)}{M_s - M_0} + \frac{M_0}{M_s}\right) = 4.48\times10^8\ N/m^2 \text{ (obtained in step (12))}$$
$$a = \frac{A_sf_{dy} + A_ff_f}{0.85f_c'b} = 0.124\, m \text{ (obtained in step (12))}$$

$$M_r = A_sf_{dy}\left(d - \frac{a}{2}\right) + A_ff_f\left(h - \frac{a}{2}\right) - M_0$$
$$= 2.68\times10^5 \quad Nm$$

c. $M_r > M\left(\frac{L}{2}, t_m\right)$, therefore the FRP reinforcement does not rupture.

18. maximum displacement at mid-span of the beam

a. calculate the static displacement $W_2(1.5)$ form Eq. (3.149) (the value of v_c)

$$W_2\left(\frac{L}{2}\right) = v_c = 3.87 \times 10^{-6}\ m$$

b. calculate maximum displacement at mid-span of the beam from Eq. (3.33)

$$w\left(\frac{L}{2}, t_m\right) = pT_1(\tau_1)W_1(1.5) + pT_2(t_m)v_c = 0.0174\ \ m$$

The maximum displacement of the mid-span of the beam without FRP reinforcement (c.f. Section 7.1) is

$$w_{\max} = 0.0317\ \ m$$

Therefore the relative reduction of displacement is

$$\frac{0.0317 - 0.0174}{0.0317} = 45\%$$

This result shows that the deflection of the beam strengthened with FRP sheets can largely reduce the dynamic deformation of the beam subjected to air-blast loads.

7.3 Framed RC building subjected to external air-blast loading

The pressure pulse in air from the detonation of high explosives, while extremely intensive, is also of very short duration – typically measured in milliseconds. The natural period of vibration of a framed structure in which the whole of its mass is constrained to move together is much longer than the typical bomb blast duration. As a result of this 'mismatch', the blast shock wave generally does not last long enough to induce significant overall movement in the structure. In other words, the applied blast load is resisted primarily by the building's high inertia rather than by inducing structural deflection. When assessing the consequences of the agreed threats it is important to consider whether a very close detonation, particularly of a relatively small charge, could cause disproportional overall damage due to removal of a few critical members. Where appropriate the blast loading from a particular charge in a given location on individual structural elements can be assessed and the elements can be designed to resist these loads. If a credible bomb explosion could cause the loss of a number of such elements, then normal robustness may not be sufficient to confine the extent of the resulting damage to reasonable limits and may cause progressive collapse. A progressive collapse occurs when a structure has its loading pattern or boundary conditions changed such that elements within the structure are loaded beyond their capacity and fail. The residual structure is forced to seek alternative load paths in order to redistribute the loads applied to it. As a result, other elements may fail causing further load redistribution. The process will continue until the structure can find equilibrium either by shedding load as a by-product of elements failing or by finding stable alternative load paths. Fig. 7.4 shows the progressive collapse of a framed structure when a column in the first level is removed.

The first step to simulate the progressive collapse of a framed concrete building is to carry out the local damage assessment using the SDOF approach. At the instant immediately prior to failure the frame will be reacting equal and opposite shears and moments on the member and the progressive collapse can then be simulated as a quasi-static approach (Gilmour, 1998).

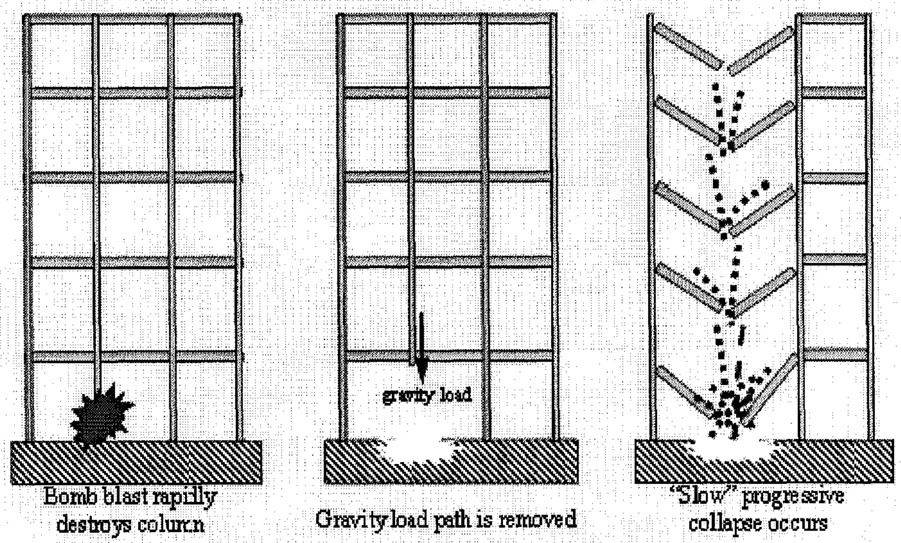

Fig. 7.4 Progressive collapse of a building

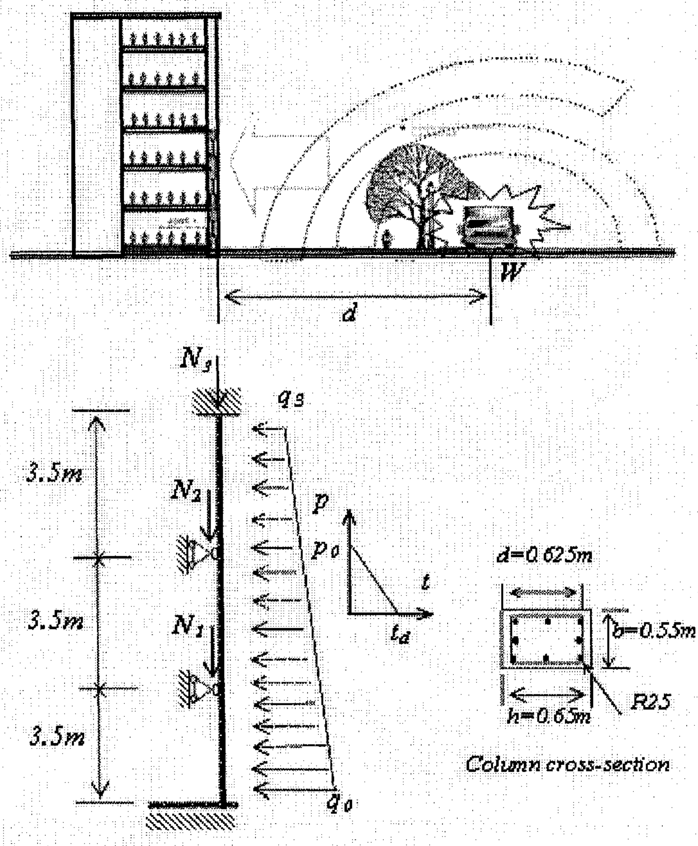

Fig. 7.5 Framed RC building subjected to external air-blast loading

This section presents an example to show how the formulas derived in this thesis can be used to carry out the local damage assessment of the columns in a framed concrete building subjected to air-blast loading.

As shown in Fig. 7.5, the columns exposed to blast overpressure are selected to be analyzed. For simplicity, only the columns in first three stories are considered and modeled as a continuous beam loaded with both static axial forces and transverse blast load.

A. initial design parameters

1. number of spans of the continuous beam

   $M=$ 3

2. length of each span

   $l=$ 5 m

3. height of the beam's cross-section

   $h=$ 650 mm

4. width of the beam's cross-section

   $b=$ 550 mm

5. effective height of the beam's cross-section

   $d=$ 625 mm

6. distributed mass including the self weight and the attached mass (such as filling walls, windows, et. al.) on the beam

   $m=$ 1716 kg/m

7. static axial loads on the beam

   $N_1=$ 500000 N

   $N_2=$ 500000 N

   $N_3=$ 1600000 N

8. Young's modulus of concrete

$E_c = 3.0\times10^{10}\ N/m^2$

9. Young's modulus of steel bar

$E_s = 2.1\times10^{11}\ N/m^2$

10. area of the tension reinforcement

$A_s = 1473\ mm^2$

11. static yield strength of the steel and concrete

$f_y = 2.7\times10^{8}\ N/m^2$

$f_c = 1.6\times10^{7}\ N/m^2$

12. air-blast load on the columns

$q_0 = 3.0\times10^{6}\ N/m$

$q_3 = 2.7\times10^{6}\ N/m$

$t_d = 0.025$ sec

B. Calculation

1. calculate bending stiffness of the cross-section

a. calculate the value of α_e

$$\alpha_e = \frac{E_s}{E_c} = \frac{2.1\times10^{11}}{3.0\times10^{10}} = 7$$

b. the depth of neutral axis is calculated from Eq. (5.4)

$c = 0.123\ m$

c. calculate bending stiffness of the cross-section from Eq. (5.3)

$E_cI = 9.12\times10^{7}\ Nm^2$

2. calculate the stress in steel reinforcement due to static axial force from Eq. (3.72)

   $\sigma_N = 0.473 \times 10^8$

3. calculate the parameters concerned with blast loading

   a. calculate the loading amplitude from Eq. (3.61)

   $$p = \frac{1}{2}(q_0 + q_3) = \frac{1}{2}(3\times10^6 + 2.7\times10^6) = 2.85\times10^6\ N/m^2$$

   b. the ratio of the loading amplitudes of the continuous column from Eq. (3.63)

   $a = -0.0526$

   c. a_k and p_k from Eq. (3.162) and (3.163), respectively

   $a_1 = -0.0169$

   $a_2 = -0.0175$

   $a_3 = -0.0182$

   $p_1 = 1.0351$

   $p_2 = 1.00$

   $p_3 = 0.965$

4. rotational stiffness of the support at bottom of the column from Eq. (3.160)

   $K_{0\theta} = 2.15\times10^{10}\ Nm$ (assume)

   $$k_0 = \frac{K_{0\theta} l}{2EI} = 590$$

5. calculate static joint rotational displacements from Eq. (3.179)

   $\theta_l = 1.01 \times 10^{-10}$ *rad.*

θ_2=-3.48×10^{-10} *rad.*

θ_3=-3.14×10^{-10} *rad.*

6. calculate the integrations concern with the static deformation from Eqs. (3.164), (3.165), (3.166) and (3.167).

$$\int_0^L W_1(x) f_1(x) dx = 1.439\times10^{-7}$$

$$\int_0^l \left(\frac{dW_1}{dx}\right)^2 dx = 3.42\times10^{-16}$$

$$\int_l^{2l} \left(\frac{dW_1}{dx}\right)^2 dx = 2.4835\times10^{-16}$$

$$\int_{2l}^{3l} \left(\frac{dW_1}{dx}\right)^2 dx = 1.1154\times10^{-16}$$

$$\sum_{k=1}^{3} \bar{N}_k \int_{(k-1)}^{kl} \left(\frac{dW_1}{dx}\right)^2 dx = 1.5893\times10^{-9}$$

$$\int_0^L W_1^2(x) dx = 1.55\times10^{-15}$$

$$\int_0^L W_1(x) dx = 1.4537\times10^{-7}$$

7. calculate the frequency ω_1 and parameter η_1 of the first dynamic response stage from Eq. (3.65).

$$\omega_1^2 = 5.34\times10^4$$

$$\omega_1 = 231 \ rad/\sec$$

8. calculate η_1 from Eq. (3.69)

$$\eta_1 = 1.003 \approx 1$$

9. determine the form of the dynamic function

$$\omega_1 t_d = 471\times0.025 = 11.78$$

since $0.4<\omega\, t_d<40$, therefore the dynamic function is in the form defined by Eq. (5.19). i.e.

$$T_1(t) = 1 - \frac{t}{t_d} - \cos\omega t + \frac{\sin\omega t}{\omega t_d} \qquad 0 \le t \le t_d$$

the dynamic function and its derivative are

$$T_1(t) = 1 - 40t - \cos 471t + \frac{1}{11.78}\sin 471t$$

$$\dot{T}_1(t) = -40 + 471\sin 471t + \frac{471}{11.78}\cos 471t$$

10. calculate the bending moment *Mp1* from Eqs. (3.180) and (3.181)

   a. calculate M_{11} and M_{21} from Eqs. (3.180) and (3.181) respectively

   $$M_{11} = 2.18 \quad M_{21} = 2.13$$

   b. calculate M_{1p1} and M_{2p1}

   $$M_{1p1} = p\ M_{11} = 2.85\times10^6 \times 2.18 = 6.2\times10^6\,Nm$$

   $$M_{2p1} = p\ M_{21} = 2.85\times10^6 \times 2.13 = 6.06\times10^6\,Nm$$

   c. determine value of M_{p1}

   $M_{1p1} > M_{2p1}$, therefore the cross-section at joint 1 yields first, i.e.

   $$M_{p1} = 6.2\times10^6\,Nm$$

11. calculate the static yield bending moment M_{s1} from Eq. (5.5)

   For axial loaded beam, f_y *should be replaced with* $f_y + \sigma_N$ (*see* Eq. (3.71))

   $$M_{1s} = 2.73\times10^5\ Nm$$

12. calculate the time when steel bar yield

   a. calculate u from Eq. (5.42)

   $$u = \omega t_d = 5.78$$

b. calculate d from Eq. (5.43)

$d = 0.0602$

c. calculate $\omega\tau_1$ from Eq. (5.41)

$\omega\tau_1 = 0.476$

$$\tau_1 = \frac{\omega\tau_1}{\omega} = 0.00206007 \quad \text{sec}$$

13. calculate the value of $T_1(\tau_1)$ and $\dot{T}_1(\tau_1)$ form the expression obtained in step 8.

$T_1(\tau_1) = 0.108$

$\dot{T}_1(\tau_1) = 102$

14. bending moment M_1 at time τ_1

$M_1(\tau_1) = 6.12\times10^6 \times 0.108 = 6.71\times10^5 \ Nm$

After the time $\tau_1 = 0.00206\,\text{sec}$. the column will deform further with the simply supporting condition at bottom end.

15. rotational stiffness of the support at bottom of the column

k_0=0.00E+00 Nm (cross-section at bottom of column has yielded)

16. static joint rotational displacements from Eq. (3.179)

$\theta_1 = 8.3\times10^{-9}$ *rad.*

$\theta_2 = -2.29\times10^{-9}$ *rad.*

$\theta_3 = 4.77\times10^{-9}$ *rad.*

17. calculate the integrations concern with the static deformation from Eqs. (3.164), (3.165), (3.166) , (3.167) and (3.169).

$\int_0^L W_2(x) f_1(x)\,dx = 2.13544\times10^{-7}$

$$\int_0^l \left(\frac{dW_2}{dx}\right)^2 dx = 2.1586\times10^{-15}$$

$$\int_l^{2l} \left(\frac{dW_2}{dx}\right)^2 dx = 9.918\times10^{-17}$$

$$\int_{2l}^{3l} \left(\frac{dW_2}{dx}\right)^2 dx = 1.562\times10^{-16}$$

$$\sum_{k=1}^{3} \bar{N}_k \int_{(k-1)l}^{kl} \left(\frac{dW_2}{dx}\right)^2 dx = (26\times12.6+21\times0.578+16\times0.91)\times10^{-12}$$
$$=3.54\times10^{-10}$$

$$\int_0^L W_2(x)\,dx = 2.121\times10^{-7}$$

$$\int_0^L W_2^2(x)\,dx = 3.2\times10^{-16}$$

$$\int_0^l W_2(x)\,dx = 1.41\times10^{-7}$$

18. calculate the frequency of the second dynamic response stage from Eq. (3.65)

    $\omega_2^2 = 21960$

    $\omega_2 = 148\ \text{rad/sec}$

19. calculate η of the second dynamic response stage from Eq. (3.69)

    $\eta_2 = 1.007 \approx 1$

20. determine the form of the dynamic function

    a. $\omega_2\ (t_d - \tau_1) = 148\times(0.025-0.00206) = 3.4$

    since $0.4<\omega(t_d - \tau_1)<40$, therefore the dynamic function is in the form as shown Eq.(5.50), i.e.

    $$T_2(t) = 1 - \frac{t}{t_d} - T_1(\tau_1) + C_2 \sin\omega_2(t-\tau_1) - D_2\cos\omega_2(t-\tau_1)\ ,\quad \tau_1 \le t \le t_d$$

    b. calculate C_2 and D_2 from Eqs. (5.46) and (5.47) respectively

    $C_2 = 0.739$
    $D_2 = 0.809$

c. the dynamic function and its derivative are

$$T_2(t) = 0.892 - 40t + 0.739\sin 148(t - 0.00206)$$
$$- 0.809\cos 148(t - 0.00206)$$

$$\dot{T}_2(t) = -40 + 120\sin 148(t - 0.00206017) + 109\cos 148(t - 0.00206017)$$

21. calculate the bending moment *Mp* from Eqs (3.180) and (3.181)

a. calculate M_{12} and M_{22} from Eqs. (3.180) and (3.181) respectively

$$M_{12} = 0 \quad , \quad M_{22} = 2.71$$

b. calculate M_{1p2} and M_{2p2}

$$M_{1p1} = p \;\; M_{12} = 2.85\times10^6 \times 0 = 0 \; Nm$$

$$M_{2p2} = p \;\; M_{22} = 2.85\times10^6 \times 2.71 = 7.73\times10^6 \, Nm$$

c. determine value of M_{p2}

$$M_{p2} = M_{2p2} = 7.73\times10^6 \, Nm$$

22. calculate the static yield bending moment M_{s2} from Eq. (5.5)

For axial loaded beam, f_y *should be replaced with* $f_y + \sigma_N$ (*see* Eq. (3.71))

$$M_{2s} = 2.73\times10^5 \, N\cdot m$$

23. calculate $T_2(\tau_2)$ and τ_2 form Eq. (5.88) and Eq. (5.89) respectively

a. calculate the known values in Eq. (5.83)

$$T_1(\tau_1)M_{2p1} = 6.55\times10^5 \, Nm$$

$$M_{2p2} = 7.73\times10^6 \, Nm$$

b. calculate the functions d from Eq. (5.84)

$$d = 2.65\times10^{-4}$$

c. calculate the value of x from Eq. (5.88)

$$x = 8.1323\times10^{-5}$$

d. calculate $T_2(\tau_2)$ from Eq. (5.89)

$$T_2(\tau_2) = 6.9\times10^{-6}$$

e. calculate τ_2 from Eq. (5.90)

$$\tau_2 = 0.00206017$$

f. calculate A and B from Eqs. (5.64) and (5.65) respectively

$$A = 0.913$$
$$B = 3$$

g check condition defined by Eq. (5.92)

$$\tau_1 + \frac{1}{\omega_2}\left(\arccos\frac{1}{B\sqrt{A^2+1}} + \arccos\frac{A}{\sqrt{A^2+1}}\right) = 1.6\times10^{-3}$$
$$> 2.06017\times10^{-3} = \tau_2$$

Therefore, Eq. (5.92) is satisfied.

24. calculate the value of $\dot{T}_2(\tau_2)$ from the expression obtained in step 20.

$$\dot{T}_2(\tau_2) = 80$$

25. calculate bending moment M_2 at time τ_2 from Eq. (3.33)

$$M_2(\tau_2) = M(l, \tau_2) = 6.55\times10^5 \ Nm$$

After the time $\tau_2 = 2.06017\times10^{-2}$ sec., the column between first and second floor will deform further with the simply supporting conditions at both ends.

26. calculate the frequency, ω_3, from Eq. (3.207)

k=1, a_1= - 0.0169(obtained in step 2), k_0=0 (obtained in step 15)

$$g_1(0, \ -0.0169) = 34425$$

$$g_2(0, \ -0.0169) = 340201$$

$$g_3(0, \ -0.0169) = 306900$$

$$\overline{N}_1^* = \frac{l^2}{EI}\overline{N}_1 = \frac{5^2\times2600000}{3.78\times10^8} = 0.713$$

$$\omega_3 = 88 \ rad/\text{sec}.$$

27. calculate γ_3 from Eq. (3.208)

$\gamma_3^2 = 8291$

28. calculate η_3 form Eq. (3.69).

$\eta_3 = 1.08$

29. calculate the integration $\int_0^l W_3(x)dx$ from Eq. (3.206)

k_0=0 (obtained in step 15) , p_1=1.04 and a_1= -0.0169 (obtained in step 2)

$\int_0^l W_3(x)dx = 2.957\times10^{-7}$

30. determined the form of the dynamic function $T_3(t)$

a. $\omega_3(t_d - \tau_2) = 139\times(0.025 - 0.0010032) = 3.34 > 0.4$

therefore the dynamic function in third stage is in the form defined by Eq.(5.50), i.e.

$$T_3(t) = 1 - \frac{t}{t_d} - T_1(\tau_1) - T_2(\tau_2) + C_3 \sin\omega_3(t-\tau_2) - D_3\cos\omega_3(t-\tau_2)$$

b. calculate C_3 and D_3 from (5.51) and (5.52), respectively

$C_3 = 0.86$
$D_3 = 0.809$

c. therefore the dynamic function and its derivative are

$$T_3(t) = 0.892 - 40t + 0.86\sin 88(t - 0.00206017) - 0.809\cos 88(t - 0.00206017)$$

and

$$\dot{T}_3(t) = -40 + 99.3\cos 139(t - 0.0010032) + 119\sin 139(t - 0.0010032)$$

31. calculate the joint rotational displacements from Eqs. (3.200) and (3.201)

$\theta_1 = 5.9207\times10^{-8}$
$\theta_2 = -5.9073\times10^{-8}$

32. calculate the position where the bending moment is a maximum value in third

stage (assume $\eta_3 T_3(\tau_3) = 0.05$)

a. dynamic deformation of the column at the time τ_3 can be calculated from

$$w(x,\tau_3) = p\left[\eta_1 W_1(x) T_1(\tau_1) + \eta_2 W_2(x) T_2(\tau_2) + \eta_3 W_3(x) T_3(\tau_3)\right], \quad 0 \le x \le l$$

$(\eta_1 T_1(\tau_1) = 0.108, \quad \eta_2 T_2(\tau_2) = 6.9\times10^{-6})$

Because τ_3 is unknown, start a "trial & error" iteration by assuming

$\eta_3 T_3(\tau_3) = 0.05$

i.e.

$$w(x,\tau_3) = p\left[3.67\phi_2(s) - 3.62\phi_4(s) + 1.78\phi_5(s,a_1)\right]\times10^{-9}, \quad s = \frac{x}{l}$$

where $\phi_2(s), \phi_4(s), and \quad \phi_5(s,a)$ are shown in Eq. (3.105).

b. with the condition $\dfrac{\partial^3 w(x,\tau_3)}{\partial x^3} = 0$ the position x_m where the bending moment is maximum at time τ_3 is determined as

$x_m = 2.4984\,m$

33. the amplitude of the dynamic bending moment at position $x_m = 2.4984\,m$ in first, second and third elastic stages can be calculated as

$$M_{3p1} = -pEI\left.\frac{d^2W_1(x)}{dx^2}\right|_{x=2.4984} = 3096215\ Nm$$

$$M_{3p2} = -pEI\left.\frac{d^2W_2(x)}{dx^2}\right|_{x=2.4984} = 5357449\ Nm$$

$$M_{3p3} = -pEI\left.\frac{d^2W_3(x)}{dx^2}\right|_{x=2.4984} = 9218779\ Nm$$

34. calculate $T_3(\tau_3)$ and τ_3 from Eq. (5.88) and Eq. (5.89), respectively

   a. calculate the known values in Eq. (5.83)

   $$T_1(\tau_1)M_{3p1} = 3.35\times10^5\,Nm$$

   $$T_2(\tau_2)M_{3p2} = 3.69\times10^5\,Nm$$

   $$M_{3p3} = 9.22\times10^6\,Nm$$

   b. calculate the functions d from Eq. (5.84)

   $d = 43.46$

   c. calculate the value of x from Eq. (5.88)

   $$x = \left(d\frac{(C_3\omega_3 t_d - 1)M_{3p3}}{\omega_3 t_d \sum_{k=1}^{2} M_{3pk}T_k(\tau_k)} + 1 \right)^{\frac{1}{18}} - 1 = 0.41576$$

   d. calculate $T_3(\tau_3)$ from Eq. (5.89)

   $$T_3(\tau_3) = \frac{\sum_{k=1}^{2} M_{3pk}T_k(\tau_k)}{M_{3p3}}x = 0.0151$$

   e. calculate τ_3 from Eq. (5.90)

   $$\tau_3 = \tau_2 + \frac{x\,t_d \sum_{k=1}^{2} M_{3pk}T_k(\tau_k)}{c_3(C_3\omega_3 t_d - 1)M_{3p3}} \left(1 - \frac{x(\omega_3 t_d)^2 \sum_{k=1}^{2} M_{3pk}T_k(\tau_k)}{2c_3(C_3\omega_3 t_d - 1)^2 M_{3p3}} \right)$$

   $= 0.00244$ sec.

   f. calculate A and B from Eqs. (5.63) and (5.64), respectively

   $A = 1.06$

   $B = 1.77$

   g. check condition defined by Eq. (5.92)

$$\tau_2+\frac{1}{\omega_3}\left(\arccos\frac{1}{B\sqrt{A^2+1}}+\arccos\frac{A}{\sqrt{A^2+1}}\right)=0.0241>0.00244=\tau_3$$

therefore, Eq. (5.92) is satisfied.

35. calculate the new value of $\eta_3 T_3(\tau_3)$ using new value of $T_3(\tau_3)=0.0151$

$\eta_3 T_3(\tau_3)=1.77\times 0.0151=0.0163$

36. replace the assumed value of $\eta_3 T_3(\tau_3)=0.05$ with 0.0163 and calculate the position x_m where the bending moment is maximum at time $t=\tau_3$ again.

   a. dynamic deformation and displacement at $x_m=2.4984$

   $T_1(\tau_1)=0.108,\quad T_2(\tau_2)=6.9\times 10^{-6},\quad \eta_3 T_3(\tau_3)=0.0163$

   the dynamic deformation of the column at $\tau_3=0.00244\,\text{sec}$ is

$$w(x,\tau_3)=p\left[1.49\phi_2\left(\frac{x}{l}\right)-1.5\phi_4\left(\frac{x}{l}\right)+0.935\phi_5\left(\frac{x}{l},a_1\right)\right]\times 10^{-8}$$

   where $\phi_2(s)$, $\phi_2(s)$ and $\phi_5(s,a)$ are shape functions used in Eq. (3.104).

   b. with the condition $\frac{\partial^3 w(x,\tau_3)}{\partial x^3}=0$ determine the position x_m where the bending moment gets its maximum value at time τ_3

   $x_m=2.4999m$

37. the amplitude of the dynamic bending moment at position $x_m=2.4999m$ in first ,second and third elastic stages can be calculated as

$$M_{3p1} = -pEI \left. \frac{d^2W_1(x)}{dx^2} \right|_{x=2.4999} = 3096223\ Nm$$

$$M_{3p2} = -pEI \left. \frac{d^2W_2(x)}{dx^2} \right|_{x=2.495} = 5355129\ Nm$$

$$M_{3p3} = -pEI \left. \frac{d^2W_3(x)}{dx^2} \right|_{x=2.495} = 9218752\ Nm$$

the bending moments are almost the same as the values calculated in step (33) where $T_3(\tau_3) = 0.05$ is assumed. If they were not close to each other, a further iteration should be carried out, i.e. the calculations in step (36) should be repeated with the new values of

$\eta_3 T_3(\tau_3) = 0.0163,$

$M_{3p1} = 3096223,$

$M_{3p2} = 5355129,$

and

$M_{3p3} = 9218752$

to get more accurate values of x_m and τ_3.

38. calculate the value of $\dot{T}_3(\tau_3)$ from the results obtained in step 30.

$\dot{T}_3(\tau_3) = 67$

39. bending moment M_3 at time τ_3 from Eq. (3.33)

$$M_3(\tau_3) = M(2.5, \tau_3)$$
$$= M_{3p1}T_1(\tau_1) + M_{3p2}T_2(\tau_2) + \eta_3 M_{3p3}T_3(\tau_3) = 4.85 \times 10^5\ \ Nm$$

After the time $\tau_3 = 2.44\times10^{-3}$ sec., the column between first and second floor will deform further with a plastic hinge in the span and the simply supporting conditions at both ends of the single span column.

40. calculate ω_p^2 from Eq. (3.85)

$$\omega_p^2 = 727$$

41. calculate γ_p^2 from Eq. (3.86)

$$\gamma_p^2 = 0.000874$$

42. calculate $\beta_i \quad i = 1,2,3$ from Eq. (3.87).

$$\beta_1 = 5.25\times10^{-12}, \quad \beta_2 = 1.12\times10^{-11}, \quad \beta_3 = 2.79\times10^{-11}$$

43. calculate the initial value of $\dot{T}_p(\tau_3)$ from Eq. (3.89)

$$\dot{T}_p(\tau_3) = 1.37\times10^{-8}$$

44. calculate constants A and B from Eqs. (3.91) and (3.92) respectively

$$\frac{\gamma_p^2}{2\omega_p^2} = 6.01\times10^{-7}$$

$$\sum_{k=1}^{3} \eta_k T_k(\tau_k) = 0.124$$

$$\bar{N}_1 = 500000 + 500000 + 1600000 = 2.6\times10^6\, N$$

$$\bar{N}_1 \sum_{k=1}^{3} \beta_k T_k(\tau_k) = 2.57\times10^{-6}$$

$$A = -4.22\times10^{-7}$$
$$B = 1.36\times10^{-6}$$

45. calculate the time when plastic deformation reaches its maximum value from Eq. (3.87)

$$t_m = \tau_n + \frac{1}{\omega_p} \ln \left\{ \frac{ -\frac{1}{t_d}\frac{\gamma_p^2}{\omega_p^2} \pm \sqrt{\left(\frac{1}{t_d}\frac{\gamma_p^2}{\omega_p^2}\right)^2 + 4\omega_p^2 AB} }{2\omega_p A} \right\} = 4.59\times10^{-2}\ \text{sec}.$$

$$t_m > t_d = 0.025$$

46. calculate the plastic displacement at the mid-span at the time $t = t_d = 0.025\,\text{sec}$ from Eq. (3.83).

$$T_p(t_d) = A\ e^{\omega_p(t_d-\tau_3)} + B\ e^{-\omega_p(t_d-\tau_3)} - \frac{\gamma_p^2}{\omega_p^2}\left(-\sum_{k=1}^{3}\eta_k T_k(\tau_k)\right) - \frac{\bar{N}_1}{\omega_p^2}\sum_{k=1}^{3}\beta_k T_k(\tau_k)$$
$$= 1.11\times10^{-7}$$

$$w_p(l_A, t_d) = pT_p(t_d) + p\sum_{i=1}^{3}\eta_i W_i(l_A) T_i(\tau_i)$$
$$= 0.368\ m$$

47. calculate C and D from Eqs. (3.99) and (3.100) respectively

$C = 1.1629\times10^{-7}$

$D = -1.5102\times10^{-7}$

48. calculate *tm* from Eq. (3.102)

For $C = 1.1629\times10^{-7}$ and $D = -1.5102\times10^{-7}$, the function on the left side of Eq. (3.101) is greater than zero. That means the dynamic function $T_p(t)$ is a mono-increased function. Therefore, the dynamic deformation of the column increases until the column collapses.

The column above the second floor can be analyzed with the similar procedure. The starting time should be $t = \tau_2 = 0.00206017$ sec.and the initial condition should be

$$T(\tau_2) = 0$$

and

$$\dot{T}(\tau_2) = \dot{T}_2(\tau_2)\frac{\int_l^{3l} W_2(x)\,dx}{\int_l^{3l} W(x)\,dx}$$

where $W(x)$ is the static deformation of the two-span continuous column above second floor for which the bending stiffness of the column below the second floor is ignored. Because the calculation procedure is similar to the procedure conducted above, it is not given in this thesis.

7.4 Simply-supported square RC plate subjected to air-blast loading

This section gives two examples. The first example in this section is cited from Боданский's book (Боданский, 1974) to validate the formulas derived in this thesis for the analysis of plate subjected to air-blast load. The reinforced concrete plate in the first example is subjected to an air-blast load from nuclear explosion. The reinforced concrete plate in the second example is subjected to an air-blast load from a conventional explosion. The response of the plate in the second example will be compared with the response of the concrete plate reinforced with combined steel bars and FRP mat, which will be given in Section 7.5.

Example 1.

Fig. 7.6 shows a buried concrete shelter structure. The roof of this structure is a square pre-cast concrete slabs with size of 6000×6000×350mm^3. The idealized triangular blast load has $p = 2.2\times10^5\ N/m^2$ and $t_d = 2.3\,\text{sec}$.

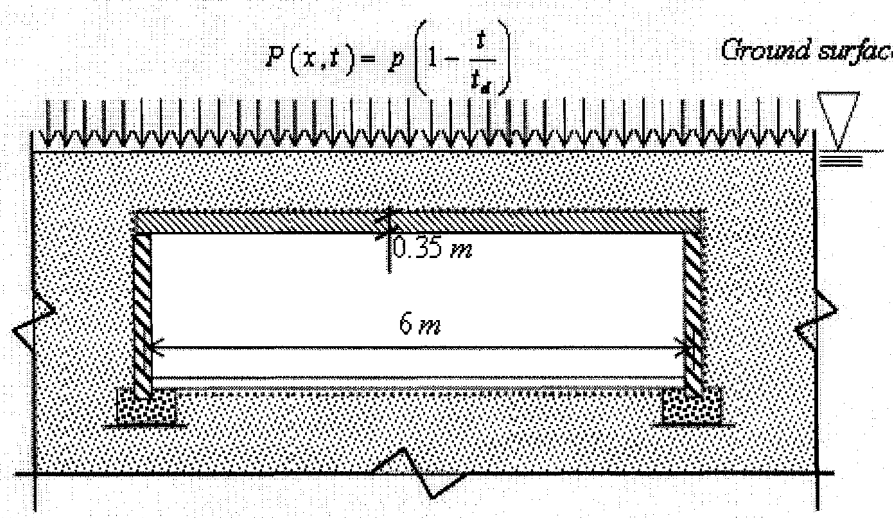

Fig. 7.6 Buried shelter structure with roof of two-way square pre-cast RC slab subjected to blast loading on ground surface generated by a nuclear explosion

The simply-supported concrete plate and the blast loading are shown in Fig. 7.7.

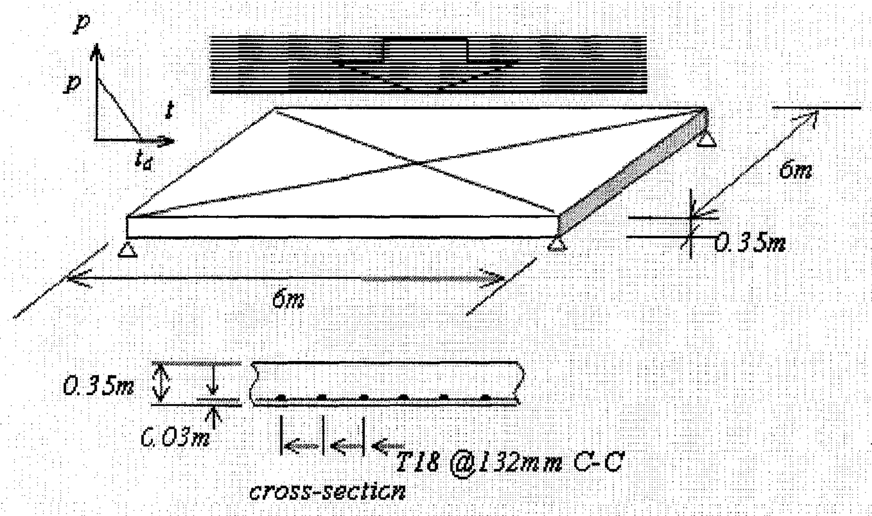

Fig. 7.7 Simply-supported square RC plate subjected to blast loading generated by a nuclear explosion

A. initial design parameters

1. slab length

   $a = 6m$

2. slab width

   $b = 6m$

3. slab thickness (cross-section height)

   $h = 0.35m$

4. effective cross-section height

   $d = 0.32m$

5. distributed mass of the slab including the attached mass (soil)

   $m = 2000 kg/m^2$

6. concrete compressive strength

   f_c =1.88e+07N/m^2

7. steel reinforcement tension strength

   f_y = 5.1e+08N/m^2

8. concrete modulus of elasticity

   E_c =3.15e+10N/m^2

9. steel modulus of elasticity

   E_s =2.1e+11N/m^2

10. concrete Poisson's ratio

    μ =0.16

11. tension reinforcement ratio

    ρ =0.006

12. blast loading amplitude

    p =180000N/m^2

13. positive phase duration

    t_d =2.27sec

B. calculation

1. Calculate bending stiffness of the plate from Eq. (4.2)

$$D = \frac{E_c h^3}{12(1-\mu^2)} = \frac{3.15\times10^{10}\times0.35^3}{12\times(1-0.16^2)} = 115503772\ Nm$$

2. Calculate natural frequency of the SDOF system from Eq. (4.44)

$$\omega = \frac{\pi^2}{a^2}\left(1+\frac{a^2}{b^2}\right)\sqrt{\frac{D}{m}} = \frac{2\pi^2}{6^2}\sqrt{\frac{115503772}{2000}} = 132\ rad/sec$$

3. $\omega t_d = 299 > 40$

4. dynamic function (for $\omega t_d > 40$, use Eq. 5.18)

   $T(t) = 1 - \cos 132\, t$

5. calculate the depth of compression zone, *a*, from Eq. (5.8)

   $\beta_1 = 0.85$
   $a = 0.0612$

6. calculate the static yield bending moment M_s from Eq. (5.6)

$$M_s = A_s f_y\left(d - \frac{a}{2}\right) = 0.00192\times 5.1\times 10^8 \times\left(0.32 - \frac{0.0612}{2}\right)$$
$$= 2.83\times 10^5\ \ Nm$$

7. calculate the bending moment M_0 at plate center due to self-weight and weight of soil above the plate (static load)

   $M_0 = 0.0364 q_0 a^2 = 0.0364\times 20000\times 6^2 = 2.62\times 10^4\ \ Nm$

8. calculate the bending moment M_p at center of the plate

   $M_p = 0.0364 pa^2 = 0.0364\times 180000\times 6^2 = 2.36\times 10^5\ \ Nm$

9. calculate the time when the steel bar yield (strain effect is not considered in this example) is calculated from $M_p T(\tau) = M_{sy} - M_{s0}$, i.e.

$$\tau = \frac{2}{\omega}\arcsin\sqrt{\frac{M_{sy} - M_{s0}}{2M_p}}$$
$$= \frac{2}{132}\arcsin\sqrt{\frac{2.83\times 10^5 - 2.62\times 10^4}{2\times 2.36\times 10^5}} = 0.0126\,\text{sec}.$$

10. calculate the values of $T(\tau)$ and $\dot{T}(\tau)$

$T(\tau)=1.09$

$\dot{T}(\tau)=131$

11. deformation mode of the plate is

$$W(x,y)=\frac{16a^4\sin\frac{\pi}{b}x\sin\frac{\pi}{a}y}{\pi^6 D\left(1+\frac{a^2}{b^2}\right)^2}=4.67\times10^{-8}\sin\frac{\pi}{6}x\sin\frac{\pi}{6}y$$

12. maximum deformation of the plate at time τ

$w(3,3,\tau)=180000\times1.09\times4.67\times10^{-8}=0.00916$ m

13. calculate $\dot{T}_p(\tau)$ from Eq. (4.37)

$\dot{T}_p(\tau)=7.47\times10^{-6}$

14. calculate ω_p^2 from Eq. (4.31)

$$\omega_p^2=\frac{1}{1000}\ (\text{rad}/\text{sec})^2$$

15. calculate the time when relative rotation angle of the plastic hinge reaches its maximum value t_m from Eq. (4.42)

$$t_m=t_d\left\{\sqrt{\left(1-T(\tau)-\frac{\tau}{t_d}\right)^2+\frac{2\dot{T}_p(\tau)}{t_d\omega_p^2}}+1-T(\tau)\right\}=0.094\,\text{sec}.$$

16. calculate the value of $T(t_m)$ from Eq. (4.40)

$$T_p(t_m)=-\frac{\omega_p^2(t_m-\tau)^2}{6t_d}\left[(t_m-\tau)+3t_dT(\tau)-3(t_d-\tau)\right]+\dot{T}_p(\tau)(t_m-\tau)$$
$$=3.25\times10^{-7}$$

17. calculate maximum displacement at the center of the plate from Eq. (4.17)

$w(3,3,t_m)=0.0675$ m

18. maximum open angle of the plastic hinge from Eq. (4.43)

$$\psi_{\max} = p\frac{4}{a}T_p\left(t_{\max}\right) + \frac{64pa^3}{\pi^6 D\left[1+\left(a/b\right)^2\right]^2}T\left(\tau\right) = 0.037 \ \ rad.$$

19. calculate the limit open angle of the plastic hinge from Eq. (6.2)

$$\psi_d = 0.035 + 0.003\frac{f_c}{f_s}\frac{bd}{A_s} = 0.035 + 0.003\frac{1.6\times 1\times 0.32}{51\times 1.92\times 10^{-3}}$$

$$= 0.05 \quad rad.$$

20. $\varphi_{c\,max} < \psi_d$, i.e. the slab is capable to resist the design blast load.

The maximum open angle of the plastic hinge given by Боданский (Боданский, 1974) is

$$\varphi_{c\max} = 0.039$$

The relative error is

$$\frac{0.039 - 0.037}{0.039} = 0.05 \quad \text{or} \ \ 5\%$$

Example 2.

As shown in Fig. 7.8, the second example in this section is a simply-supported square concrete plate subjected to air-blast load of conventional explosive.

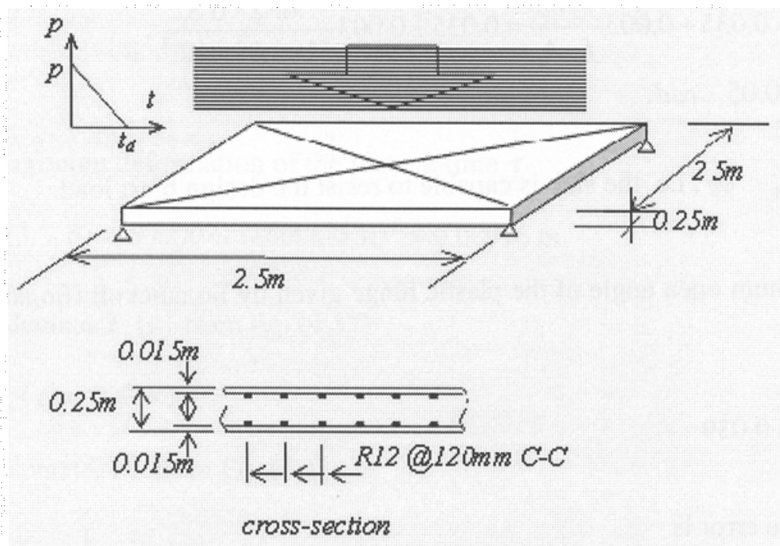

Fig. 7.8 Simply-supported square RC plate subjected to air-blast loading

A. initial design parameters

1. slab length

   a =2.5 m

2. slab width

   b =2.5 m

3. slab thickness (cross-section height)

   h =0.25 m

4. effective cross-section height

   d =0.235 m

5. distributed mass of the slab

   $m = 600\ kg/m^2$

6. concrete compressive strength

   $f_c = 4.0\text{e+}07\ N/m^2$

7. steel reinforcement tension strength

   $f_y = 2.5\text{e+}08\ N/m^2$

8. concrete modulus of elasticity

   $E_c = 3.3\text{e+}10 N/m^2$

9. steel modulus of elasticity

   $E_s = 2.0\text{e+}11 N/m^2$

10. concrete Poisson's ratio

    $\mu = 0.2$

11. tension reinforcement ratio

    $\rho = 0.005$

12. blast loading amplitude

    $p = 1000000 N/m^2$

13. positive phase duration

    $t_d = 0.0095$ Sec.

B. calculation

1. calculate plate bending stiffness from Eq. (4.3)

$$D = \frac{E_c h^3}{12\left(1-\mu^2\right)} = 44759114.58 \text{ Nm}$$

2. The natural frequency can be calculated from Eq. (4.44)

$$\omega = \frac{\pi^2}{a^2}\left(1+\frac{a^2}{b^2}\right)\sqrt{\frac{D}{m}} = 863 \text{ rad/sec}$$

3. $\omega t_d = 8.195 < 40$

4. determine the form of dynamic function $T_1(t)$

   a. for $0.4<\omega t_d<40$, use Eq. 5.19

   $$T_1(t)=1-\frac{t}{0.0095}-\cos 863t \; +\frac{\sin 863t}{8.195}$$

   b. derivative of dynamic function $T_1(t)$ is then obtained as

   $$\dot{T}(\tau)=-\frac{1}{0.0095}+863\sin 863t+\frac{1}{0.0095}\cos 863t$$

5. calculate the depth to neutral axis, c, from Eq. (5.4)

   $$c=\sqrt{\left[\alpha_e\left(A_s+A'_s\right)\right]^2+2\alpha_e\left(A_s d+A'_s d'\right)}-\alpha_e\left(A_s+A'_s\right)=0.0471\ m$$

6. calculate the static yield bending moment M_s from Eq. (5.5)

   $$M_s=A_s f_y\left(d-\frac{c}{3}\right)=64454\ Nm/m$$

7. calculate M_p at the center of the plate from Eq. (4.45)

   $$M_p=0.0364pa^2=0.0364\times 1000000\times 2.5^2=227500Nm$$

8. calculate the time τ when the steel bar yield

   a. calculate u from Eq. (5.42)

   $$u=\omega t_d=8.195$$

   b. calculate d from Eq. (5.43)

   $$d=(0.895\omega)^{\frac{1}{17}}\frac{M_s}{M_p}=0.418$$

   c. calculate $\omega\tau$ from Eq. (5.41)

   $$\omega\tau=1.08$$

   $$\tau=\frac{\omega\tau}{\omega}=0.00125\text{ sec.}$$

9. calculate the values of $T_1(\tau_1)$ and $\dot{T}_1(\tau_1)$ from the results of step 4

   $$T(\tau)=0.504$$

$$\dot{T}(\tau)=705$$

10. calculate deformation mode of the plate from Eq. (4.38)

$$W(x,y)=\frac{16\ a^4\sin\frac{\pi}{b}x\ \sin\frac{\pi}{a}y}{\pi^6 D\left(1+\frac{a^2}{b^2}\right)^2}=3.63\times\ 10^{-9}\sin\frac{\pi}{2.5}x\ \sin\frac{\pi}{2.5}y$$

11. maximum deformation of the plate at time τ from Eq. (4.1)

$$w(1.25,1.25,\tau)=W_1(1.25,1.25)T(\tau)=0.00183\,m$$

12. calculate $\dot{T}_p(\tau)$ from Eq. (4.40)

$$\dot{T}_p(\tau)=\frac{384a^4\dot{T}(\tau)}{\pi^8 D\left(1+\frac{a^2}{b^2}\right)^2\left(3-\frac{a}{b}\right)}=3.113\times10^{-6}$$

13. calculate ω_p^2 from Eq. (4.34)

$$\omega_p^2=\frac{1}{m}\frac{3b-a}{2b-a}=\frac{1}{300}\ (\text{rad/sec})^2$$

14. calculate the time, t_m, when relative rotation angle of the plastic hinge reaches its maximum value from Eq. (4.42)

$$t_m=t_d\left\{\sqrt{\left(1-T(\tau)-\frac{\tau}{t_d}\right)^2+\frac{2\dot{T}_p(\tau)}{t_d\omega_p^2}}+1-T(\tau)\right\}=0.01016\text{ sec.}$$

15. calculate the value of $Tp(td)$ from Eq. (4.26)

$$T_p(t_d)=-\frac{\omega_p^2(t_d-\tau)^2}{6t_d}\left[(t_d-\tau)+3t_dT(\tau)-3(t_d-\tau)\right]+\dot{T}_p(\tau)(t_d-\tau)$$

$$=3.41\times10^{-8}$$

16. Calculate $\dot{T}_p(t_d)$ from Eq. (4.24)

$$\dot{T}_p(t_d)=-\frac{\omega_p^2(t_d-\tau)^2}{2}T(\tau)+\dot{T}_p(t_d)(t_d-\tau)+T_p(t_d)$$

$$=1.19\times10^{-6}$$

17. calculate t_m from Eq. (4.31)

$$t_m = t_d + \frac{\dot{T}_p(t_d)}{\omega_p^2 \sum_{k=1}^{n} ik\, T_k(\tau_k)} = 0.010205 \text{ sec}$$

18. calculate the value of $T_p(t_m)$ from Eq. (4.29)

    $T_p(t_m) = T_{p1}(t_m) = 3.59\times10^{-8}$

19. calculate maximum plastic displacement at the center of the plate from Eq. (4.17)

    $w(1.25,1.25,t_m) = pT_p(t_m)W_p(1.25,1.25) + pT(\tau)W(1.25,1.25)$

    $= 0.0377\ m$

This example can also be calculated by using Biggs' method. The strain rate effect has been calculated in this example and the increase factor of the yielding bending moment can be calculated using the result of step 9 in above calculations:

$$f_d = \frac{0.5044M_p}{M_s} = 1.78$$

The calculation procedure is as follows:

Initial data:

a	=	2.5	*m*	:plate length
b	=	2.5	*m*	:plate length
m	=	600	*kg/m*	:distributed mass
EIa	=	4.30e7	*Nm*^{2}	:bending stiffness
Mt	=	3750	*kg*	:total mass of the beam
td	=	0.0095	*sec.*	:duration of the blast load
P	=	1.0e6	*N/m*^{2}	:amplitude of the uniformly distributed blast load
Ft	=	6.25.0e6	*N*	:amplitude of the total force on the beam

Transformation factors for simply supported beam

Elastic		Plastic	
Load factor	Mass factor	Load factor	Mass factor
$K_{eL}=0.46$	$K_{eM}=0.31$	$K_{pL}=0.333$	$K_{pM}=0.17$

(Notes: the factors are obtained from Table 5.4 in Biggs' book (Biggs, 1964))

The maximum spring constant (k) and maximum resistance (R_m) are

$$k=\frac{252EI_a}{a^2}=1.863\times10^9\ N/m\ ,\quad R_m=\frac{12f_d\left(M_s+M_s\right)}{a}=2754024\ N\ ,$$

$$R_{em}=K_{eL}R_m=0.46\times2754024=1266851N$$

$$F_e=K_{eL}F_t=0.46\times6250000=2875000N$$,

$$M_e=K_{eM}M_t=0.5\times3750=1162.5kg$$

$$\omega=\sqrt{\frac{k_e}{M_e}}=858.62,\qquad y_{el}=\frac{R_{em}}{k_e}=0.001478m,\qquad y_{st}=\frac{F_e}{k_e}=0.003355m$$

The time when elastic stage terminates, t_{el}, is determined by solving following equation:

$$1-\cos858.62t_{el}-\frac{t_{el}}{0.0095}+\frac{1}{8.16}\sin858.62t_{el}=\frac{y_{el}}{y_{st}}=0.44$$

The solution is: $t_{el}=0.001165$ sec.

$$M_{pe}=K_{pL}M_t=0.17\times3750=625kg$$,

$$F_{pe}=K_{pL}F_t=0.33\times6250000=2083333N$$

$$R_{pm}=K_{pL}R_m=0.33\times2754024=918000N$$

$$\ddot{y}_p(t_1) = \frac{F_{pe}}{M_{pe}}\left(1 - \frac{t_1 + t_{el}}{t_d}\right) - \frac{R_{pm}}{M_{pe}}, \qquad \ddot{y}_p(t_1) = -350877t_1 + 1455.67$$

$$\dot{y}_p(t_1) = -175438.6t_1^2 - 1455.67t_1 + \frac{K_{eL}}{K_{pL}} y_{st}\omega \sin \omega t_{el} \quad ,$$

$$\dot{y}_p(t_1) = -175438.6t_1^2 - 1455.67t_1 + 1.639127$$

The time when the dynamic deformation reaches its maximum value is determined by solving following equation:

$$\dot{y}_p(t_{1m}) = -175438.6t_{1m}^2 - 1455.67t_{1m} + 1.639127 = 0$$

The solution is: $t_m = 0.0093$ sec.

$$y_p(t_1) = -58479.5t_1^3 - 727.83t_1^2 + 1.639127t_1 + y_{el}$$

The maximum displacement in plastic stage is then obtained as:

$$y_p(t_{1m}) = y_p(0.0093) = 0.0326m$$

The result obtained by using Biggs' method is very close to the value (0.0377m) obtained by using the formulae derived in this thesis.

7.5 Simply-supported square RC plate strengthened with FRP sheet subjected to air-blast loading

As shown in Fig. 7.9, a square RC plate strengthened with FRP sheet is subjected to the air-blast loading.

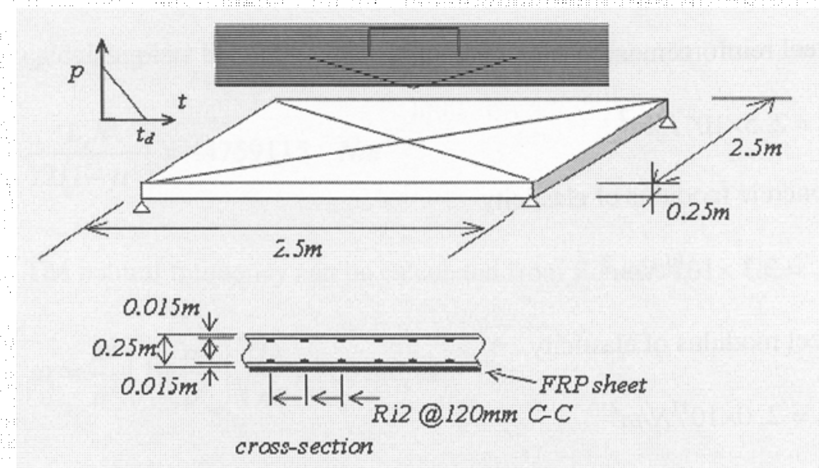

Fig. 7.9 Simply-supported square RC plate strengthened with FRP sheet subjected to air-blast loading

A. initial design parameters

1. Slab length

   $a = 2.5\ m$

2. Slab width

   $b = 2.5\ m$

3. Slab thickness (cross-section height)

   $h = 0.2\ m$

4. effective cross-section height

$d = 0.185\ m$

5. distributed mass of the slab

   $m = 600\ kg/m^2$

6. concrete compressive strength

   $f_c = 4.0 \times 10^7\ N/m^2$

7. steel reinforcement tension strength

   $f_y = 2.5 \times 10^8\ N/m^2$

8. concrete modulus of elasticity

   $E_c = 3.3 \times 10^{10}\ N/m^2$

9. steel modulus of elasticity

   $E_s = 2.0 \times 10^{11}\ N/m^2$

10. concrete Poisson's ratio

    $\mu = 0.2$

11. tension reinforcement ratio

    $\rho = 0.005$

12. parameters of S&P G-Sheet E 50/50 A

    a. modulus of elasticity

       $E_f = 7.3 \times 10^{10}\ N/m^2$

    b. tensile strength

       $f_f = 3.4 \times 10^9\ N/m^2$

    c. fiber cross-section area per meter in both two orthogonal directions

    $A_f = 6.7 \times 10^{-5}\ m^2$

13. blast loading amplitude

$p = 1000000\ N/m^2$

14. positive phase duration

$t_d = 0.0095\text{sec}$

B. calculation

1. calculate plate bending stiffness from Eq. (4.3)

$$\frac{E_c h^3}{12\left(1-\mu^2\right)} = 44759115 \quad Nm$$

2. The natural frequency can be calculated from Eq. (4.44)

$$\omega_1 = \frac{\pi^2}{a^2}\left(1+\frac{a^2}{b^2}\right)\sqrt{\frac{D}{m}} = 863 \text{ rad/sec}$$

3. $\omega_1 t_d = 8.195$

4. determine the form of dynamic function $T_1(t)$

   a. for $0.4<\omega t_d<40$, use Eq. (5.19)

$$T_1(t) = 1 - \frac{t}{0.0095} - \cos 863t \ + \frac{1}{8.195}\sin 863t$$

   b. the derivative of dynamic function $T_1(t)$ can be obtained as

$$\dot{T}_1(t) = -\frac{1}{0.0095} + 863\sin(863t) + \frac{1}{0.0095}\cos(863t)$$

5. calculate the depth to neutral axis, c, from Eq. (5.4)

$$\begin{aligned} c &= \sqrt{\left[\alpha_e(A_s + A_s') + \alpha_f A_f\right]^2 + 2\alpha_e\left(A_s d + A_s' d'\right) + 2\alpha_f A_f h} \\ &\quad -\left[\alpha_e(A_s + A_s') + \alpha_f A_f\right] \\ &= 0.0476 \end{aligned}$$

6. calculate the static yield bending moment M_s from Eq. (5.3)

$$M_s = A_s\sigma_{sy}\left(d-\frac{c}{3}\right)+A_fE_f\frac{h-c}{d-c}\frac{f_y}{E_s}\left(h-\frac{c}{3}\right)=64415\ Nm/m$$

7. calculate the bending moment M_{p1} at the center of the plate

$$M_{p1}=0.0364pa^2=227500\ Nm/m$$

8. calculate the time when the steel bar yield from Eq. (5.37)

   a. calculate d from Eq. (5.43)

$$d=(0.895\omega)^{\frac{1}{17}}\frac{M_s}{M_{p1}}=0.418$$

   b. calculate u from Eq. (5.42)

$$u=\omega t_d=6.559$$

   c. calculate $\omega\tau_1$ from Eq. (5.41)

$$\omega\tau_1=1.08$$

$$\tau_1=\frac{\omega\tau_1}{\omega}=0.00125$$

9. calculate the values of $T_1(\tau_1)$ and $\dot{T}_1(\tau_1)$ from the results obtained in step 4

$$T_1(\tau_1)=0.504$$

$$\dot{T}_1(\tau_1)=705$$

10. deformation mode of the plate in first stage is

$$W_1(x,y)=\frac{16\ a^4\sin\frac{\pi}{b}x\ \sin\frac{\pi}{a}y}{\pi^6D\left(1+\frac{a^2}{b^2}\right)^2}=3.63\times10^{-9}\sin\frac{\pi}{2.5}x\sin\frac{\pi}{2.5}y$$

11. calculate the integration $\int_0^a \int_0^b W_1(x,y)\,dxdy$ from Eq. (4.39)

$$\int_0^a \int_0^b W_1(x,y)\,dxdy = \frac{64a^5b^5}{\pi^8 D(a^2+b^2)^2} = 9.195\times10^{-8}$$

12. calculate maximum deformation of the plate at time τ_1 from Eq. (4.1)

$$w(1.25, 1.25, 0.00125) = 1.83\times10^{-3}\,m$$

13. calculate the frequency of the second elastic stage from Eq. (4.81)

a. calculate the width of the band shaped yielded zone from Eq. (3.19)

$k_1 = 0.7,\quad k_2 = 1,\quad z = 1.25,\quad d = 0.235,\quad c = 0.0476$ (obtained in step 5)

$l_p = 0.0851\quad m$

b. calculate f_{dy} from Eq. (5.12)

$f_{dy} = 4.45\times10^8\quad N/m^2$

c. calculate depth of neutral axis of yielded zone, c, from Eq. (5.11)

$c = 0.0192\quad m$

d. calculate c_f from Eq. (5.14)

$c_f = 0.0181\quad m$

e. calculate a_1 from Eq. (5.15)

$a_1 = 0.0131\quad m$

f. calculate bending stiffness of the band shaped yielding zone from Eq. (5.13)

$(E_c I)_y = 2.67\times10^5\quad Nm/m$

g. calculate stiffness of the distributed rotational spring from Eq. (4.4)

$k_c = 1.56 \times 10^6 \quad Nm/m$

h. calculate the maximum displacement of the plate after steel bars have yielded from Eq. (4.54)

$\delta = 2.94 \times 10^{-7}$

i. calculate the integration in Eq. (4.50)

$$\iint_\Omega W_2(x, y)\, dxdy = \frac{a\delta}{6}(3b - a) = 6.12 \times 10^{-7}$$

j. calculate the frequency of the equivalent SDOF system of the plate after steel bars have yielded from Eq. (4.50)

$$\omega_2^2 = \frac{48k_c(b + 0.141a)}{ma^3(2b - a)} = 11349$$

$\omega_2 = 107 \quad rad/\sec$

14. determine the form of the dynamic function of the second elastic response stage

a. $\omega_2(t_d - \tau_2) = 8.79 > 0.4$. $T_2(t)$ is in the form given by Eq. (5.50)

b. calculate C_2 and D_2 from Eq. (5.51) and Eq. (5.52), respectively

$C_2 = 1.09$, $D_2 = 0.36488$

c. the dynamic function of the second elastic response stage is

$$T_2(t) = 1 - T_1(\tau_1) - \frac{t}{t_d} + 1.9833 \sin \omega_2 (t - \tau_1) - 0.36488 \cos \omega_2 (t - \tau_1)$$

15. calculate the bending moment M_r at which the FRP sheet ruptures

a. calculate depth of neutral axis of yielded zone, c, from Eq. (5.11)

$c = 0.0192 \quad m$

b. calculate a from Eq. (5.10)

$a = 0.0163\, m$ ($\beta_1 = 0.85$)

c. $f_{dy} = 4.45 \times 10^8\ N/m^2$ (obtained in step 13.b.)

d. calculate M_r from Eq. (5.9)

$M_r = 172351\ \ Nm/m$

16. calculate M_{p2}, which is the amplitude of the dynamic bending moment at center of plate after steel bars have yielded, from Eq. (4.53)

$$M_{p2} = pM_c = \frac{pa^2(3b-a)}{12(b+0.414a)} = 736577\ \ N$$

17. calculate t_m when the dynamic function reaches its maximum value

a. calculate A from (5.64)

$$A = \frac{C_2}{D_2} = 2.985$$

b. calculate B from (5.65)

$$B = D_2\omega_2 t_d = 0.369$$

c. calculate t_m from Eq. (5.92)

$$t_m = \tau_1 + \frac{1}{\omega_2}\left(\arccos\frac{1}{B\sqrt{1+A^2}} + \arccos\frac{A}{\sqrt{1+A^2}}\right) = 0.00929 \text{ sec}$$

18. calculate the maximum value of dynamic function $T_2(t)$ from Eq. (5.50)

$$T_2(t_m) = 0.101$$

19. calculate the maximum dynamic bending moment from Eq. (5.57)

$$M_2(t) = T_1(\tau)M_{p1} + T_2(t_m)M_{p2} = 189095\ \ Nm/m$$

which is larger than the rupture bending moment $M_{r2} = 172351\ \ Nm/m$. Therefore the FRP sheet will rupture at a time $\tau_2 < t_m = 0.00929$ sec.

20. calculate the value of $x = \omega_2(\tau_2 - \tau_1)$ from Eq. (5.67) (assume $|x| < 1$)

$a = 3.916$, $b = 1.063$, $c = -1.624$

$$x = \frac{1}{2a}\left(-b + \sqrt{b^2 - 4ac}\right) = 0.522$$

$\tau_2 = 0.00616$ sec.

21. calculate values of dynamic function $T_2(t)$ and its derivative at time τ_2

$T_2(\tau_2) =$ 0.0285

$\dot{T}_2(\tau_2) =$ 106.637

22. calculate ω_p^2 from Eq. (4.34)

$$\omega_p^2 = \frac{1}{m}\frac{3b - a}{2b - a} = \frac{1}{300}$$

23. calculate initial value of $\dot{T}_p(t)$

a. calculate U_{pp} from Eq. (4.24)

$U_{pp} = 21146$

b. calculate $\dot{T}_p(\tau_2)$ from Eq. (4.33)

$$\iint_\Omega W_p(x, y)\,dxdy = \frac{ab}{3} = 2.08333$$

$\dot{T}_p(\tau_2) = 3.1345\times10^{-5}$

24. calculate t_m when dynamic function $T_p(t)$ reaches its maximum vale from Eq. (4.27)

$t_m = 0.0123$ sec.

since $t_m = 0.0123 > t_d = 0.0095$, the dynamic function $T_{p1}(t)$ should be calculated

25. calculate $T_p(t_d)$ from Eq.(4.26)

$T_p(t_d) = 2.74 \times 10^{-8}$

26. calculate $\dot{T}_p(t_d)$ from Eq.(4.25)

$\dot{T}_p(t_d) = 6.03 \times 10^{-6}$

27. calculate t_m from Eq. (4.31)

$t_m = 0.0131 \text{ sec}$

28. calculate $T_{p1}(t_m)$ from Eq.(4.30)

$T_{p1}(t_m) = 3.82 \times 10^{-8}$

29. calculate maximum dynamic deformation from Eq. (4.17)

$w(1.25, 1.25, t_m) = 1.0 \times 10^{6} \times 3.82 \times 10^{-8} + 1.83 \times 10^{-3} = 0.04003\ m$

Chapter 8

SUMMARY AND FUTURE WORK

8.1 Summary

With the weighted residual method, a structural component subjected to air-blast load is transformed into a single-degree-of-freedom system model, while the laws of energy conservation and kinetic momentum conservation are used to set up the initial conditions of the mathematical equations of the SDOF system model.

A new concept of equivalent rotational spring has been proposed to set up the dynamic equivalent SDOF system of the structure reinforced with both steel bars and external FRP plate/mat, and based on the law of energy conservation and the law of kinetic momentum conservation, a stage-tracing method has been presented to compute the dynamic response of structures with progressively reducing stiffness.

Simple and accurate formulas have been proposed to calculate the yielding delay time of steel reinforcement (strain rate effect).

A significant number of formulas to set up the SDOF system of different structures have been derived, which largely simplify the design procedure of the structure subjected to air-blast loading. A number of examples were provided to validate the derived approach.

8.2 Future work

This study focused mainly on the derivations to set up the mathematical model of the SDOF system of a structure. Experiments to determine the properties of the materials at high strain rate are also very important for the analysis and design of the structures subjected to air-blast loading. The parameters in the equation to determine the yielding delay time of mild steel were obtained many years ago. Now, metallurgy technique has been largely improved and many new types of steel have been used in the construction industry. On the other hand, testing techniques have been largely improved. Therefore, tests of different kinds of steels on strain rate effect should be done to satisfy the requirements of analysis and design of blast resist structures.

The design criteria listed in Chapter 6 is obtained from public literature. They are all based on the results of static experiments. Although one can use dynamic factors to make them "suitable" for the design and analysis of blast resist structures, it should be noted that there are many unknowns concerned with failure mechanisms when the structure deforms at very high speed. Therefore, tests to set up the dynamic criteria for the design of blast-resistant structures should be carried out.

The stiffness of the equivalent rotational spring to model the beam segment (in which steel bars have yielded) in RC beam strengthened with FRP plate/sheet is dependent on the length and remaining bending stiffness of the beam segment. The length of the yielding zone in the tension steel bars should be determined with test result by measuring the plastic strain of the steel bars over the span of the tested RC beam strengthened with FRP plate/sheet.

For a RC beam/slab subjected to air blast loads, one likely failure mode is shear failure, which occurs before the tension reinforcement yields. The shear failure of a RC beam/slab is usually due to the crushing of the concrete. Anyway, by using SDOF method, it is difficult to trace the dynamic response of a RC beam/slab subjected to air blast loads after the concrete crushes, because it is difficult to estimate the bending and shearing stiffness of the RC beam/slab after the concrete has crushed. FRP strips/mats can also be used to increase the shear capacity of a reinforced concrete beam by partial or complete beam wrapping (MBrace 2002). Sufficient FRP wrap reinforcement for the strengthening of the concrete beam subjected to air blast loads can confine the concrete and prevent concrete from crushing. Therefore, the shear resistance of a web-reinforced concrete beam may be modeled as a parallel chord truss (truss mechanism) and the SDOF method for the analysis of the RC beam, in which the shear failure mode is considered, can be developed. Anyway, to develop such a reliable SDOF method, more theory and experimental research work should be carried out.

REFERENCES

Alsayed S. H., Al-Sallom Y. A., and Almusallam T. H. (2000) "Fiber-Reinforced Polymer Repair Materials – some facts," New Civil Engineer International, pp. 29-32. U.K.

Arduini, M. and Nanni, A. (1997), "Behavior of Pre-cracked RC Beams Strengthened with Carbon FRP sheets", Journal of Composites for Construction, May pp. 63-70.

Atkash R. S., Chan K. K., Stultz K. G., Dillworth J. R., and Maranda M. L., (1994), Theoretical Guidebook, Reversion G. Weidlinger Associates, New York, USA.

Baker, A. L. L., (1956), Ultimate Load Theory Applied to the Design of Reinforced and Prestressed Concrete Frame, Concrete Publications Ltd, London, 1956, 91pp.

Biggs J. M. (1964), Introduction to Structural Dynamics, McGRAW-HILL Book Company, New York, USA.

Brebbia C. A. and Sanchez-Galvez V. (1994), Shock and Impact on Structures, Computational Mechanics Publications, Southampton, U. K. and Boston, USA.

Brezinski C. and Iseghem J. V. (1994), "Pade Approximations", Handbook of Numerical Analysis Vol. III , Elsevier Science, North-Holland.

Britt J. R. and Lumsden M. G. (1994), Internal Blast and Thermal Environmental from internal and External Explosions: A User's Guide for the BLAXT Code, Version 3.0, U.S.A.E. Waterways Experiment Station, Vicksburg, MS, USA.

Campbell, J. D. (1953), "The Dynamic Yielding of mild steel", Acta Metallurgica, Vol. 1, No. 6. pp. 706-710.

Chajes, M. J., Finch, Jr. W. W., Januszka, T. F. and Thomson, Jr. T. A. (1996), "Bond and Force Transfer of Composite Material Plates Bonded to Concrete", ACI Structural Journal, V. 93, No. 2, March-April. 1996, pp. 208-217.

Design Guide Line for S&P FRP Systems (2002) S&P Product Company, Texas, USA.

DOE/TIC-11268 (1992), A Manual for the Prediction of Blast and Fragment Loadings on Structures. U.S. Department of Energy, Washington DC, USA.

Edward R. F., Duane J. G., and Milligan P. B. (1998), "Composite Systems for Seismic Applications". Concrete International. June 1998, pp. 31-33.

ESL-TR-87-57 (1989), Protective Construction Design Manual. Air Force Engineering Center, Engineering & Services Laboratory, Tyndall Air Force Base, Florida, USA.

FEMA 273/274, (1997), NEHRP Guidelines for Seismic Rehabilitation of Buildings. 1997 Edition. FEMA 356/357. 2000: USA.

FEMA 368/307/308, (1998), NERHRP Evaluation and repair of earthquake damaged concrete and masonry buildings. USA.

FEMA 368/369, (2000), NEHRP Recommended Provisions for Seismic Regulations for New Buildings and Other Structures. USA.

Gilmour, J. R. (1998), Numerical Modeling of the Progressive Collapse of Structures Under Dynamic Loading Condition, PhD Thesis, City University, London, UK.

Glasstone, S., and Dolan P. (1977), The Effects of Nuclear Weapons, 3rd ed. Washington D.C., U.S. Department of Defense and U.S. Department of Energy.

Goldsmith, W. (1965), ГоЛдшит, В., Удар (Shock) СИ Моква.

Henrych J. (1979), The Dynamics of Explosion and Its Use, Elsevier Scientific Publishing Company, New York, USA.

James G. Macgregor (1997), REINFORCE CONCRETE Mechanics and Design (Third Edition), PRENTICE-HALL International, Inc. New Jersey, USA.

Jones, R., Swamy, R. N. and Charif, A. (1988), "Plate Separation and Anchorage of Reinforced Concrete Beams Strengthened by Epoxy-bonded Steel Plates", The Structural Engineer, Vol. 66, No. 5. March 1988, pp. 85-94.

Kotlyarevskii, V. A. (1961), "Mechanical Characteristic of Low-Carbon Steel Subjected to An Impulse Load with Regard to Creeping and Viscoplastic Properties", ПМТФ No 6, Моква.

Macgregor J. G. (1988), Reinforced Concrete Mechanics and Design, Prentice-Hall International, Inc. New Jersey, USA.

Malek, A. M. , Saadatmanesh, H. and Ehsani, M. R. (1998), "Prediction of failure Load of R/C Beams Strengthened with FRP Plate due to Stress Concentration at Plate End", ACI Structural Journal, V. 95, No. 2, March-April 1998. pp. 1-11.

Malvar L. J. (1990), "Review of Static and Dynamic Properties of Steel Reinforcing Bars", ACI Materials Journal, V95, 5, pp. 609-616.

Mosley W. H. and Bungey J. H. (1990), Reinforced Concrete Design, Macmillan Press Ltd, London, UK.

National Research Counncil. (1995) Protecting Buildings from Bomb Damage: Transfer of Blast-Effects Mitigation Technologies from Military to Civilian Applications, Washington, D. C. National Academic Press, USA.

Nguyen, D. M., "Behaviour of Reinforced Concrete Elements Externally Strengthened with Fibre Reinforced Plastic Plates", PhD. Thesis, School of Civil and Environmental Engineering, Nanyang Technological University, 2001.

Nguyen, D. M., Chan, T. K. and Cheong, H. K. (1999), "Interaction Behaviour Between Plate-Adhesive-Concrete and Premature Failures of FRP Strengthened Beams", East Asia-Pacific Conference on Structural Engineering and Construction, Kochi, Japan, August, pp. 1289-1294.

Park, R. and Paulay, T, (1975), Reinforced Concrete Structures, John Wiley and Sons, New York.

Quantrill, R. J., Hollaway, L. C. and Thorne, A. M. (1996), "Prediction of The Maximum Plate End Stresses of FRP Strengthened Beams Response: Part II", Magazine of Concrete Research, 48, No. 117. Dec. 1996, pp. 331-342.

Ray W. Clough and Joseph Penzien (1993) "Dynamics of Structures" McGraw-Hill, Inc, Singapore.

Roberts, T. M. (1989), "Approximate Analysis of Shear and Normal Stress Concentrations in the Adhesive Layer of Plated RC Beams", The Structural Engineer, Vol. 67, No. 12, June 1989, pp. 229-233.

Saeed Moaveni, (1999), Finite Element Analysis: Theory and Application with

ANSYS, Prentice Hall; 1st Ed.

Save M. A., D. C., and de Saxce G. (1997), Plastic Limit Analysis of Plates, Shell and Disks, Elsevier Science B. V.

Sharif, A. M., Al-Sulaimani, G. J., Basunbul, I. A., Baluch, M. H. and Ghaleb, B.N. (1994), "Strengthening of Initially Loaded Reinforced Concrete Beams using FRP Plates", ACI Structural Journal, V. 91, No. 2, pp. 160-168.

Sharif, A. M., Al-Sulaimani, G. J., Basunbul, I. A., Baluch, M. H. and Ghaleb, B. N., (1991), "Strengthening of Initially Bonded Concrete Beams Using FRP Plates", ACI Structural Journal, 91(2), pp. 160-168.

Smith P. D. and Hetherington J. D. (1994), Blast and Ballistic Loading of Structures, Butterworth- Heinemann Ltd, UK.

Spadea G., Bencarding F., and Swamy N. (1997) "Strengthening and Upgrading Structure with Bonded CFRP Sheets: Design Aspects for Structural Integrity", Proceedings of 3rd International Symposium on Non-Metallic (FRP) Reinforcement for Concrete Structures, Sapporo, Japan, 1997, I, pp. 629-636.

TM5-1300 (1987), Design of Structures to Resist the Effects of Accidental Explosion, Dept. of the Army, Navy and Air Force, Washington, USA.

TM5-855-1, (1986), Fundamentals of Protective Design for Conventional Weapons, HQ Department of the Army, Washington, USA.

Triantafillou, T. C., Plevris, N. (1992), "Strengthening of RC Beams with Epoxy-Bonded Fiber-Composite Materials", Materials and Structures, V. 25, 1992, pp. 201-211

Whirley R. G. and Engelmann B. E., (1993), "DYNA3D: A Nonlinear Explicit, Three Dimensional Finite Element Code for Structural Mechanics, User Manual, Revision 1", Livermore Software Technology Corporation, LSTC, Livermore, California, USA.

Zienkiewicz, O. C. and Taylor, R. C., (1989), The Finite Element Method, Vol. 1: Basic Formulation and Given Problems, 4th Ed., McGraw-Hill, UK.

Боданский М. Д., Горшков Л. М. Морозор В. И. Расторгуев Б. С., (1974), Calculations of Shield Structures(Chinese translation), Гтройиздат, Москва.